AC Microgrid protection based on machine learning and multi-agent systems

by

Muhammad Uzair

Thesis submitted in fulfilment of

the requirements for the degree of

Doctor of Philosophy

under the supervision of

A/Prof. Li Li &

Prof. Jian Guo Zhu

Faculty of Engineering and Information Technology

School of Electrical and Data Engineering

University of Technology Sydney

Sept, **2023**

Certificate of Original Authorship

I, Muhammad Uzair, declare that this thesis is submitted in fulfilment of the requirements for the award of Doctor of Philosophy, in the School of Electrical and Data Engineering at the University of Technology Sydney.

This thesis is wholly my own work unless otherwise referenced or acknowledged. In addition, I certify that all information sources and literature used are indicated in the thesis. This document has not been submitted for qualifications at any other academic institution.

Lastly, this research is supported by the Australian Government Research Training Program.

Signature: Production Note: Signature removed prior to publication.

Date: September 22, 2023

Abstract

The increasing demand for power, aging distribution systems, and concerns over greenhouse gas emissions have significantly increased distributed generation (DG) integration within distribution networks. This integration challenges conventional protection methods due to the bidirectional power flow and the constraints of anti-islanding protection. The microgrid concept offers a promising solution but also presents challenges, including the significant variation in fault currents between grid-connected and autonomous modes and the arbitrary output impedance of inverter-interfaced DG units during faults and current limiting modes. These issues complicate the development of a robust protection scheme. Therefore, an intelligent and adaptive protection scheme is required to protect microgrids against various faults and operational conditions.

Artificial intelligence, especially supervised machine learning (ML), holds significant potential for solving microgrid protection challenges. However, the limited availability of datasets and the need for innovative feature extraction techniques have impeded progress. To address these issues, this research develops different radial and meshed AC microgrid models for collecting fault and no-fault data. Three comprehensive datasets are prepared to train various supervised ML and deep learning (DL) algorithms. The largest dataset consists of 16,000 fault cases and 432 no-fault cases.

Additionally, innovative feature extraction techniques, such as Peaks Metric and Max Factor, are formulated and applied alongside investigating eight other methods to extract features, not commonly used for microgrid fault detection and classification. Various feature ranking techniques are employed to reduce the number of predictors. A novel hybrid DL-based fault detection and classification protection method is developed and validated using unseen data to ensure robust predictive performance.

Moreover, a multi-agent system (MAS) framework is established to integrate data-driven ML models within a process-driven MAS structure, enhancing coordination and adaptive protection. Simulation results show that the proposed scheme, combining ML and MAS, outperforms previous methods, achieving high fault detection and classification accuracy and exceptional protection sensitivity for both microgrid operational modes across various fault scenarios.

This research develops comprehensive models of radial and meshed microgrids, formulates new feature extraction techniques, and evaluates the performance of the intelligent protection scheme under varying conditions. The result is a robust protection scheme that improves system resilience and economic benefits by providing precise fault detection, classification, and phase identification, which are essential for future intelligent grids.

Dedication

This thesis is dedicated to my beloved father, *Muhammad Arif*, who passed away on 3 April 2023. He was the one who encouraged me to pursue this Doctoral Degree, and I am sure he would have been so proud to see me graduate. I will forever miss you, Dad.

Acknowledgements

"So all the praises and thanks are to Allah, the Lord of the heavens and Lord of the earth, Lord of the worlds." (Qur'an, chapter 45, verse 36)

After praising Allah, I would like to extend my utmost gratitude to my family, *my wife, my children, my parents, my parents-in-law, colleagues and friends*, without their understanding, support and prayers, it would have not been possible for me to complete this thesis.

I would also like to express my deep appreciation to the principal supervisor A/Prof. Li Li for his endless support, and the co-supervisor, Prof. Jian Guo Zhu for his help and advice. Lastly, I would like to thank the University of Technology Sydney and the Australian government for the scholarship.

Muhammad Uzair

September 22, 2023

Sydney, Australia

List of Publications

Journal Papers

PJ1. **M. Uzair**, L. Li, M. Eskandari, J. Hossain, J. G. Zhu, "Challenges, advances and future trends in AC microgrid protection", *Renewable and Sustainable Energy Reviews*, vol. 178, p. 113228, 2023.

PJ2. **M. Uzair**, M. Eskandari, L. Li, and J. Zhu, "Machine Learning Based Protection Scheme for Low Voltage AC Microgrids," *Energies*, vol. 15, no. 24, p. 9397, 2022.

SJ3. **M. Uzair**, L. Li, J. G. Zhu, "Hybrid deep learning based microgrid protection", *preparing to submit in IEEE Transactions on Power Delivery.*

Conference Papers

PC1. **M. Uzair**, L. Li, J. G. Zhu, "Identifying line-to-ground faulted phase in low and medium voltage ac microgrid using principal component analysis and supervised machine-learning", *Proc. IEEE 2018 Australasian Universities Power Engineering Conference (AUPEC)*, pp. 1–6, Nov 2018.

PC2. **M. Uzair**, L. Li, J. G. Zhu, M. Eskandari, "A protection scheme for ac microgrids based on multi-agent system combined with machine learning", *Proc. IEEE 2019 Australasian Universities Power Engineering Conference (AUPEC)*, pp. 1–6, Nov 2019.

Book Chapter

PB1. **M. Uzair**, L. Li, S. B. A. Bukhari, "Deep learning-based microgrid protection", in *Microgrids and Virtual Power Plants.* Singapore: Springer Nature Singapore. Approved and awaiting publication.

Contents

List of Figures

List of Tables

List of Symbols and Abbreviations

$\bar{x}$ Mean of signal x

$\bar{x}_{peaks}$ Mean of the peak values in signal x

$e\vec{v}_1$ First eigenvector

C_M Covariance matrix

cov Covariance

$Freq$ Frequency

Iph_{ABC} Three phase current

Ish_{ABC} Three phase short-circuit current

pc_1 First principal component

pc_2 Second principal component

$Sym5$ Symlets 5

Vph_{ABC} Three phase voltage

x_{max} Maximum value of the signal x

x_{rms} RMS value of x

AI Artificial intelligence

ANN Artificial neural network

AP Adaptive OC protection

BA Backup agent

BT Bagged Trees

CA Central agent

CB Circuit breaker

CNN Convolutional neural network

DER Distributed energy resource

DG Distributed generation

DN Distribution network

DNN Deep neural network

DP Differential protection

DT Decision Tree

DWT Discrete wavelet transform

ELM Extreme learning machine

FC Fault current

FCL Fault current limiter

FD Fault detection

FE Feature extraction

FFT Fast Fourier transform

FL Fault location

FNN Feedforward neural network

FP Faulted phase

FTC Fault type classification

GA Grid agent

HDLBPS Hybrid deep learning-based protection system

IDMT Inverse definite minimum time

IED Intelligent electronic device

IIDG Inverter interfaced distributed generator

LA Local agent

LG Line-to-ground

LL Line-to-line

LLG Line-to-line-to-ground

LLL Line-to-line-to-line

LLLG Line-to-line-to-line-to-ground

LSTM Long short-term memory

LVRT Low voltage ride-through

MA Measurement agent

MAS Multi-agent systems

MG Macro grid / Main grid

ML Machine learning

MW Mother wavelet

NB Naïve Bayes

OC Overcurrent

PA Protection agent

PCC Point of common coupling

PCP Parallel Coordinates plot

PMU Phasor measurement unit

PS Protection scheme

PV Photovoltaic

RF Random Forest

RMSE Root-mean-square error

SC Short circuit

SML Supervised machine learning

SVM Support vector machine

THD Total harmonics distortion

TW Travelling waves

VA Verification agent

WA Wide-area

WT Wavelet transform

Chapter 1

Introduction

1.1 Background

Major Australian cities have faced numerous blackouts recently as the present conventional power grid reaches its maximum capacity. Additionally, with more concerns about greenhouse gas emissions by conventional power plants in many countries, including Australia, more and more distributed generation (DG) sources are being connected to the distribution networks (DNs). Compared to large-scale traditional power plants away from the cities, generating power locally reduces infrastructure costs and greenhouse gas emissions due to renewable energy sources and the elimination of line losses associated with long transmission lines. At present, the share of renewable energy is around 36% of the total electricity generation in Australia, increasing from 32.5% in 2021 and doubling since 2017 [4]. Australia is committed to achieving net-zero greenhouse gas emissions and is changing its electrical system to rely primarily on renewable energy sources by 2050 [5].

In Australia, renewable energy generation predominantly revolves around wind and hydropower, which represent the most significant contributors. Nevertheless, over the past decade, there has been a notable surge in the adoption of rooftop grid-connected photovoltaic (PV) systems among households. This increased uptake can be attributed to the proactive support from the government in the form of subsidies and attractive financial incentives, including Renewable

Some contents of this chapter have been published in M. Uzair, L. Li, M. Eskandari, J. Hossain, J. G. Zhu, "Challenges, advances and future trends in AC microgrid protection", *Renewable and Sustainable Energy Reviews*, vol. 178, p. 113228, 2023.

Energy Certificates. Still, due to smaller size and export limitations from network operators, the PV systems have negligible impact on the distribution system. Most PV systems are sized according to load requirements to consume power produced on-site and export limited power to the grid.

1.1.1 Protection

Electrical power protection is an important aspect of the electricity network as it provides safety from shocks for humans and protects equipment from faults. An essential feature of any protection scheme is to sensitively identify faults and quickly segregate them to prevent other zones and equipment from getting affected and provide a reliable power supply to the customers instead of a grid-wide blackout.

Most distribution networks at the primary and secondary levels are radial, offering simpler fault protection and relay coordination. Protection devices in existing DNs consist of non-directional overcurrent (OC) protective relays, reclosers, fuses, and sectionalisers [6]. Typically, a recloser or an OC relay is installed at the distribution substation, and both use a circuit breaker (CB) to interrupt the fault current (FC). Primary protection for the lateral loads is provided by fuses, while OC relays and reclosers provide backup protection. Additional protection, usually DP, is required for the transformers. Sectionalisers are combined with breakers or reclosers and are designed to operate after a fixed number of breaker operations to isolate a section during faults. Different protection zones in existing DN are shown in Fig. 1.1.

The existing protection system is designed based on three assumptions. Firstly, the FC magnitude is many times larger than the nominal load current. Next, the FC magnitude is inversely proportional to the impedance between the fault and the source and thus varies with the fault location in the network. Lastly, the FC flows in one direction from the generator towards the fault due to the radial layout [7].

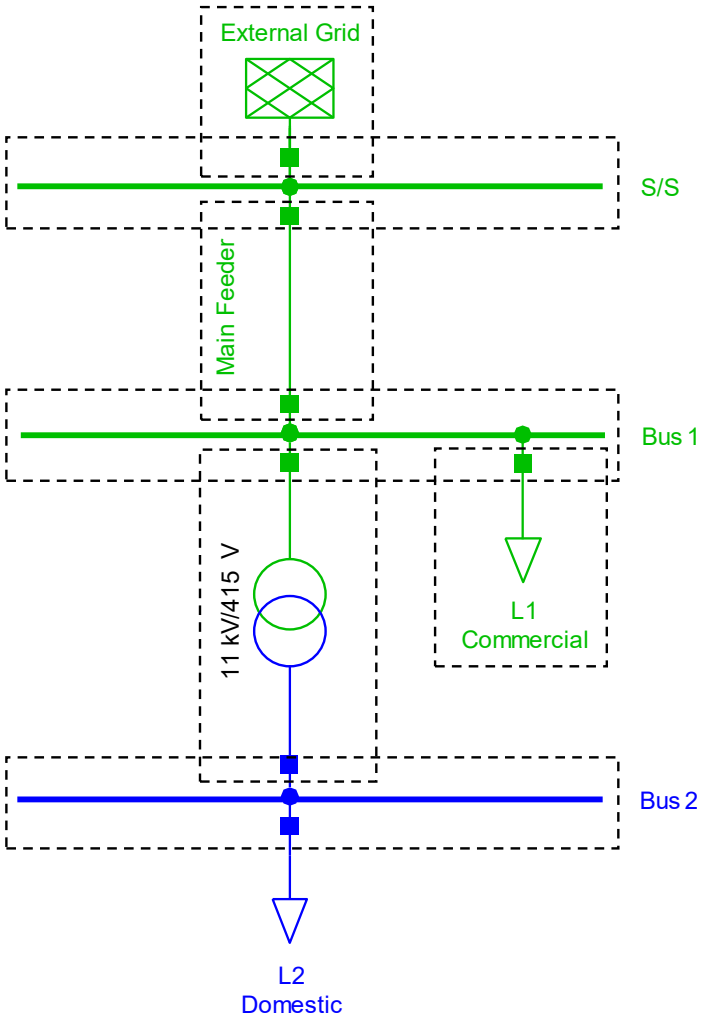

Figure 1.1: Protection zones in passive DN

1.1.2 Effects of Increased DG Penetration on Existing Protection Schemes

As mentioned above, currently, OC protection is frequently used in DNs. OC relay settings are preset to detect the fault and coordinate with other relays. With the significant penetration of DGs in DN, protection discrimination will fail, causing nuisance tripping or failure to trip. This is because OC protection for phase and earth faults employing inverse definite minimum time (IDMT) curves is commonly implemented for coordination between devices. This technique is suitable for the passive radial system, but such protection will not function correctly in a dynamic system with varying power and loads unless regularly reconfigured. Coordinating reclosers in the DN with embedded DGs brings further difficulty. Although DG penetration

is small at present, to ensure that the anti-islanding protection can function, a recloser must remain open for an extended period, but enough to ensure minimum interruption faced by users [8]. This coordination process becomes even more complex with installing fuses and sectionalisers in the DN. To avoid replacing the fuse, reclosers should be coordinated with fuses to isolate before the fuse is blown as the fault is detected. This is known as fuse-saving protection scheme (PS) [9]. Temporary faults will most likely be cleared before the first reclose.

On the other hand, the fuse will blow faster before the recloser trips if the fault is permanent. Therefore, a couple of different IDMT curves are used for recloser-fuse coordination. For temporary faults with DG presence, there is a greater chance that a fuse will blow before the recloser with the fast IDMT curve trips [10] due to FC provided by DGs. Moreover, due to the continued FC provided by local DGs, the operation of sectionalisers will also be affected, as they may fail to detect an upstream CB operation. Coordination failure of any of these devices due to the presence of DG will compromise the whole DN reliability.

In addition to the limitations mentioned, anti-islanding protection currently prevents unintentional islanding in DNs by disconnecting embedded DG supplies in the absence of utility dispatched generation. The reason is to provide safety to humans, restore the faulty network and avoid non-synchronised reconnection to the grid [11]. Under Australian Standard 4777.1:2016, an active DN should provide anti-islanding protection incorporating active anti-islanding protection such as varying output power, frequency shifting, current injection, and frequency instability. It should also offer passive anti-islanding protection, including under/over frequency and voltage protection. Additional protection function such as phase balancing is also required if not included in the inverters [12]. A simple active DN is shown in Fig. 1.2.

Hence, with the growth of various DG sources, bidirectional power flow will increase, and the existing conventional protection methods intended for passive radial distribution networks will eventually become redundant. Therefore, there is a need to develop new protection schemes, enabling maximum benefit from renewable energy sources. Moreover, the microgrid concept can solve many of the problems associated with the protection of existing DN and active DNs.

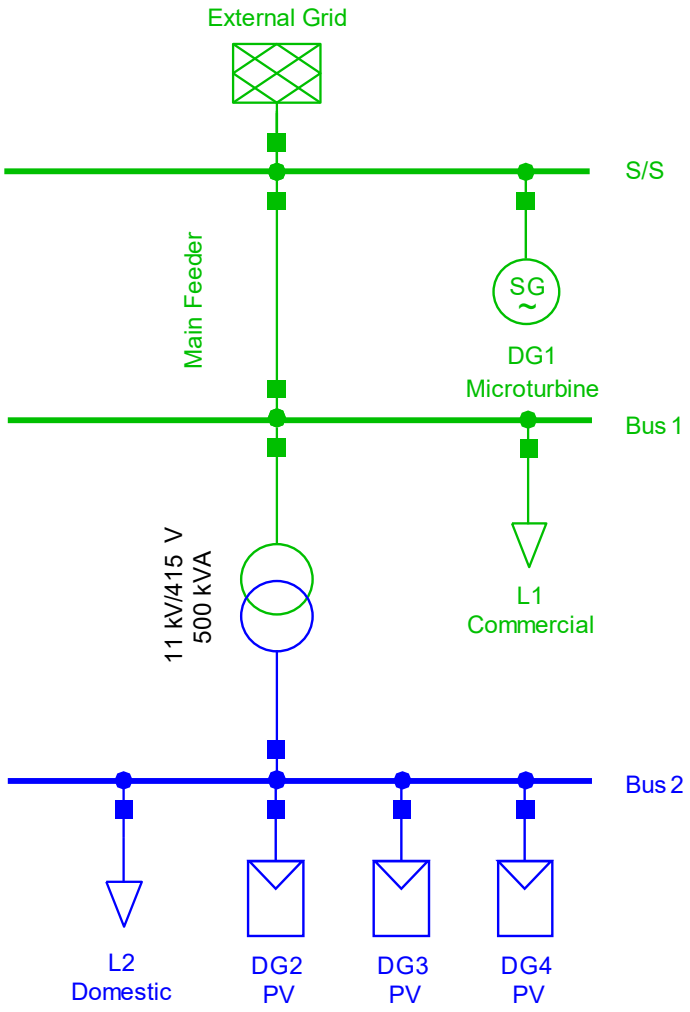

Figure 1.2: Active DN

1.1.3 The Microgrid Concept

According to the Australian Energy Market Commission, DG refers to small generation systems located on the energy user's side of the meter [13]. Many DGs, including both renewable and non-renewable sources such as photovoltaic, microturbines, synchronous generators, and others, are being connected to the DNs and will continue to grow in numbers to eventually form a local micro power system, also known as the microgrid.

A microgrid is a low-voltage controllable distribution system within a defined boundary that consists of DGs, dominated by renewable energy sources, load, and storage devices, all connected [14] as demonstrated in Fig. 1.3. It is capable of meeting customer power demands independently in an autonomous mode when disconnected from the macro grid or main grid

(MG) due to disturbances like faults, frequency drops, or voltage sags [15, 16, 17], while also providing necessary protection and control when connected to the MG [18]. This enables maximum benefit from DGs. Besides improving the resilience of power systems and reliability by reducing the load on the MG during peak demand [19], the operational and maintenance cost of large generator units will be reduced, bringing down a high generation and distribution cost. Large-scale power outages can also be prevented when the MG gets disconnected, which is currently not possible due to anti-islanding protection.

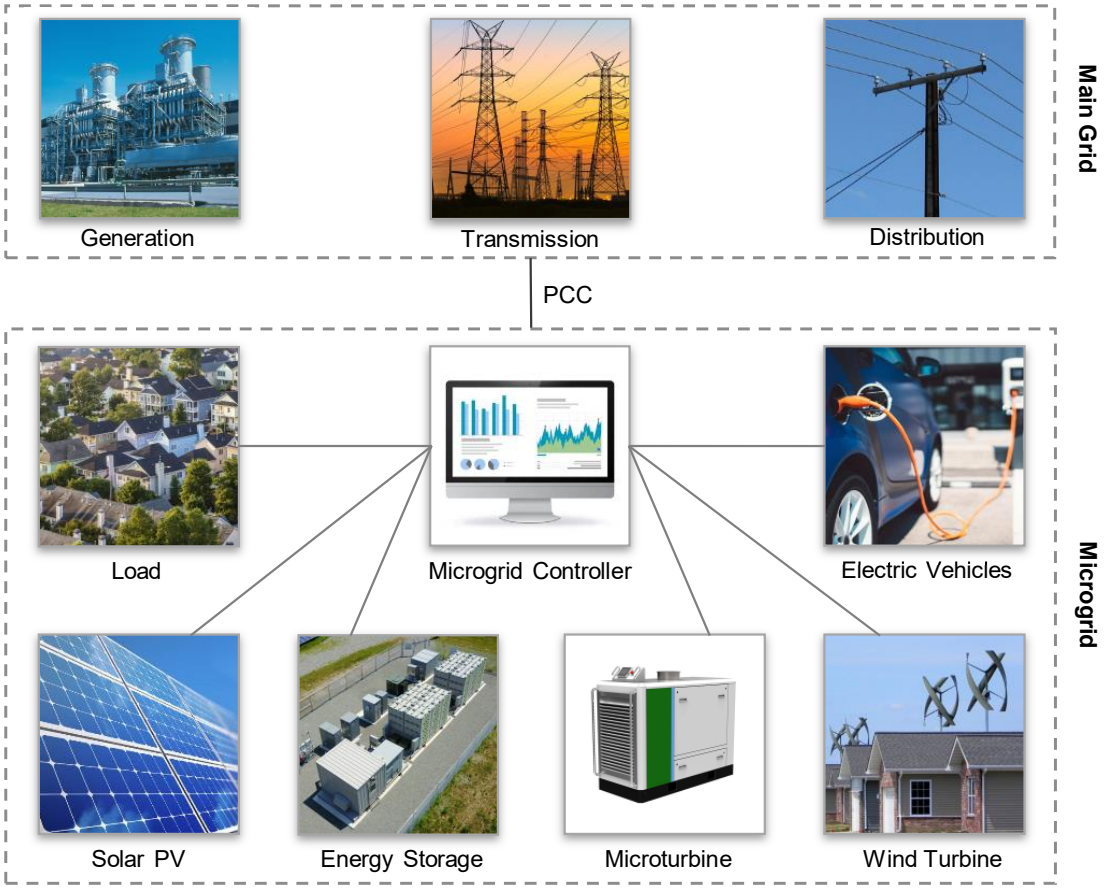

Figure 1.3: Typical microgrid schematic

Most microgrids comprise a three-phase AC common bus architecture for supplying or absorbing power at the point of common coupling (PCC) [20]. This is because transmission, distribution, and transformation of AC voltage are easier and stable voltage can be attained by reactive power control. Also, most loads in the present distribution system are AC [19]. Nevertheless, DC and AC/DC hybrid microgrids have been proposed to decrease power conversion losses. Although

DC microgrids have shown the potential to improve system efficiency by feeding the growing DC loads locally, without conversion, the absence of effective PS is a significant problem in implementing large-scale DC systems. AC system protection cannot be applied to DC systems because DC currents and voltages do not have inherent zero-crossing. Additionally, DC FC can rapidly reach dangerous levels [21]. On the other hand, in a hybrid microgrid, both DC and AC power distribution is used to avoid losses caused by the conversion of power from DC to AC for AC appliances and again from AC to DC for DC appliances [22, 23], which will bring new complications to microgrid protection, and control [24, 25]. Considering the limitations of DC and hybrid microgrids and the benefits offered by AC systems, this research is focused on AC microgrid protection.

An AC system can have asymmetrical and symmetrical faults. The most common type of unsymmetrical faults is a line-to-ground (LG) fault, accounting for 65 to 70 % of all faults, followed by line-to-line-to-ground (LLG) faults that occur around 15 to 20 % of the time, while line-toline (LL) faults make up 5 to 10 % [26]. Symmetrical faults, line-to-line-to-line (LLL) and line-to-line-to-line-to-ground (LLLG) are rare but the most severe of all electrical faults [27]. An effective and robust microgrid protection technique should protect the microgrid against all fault types in both modes under different network topologies and be financially viable.

1.1.4 Multi-Agent System and Supervised Machine Learning

In artificial intelligence, an agent or intelligent agent is a self-governing entity that includes hardware and software. It can decide its actions based on experience and information it perceives. A multi-agent system (MAS) is a computerised system comprising multiple intelligent agents that interact with each other to complete an action within an environment. Applying supervised machine learning (SML) techniques to MAS will improve the decision-making process and aid in adapting to the dynamic changes with the microgrid.

1.2 Research Methodology

1.2.1 Aims

The aims of the project are to:

1. Develop detailed models of grid-connected AC microgrid with multiple DG sources and topologies.

2. Develop a protection method to detect and classify all major faults under varying operational conditions.

3. Validate the efficiency of the proposed method.

1.2.2 Objectives

The objectives of the project are to:

1. Develop comprehensive models of radial and meshed microgrids comprising inverter interfaced distributed generation (IIDG), synchronous-based DGs, and different load profiles.

2. Develop an intelligent protection scheme that can detect symmetrical and unsymmetrical faults, classify fault types with faulted phase identification for meshed and radial topologies, for both modes of microgrid operation, different fault resistances, inception angles, and at various lines and locations along the lines.

3. Formulate and apply new feature extraction techniques and investigate the suitability of feature extraction methods not commonly used for microgrid fault detection and classification.

4. Evaluate the performance of the proposed intelligent protection scheme for AC microgrids under varying operational conditions, using unseen data for making predictions.

1.2.3 Significance

A detailed model of the microgrid is required (aim 1) for fault analysis in a commercially viable simulation tool (objective 1).

The core requirement for implementing microgrids is to develop a protection scheme that can detect and classify (aim 2) unsymmetrical and symmetrical faults. New approaches such as SML, HDL and MAS can aid in fast detection and isolation of different faults by learning to adapt to changes within the microgrid (objective 2). New feature extraction (FE) techniques will assist in training the SML algorithms (objective 3).

To check the robustness of the proposed protection scheme for sensitively detecting the faults and quickly segregating them, verification of the results will demonstrate the practicality of the proposed method (aim 3). Comprehensive simulations will be carried out to validate the protection scheme (objective 4).

1.2.4 Research Methods Chosen

This research employs a mixed-methods approach, integrating quantitative and qualitative methods to address the protection challenges in microgrids comprehensively. Quantitative methods were chosen for their ability to handle large datasets and perform statistical analysis, which is crucial for training and validating machine learning (ML) and deep learning (DL) models. Qualitative methods complemented this by providing a deeper understanding of the microgrid systems and the operational conditions that influence fault behaviour. Combining both methods ensures a robust and holistic analysis, addressing the complexity of microgrid protection more effectively than using a single method alone.

1.2.5 Method and Software Used for Data Collection and Analysis

Different radial and meshed AC microgrid models were developed to collect fault and no-fault data using Electromagnetic Transient (EMT) simulations. Three extensive datasets were prepared.

DigSilent PowerFactory is ideal for EMT simulation of microgrids, due to:

- Pre-built library of power system components: PowerFactory offers a comprehensive library of pre-built models for generators, transformers, lines, and other power system elements. This saves significant time and effort in model development compared to building everything from scratch in MATLAB.
- Focus on power system analysis: PowerFactory is specifically designed for power system analysis, with features like fault analysis, protection system coordination, and power flow studies. This makes it user-friendly and efficient for tasks related to power system simulations.
- Robust data collection: PowerFactory allows easy data collection for machine learning training, including voltages, currents, and many different signals.

MATLAB provides more flexibility in modelling custom components and control systems. It's valuable for:

- Advanced control system design: MATLAB's Simulink e allows the design and implementation of complex control systems for the microgrid.
- Fault and no-fault data collection: While PowerFactory excels in EMT simulations, MATLAB offers detailed control over fault scenarios for data collection specific to fault conditions.
- Machine Learning and Deep Learning: MATLAB is a well-established platform for training and testing various machine learning and deep learning algorithms.

AnyLogic specializes in Multi-Agent System (MAS) simulations. It's helpful for:

- Modelling agent behaviour: AnyLogic allows the modelling of the behaviour of individual

agents (e.g., distributed generators, energy storage systems) within the microgrid and analyze their interactions.

- Agent-based decision-making: Agents' decision-making can be simulated based on local information and interactions with other agents, providing valuable insights into the overall behaviour of the microgrid.

By combining these tools, I was able to leverage the strengths of each:

- PowerFactory for robust and efficient power system simulations with rich data collection.
- MATLAB is used for flexible modelling, fault scenario control, and training and testing ML and DL algorithms.
- AnyLogic for in-depth analysis of agent interactions within the microgrid.

1.2.6 Difficulties Encountered

Several challenges were encountered during data collection and analysis, including the limited availability of real-world fault data and the complexity of feature extraction. These issues were addressed by developing comprehensive simulation models to generate sufficient fault and no-fault data and formulating new feature extraction techniques. Additionally, integrating various ML algorithms and the MAS framework required extensive validation and testing to ensure reliability and accuracy, which was achieved through iterative improvements and rigorous evaluation with unseen data.

1.2.7 Evaluation of Research

The results were conclusive, demonstrating that the proposed intelligent protection scheme significantly outperformed previous methods. The choice of a mixed-methods approach proved effective in practice, providing a comprehensive understanding of microgrid fault behaviour and enabling the development of a robust protection scheme. The integration of ML, DL, and MAS frameworks enhanced the coordination and adaptive protection, contributing to the overall success and reliability of the scheme in various fault scenarios.

1.3 Summary of Research Contribution

This research develops comprehensive models for radial and meshed AC microgrids to collect fault and no-fault data, creating three extensive datasets for training 35 supervised ML and various DL algorithms. The largest dataset comprises 16,000 fault cases and 432 no-fault cases for a standard IEC meshed microgrid model. Innovative feature extraction techniques, such as Peaks Metric and Max Factor, are formulated and applied alongside investigating eight other FE methods not commonly used for microgrid fault detection and classification. Various feature ranking techniques are employed to reduce the number of predictors. A novel hybrid deep Convolutional neural network (CNN) and deep long short-term memory (LSTM) based protection method is developed, and its efficacy is validated using unseen data. A MAS framework has also been established to integrate ML and DL models, enhancing coordination, fast segregation, and adaptive protection. This intelligent protection scheme effectively detects symmetrical and unsymmetrical faults, classifies fault types, and identifies faulted phases in radial and meshed microgrids, providing robust primary and backup protection, improving system resilience, and offering economic benefits through accurate fault handling and prevention of unnecessary tripping of healthy phases.

1.4 Thesis Organisation

The report is organised into different chapters as follows:

- *Chapter 2*: This chapter presents a comprehensive literature review to identify the research gap. The focus is on recently proposed methods using modern techniques, besides critically reviewing other proposed methods.

- *Chapter 3*: This chapter starts with the shortcomings of Wavelet transform-based feature extraction, and then the application of Principal component analysis is proposed. The main focus of the chapter is the classification of bolted, low, and high-impedance LG faults using SML.

- *Chapter 4*: In this chapter, SML is used to detect and classify faults in a radial AC microgrid. New feature extraction techniques are formulated and applied, and various feature selection methods are used to find the model with the highest prediction accuracy.
- *Chapter 5*: This chapter presents a novel hybrid deep learning approach using deep CNN and deep LSTM for fault detection and fault type classification in radial and meshed AC microgrids for various operating conditions.
- *Chapter 6*: A protection scheme for AC microgrids based on MAS with SML, including HDL for detecting and classifying symmetrical and unsymmetrical faults, developed in earlier chapters, is presented in this chapter.
- *Chapter 7*: Conclusion, research contribution, and future work are given in the final chapter.

Chapter 2

Literature Review

2.1 Challenges Associated with Microgrid Implementation

Although microgrid offers many benefits, several challenges must be overcome before practical implementation.

2.1.1 Protection Challenges Associated with Microgrid

Microgrid protection is an unavoidable problem. The core aspects of any protection system include sensitivity, which means that the protection system can detect even the most minor abnormal conditions above a threshold level. The second is selectivity, i.e., only the faulted part of the network is isolated. The fault does not affect other zones and equipment or result in a complete system shutdown. Another is reliability, which is the assurance of correct operation of the protection system whenever required [28]. Other important aspects include the speed of operation, simplicity, and cost-effectiveness [29]. All these features are necessary for a microgrid.

Additionally, the protection must be adaptive to distinguish between system energisation and fault conditions for a fast trip in the latter situation and riding through the former [30]. A

This chapter is based on the work published in M. Uzair, L. Li, M. Eskandari, J. Hossain, J. G. Zhu, "Challenges, advances and future trends in AC microgrid protection", *Renewable and Sustainable Energy Reviews*, vol. 178, p. 113228, 2023.

major obstacle to effectively implementing microgrids is achieving the correct sensitivity and selectivity [31]. Moreover, in future grids, precise tripping of only the faulted phase will be required to improve supply reliability and increase financial benefits. Accurate fault type classification (FTC) and faulted phase (FP) identification will be required to achieve this [32]. The main protection challenges in a microgrid can be further subdivided as follows.

FC Direction and Dynamic Topology

Most DNs at the primary and secondary level are radial as they offer more straightforward fault protection and relay coordination [33]. In a dynamic environment where load and DGs regularly change status, coordination between fault protection devices during autonomous mode can be affected [34]. Moreover, ring main and mesh distribution systems will supersede radial systems in the future [35], and the topology of microgrids may constantly change, resulting in variable power flow and change in the direction of FC. Hence, new protection techniques that can adapt accordingly will be required.

Varying Fault Current

The intermittent nature of renewable energy sources causes FC levels in a microgrid to fluctuate [36]. The variation in FC also depends on the network topology, location, type and number of DGs, grid impedance and mode of operation. FC is comparably lower in an islanded microgrid with IIDGs because power electronic interfaces between the microgrid and IIDG inherently limit the output current for protecting semiconductor components [37]. In contrast, FC provided by the MG is usually in kilo amps [30]. Additionally, when the microgrid is connected to the MG, the combined fault contribution of numerous DGs can change short circuit (SC) levels [38], resulting in relay miscoordination. Fault levels may also vary within the microgrid as IIDGs are reported to contribute FC around 1.5 to 2 times their rated currents [39, 40]. In comparison, induction and synchronous machine-based DGs can provide FC of 5 to 10 times their rated currents [41]. This difference between the FCs in both modes and different DG types poses the biggest challenge to microgrid protection as it can lead to protection blinding or nuisance tripping.

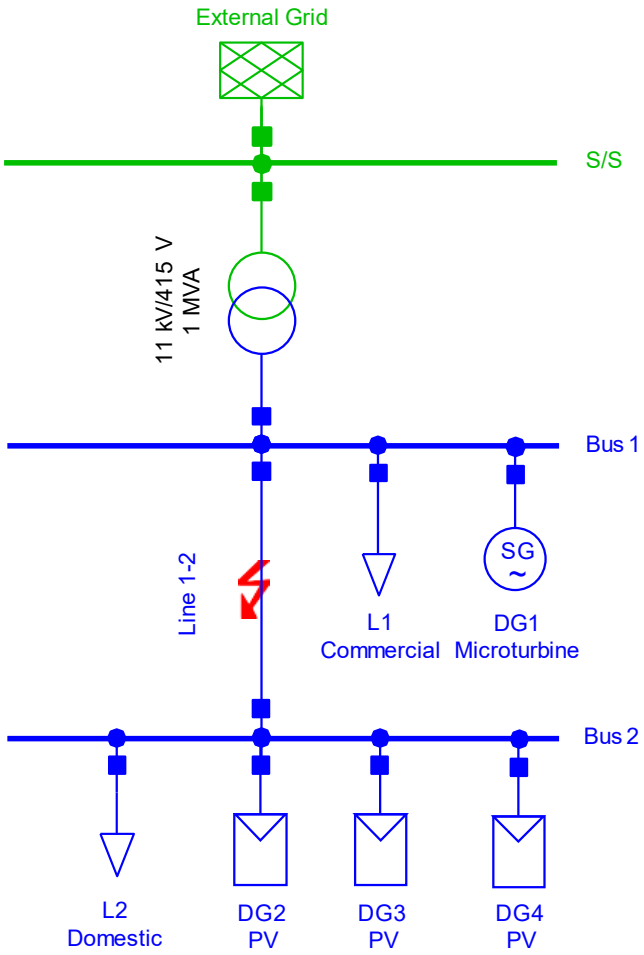

Figure 2.1: Simple AC microgrid

A simple microgrid is shown in Fig. 2.1, operating at 50 Hz and 415 V. A 600 kVA synchronous generator-based microturbine (SGM) and 400 kW commercial load are connected to Bus 1, and three 300 kVA PV IIDGs and 200 kW residential load are connected to Bus 2. When DGs are disconnected, an LG fault on phase A at 50% of a 2km line 1-2 results in a 3.305 kA SC current. If all the microgrid is linked to the MG while all the DGs are connected, the SC current increases to 4.052 kA, while it drops to 2.840 kA when all the DGs are connected in islanded mode. For the microgrid shown in Fig. 2.1, SGM has a higher merit order in islanded operation. The FC will further reduce if only IIDGs provide the power in islanded mode. This shows the FC in a microgrid can vary with varying operating conditions.

Low Voltage Ride-through

Low voltage ride-through (LVRT), also referred to as fault ride-through [42], is the ability of DGs, specifically wind and PV systems, to stay connected during short intervals of fault conditions and low voltage to avoid cascading failures resulting in widespread power outages. The existing protection system for DG sources requires modification to ensure that the microgrid meets LVRT abilities [43]. There is also a need to reconsider the time curve that defines fault ride-through requirement for the microgrid to cater to protective relay response time at the distribution level [36].

2.1.2 Control Methodology and Load Management

In grid-connected mode, the MG acts as a buffer, regulating the frequency, voltage and supplying unbalanced power requirements. In autonomous mode, managing these requirements for steady operation becomes challenging [44]. Besides voltage and frequency control, load forecasting, load management and active and reactive power control become difficult [35] due to the unpredictable nature of renewable energy sources and can result in an imbalance between power generated and load requirements [24]. Additionally, the hierarchical control scheme in microgrids consisting of primary, secondary, and tertiary levels may affect the protection system. Furthermore, with the rapid decline in the usage of rotating machines in future microgrids, the power system will have falling inertia and related dynamic frequency stability problems with sudden load variations. If the equipment fails suddenly, the system will have less time to recover. This will also limit the significant penetration of renewable energy sources to the microgrid [45, 30]. IIDG fault response heavily depends on its control method, current limiting approach and the reference frame in which they have been implemented. Lastly, connecting different types of DGs and across other vendors, control optimisation may become problematic [44].

2.1.3 Communication and Cybersecurity

For fast fault detection (FD) and coordination between protection devices and DG source dispatch and optimisation, coordination between DGs, local and central controllers, high-speed communication will be required for the future grid. This will increase the system cost. Moreover, with the advent of MAS and intelligent electronic devices (IED), standardisation of communication channel will be critical. To attain protection settings interoperability for IEDs from different vendors, a method to convert the original protection setting files to universally readable setting files will be required [46]. In [47], the authors have concluded that to achieve a standardised communication channel, there is a need to use the IEC 61850 protocol and its extensions when modelling communication infrastructure for the microgrid [48]. With increased dependency on communication for sophisticated protection and control of microgrids, a significant cybersecurity threat may arise due to natural catastrophes, human mistakes or attacks by hackers and can cause wide-scale power outages. Susceptibilities include denial of service, unauthorised access, and modification of IEDs and SCADA systems [49]. There are also concerns about communication latency, customer privacy and data protection. [50] highlighted the importance of a robust real-time monitoring setup that attains desired performance and offers security from cyber-attacks on the system.

2.2 Key Protection Schemes for The Microgrid Concept

Major PS proposed for AC microgrids are critically reviewed in this section, focusing on analysing the recently proposed protection approaches using modern techniques. A graphical illustration of the significant protection approaches reviewed in this chapter is shown in Fig. 2.2.

2.2.1 Directional OC Protection

To overcome the bidirectional power flow challenge, a communication-based PS using directional OC relays in place of reclosers, supported by blocking and inter-tripping protection, is proposed in [51]. This method assures protection selectivity, irrespective of whether the DGs

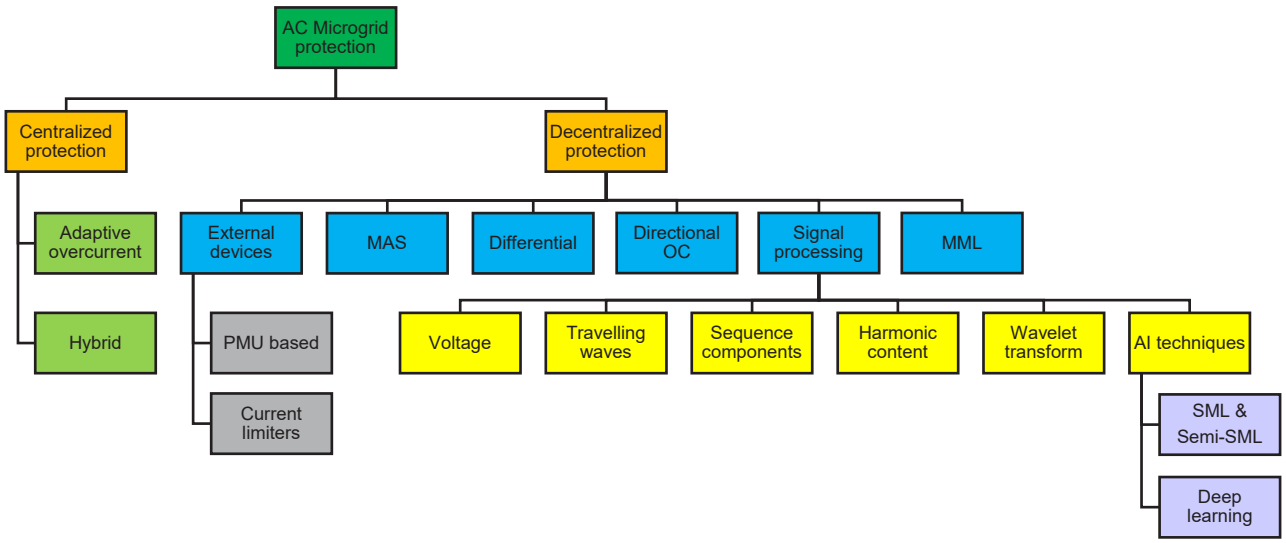

Figure 2.2: Microgrid protection methods proposed in the literature

are connected or disconnected. However, this technique will be ineffective with a fixed plug setting multiplier and time dial setting due to dynamic changes in fault levels within the microgrid [52]. Moreover, the output impedance of synchronous machines is inductive, whereas IIDG units have variable output impedance based on design and controller. Additionally, IIDGs show unpredictable output impedance in the current limiting mode, which restricts the use of conventional directional elements to protect microgrids [53, 54].

2.2.2 Adaptive OC Protection

Adaptive OC protection (AP) strategy attempts to overcome conventional and directional OC PS limitations. In this approach, relay settings are modified using an online system; when the network topology is modified, generation capacity changes or when the microgrid changes operational mode.

Two pre-defined setting groups, one for each mode of microgrid operation, obtained through several transient simulations of three-phase and single-phase faults are proposed in [55]. In contrast, three different settings for numerical OC relays, calculated offline to deal with the low value of SC currents in the autonomous mode, are suggested in [56]. In this approach, the status of the main switch at PCC and a CB dividing the microgrid determines the suitable

setting group. Initially, the relays are set to setting group A when the microgrid is connected to the MG. When it goes to the autonomous operation, and there is an upstream fault from the mid-point CB, relay settings are changed to group B. On the other hand, in the autonomous mode, when there is a downstream fault from the mid-point CB, relay settings are changed to group C. Schematic of a modified network diagram with the location of CBs is shown in Fig. 2.3. Likewise, an AP approach where the IEDs select one of eight setting groups by monitoring the status of CBs that informs about changes in topology and operational mode of the microgrid is presented in [57].

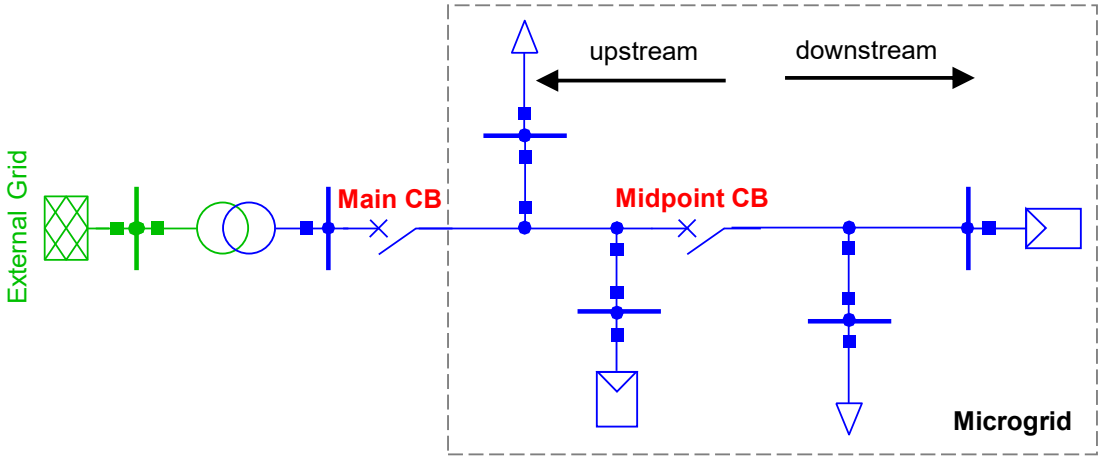

Figure 2.3: Implementation of AP scheme with three setting groups

Using pre-calculated settings is not a reliable solution for practical implementation because it requires finding all the possible configurations for correct operation [58]. Moreover, pre-calculated protection setting groups depend on simulation models with known generation capacity and topology, unlike the dynamic environment of microgrids. An active network will require continuous and tedious simulations and calculations to update settings. Also, to optimise the adaptive operation, the offline calculations need to include scenarios like symmetrical and asymmetrical faults, different DG types, and distribution systems other than radial [58].

To solve this problem, an AP scheme with online calculations based on zero sequence and quadrature components of fault current for detecting faults in microgrids with a low X/R ratio is proposed in [59]. The approach considers the mode of operation and status of DGs connected to adapt to the new settings. Contrary to other methods that consider DG fault contribution

and microgrid mode, recloser misoperation is used to calculate new pickup settings for the OC relay in an AP method, proffered in [60].

High-speed communication infrastructure is required to switch between pre-calculated protection setting groups and online setting calculations, leading to increased costs. Other downsides of AP schemes include vulnerability to DG frequency and voltage ride-through. Additionally, most AP schemes only consider the mode of operation and status of DGs, whereas FC is dependent on source impedance, fault impedance, line impedance and load impedance. Hence, further consideration needs to be given for calculating new settings.

2.2.3 Differential Protection

In the differential protection (DP) scheme, currents on both sides of the protected zone, either leaving or entering, are commonly compared. If the difference exceeds a predetermined value, the relay is operated to segregate the zone from other connected lines [34]. A current DP for islanded MV microgrids is put forward in [61]. This scheme has high sensitivity and efficient protection discrimination. A downside of using only current signals is that the PS shows incompetency for the unbalanced load [62]. To resolve this problem, DP based on impedance phase angle [63], positive sequence power angle [64], zero-sequence current [65] and zero-sequence voltages [66] have been employed.

A significant limitation of this PS is the very high implementation cost due to the requirement of a separate communication network and installation of relays at each node of a protection zone in the DN when applied to the microgrid concept [67].

2.2.4 Hybrid protection

A unique AP and DP hybrid PS is proposed in [68] to take advantage of both methods. For financial viability, AP is the default PS, and the DP scheme is implemented for susceptible areas with critical load and the areas where a high FC is expected. AP also acts as a backup for DP in case of a communication breakdown. AP and DP Hybrid protection zones are shown in Fig. 2.4.

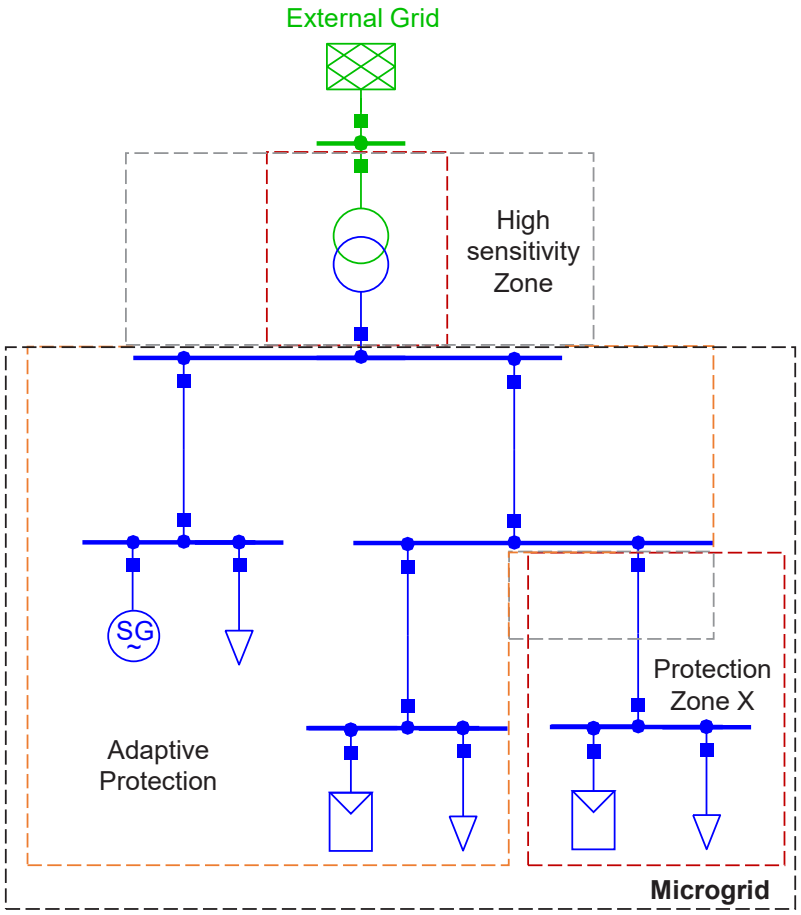

Figure 2.4: AP and DP hybrid protection zones

The techniques consider the number of DGs connected and fault direction to calculate tripping settings but do not include load contribution to the fault current. Besides, this technique heavily depends on centralised processing units and communication lines. Network latency may cause unexpected behaviour; therefore, real-time experimental investigation with a communication network is needed to verify the feasibility of this method.

Another hybrid PS is proposed in [69]. The approach combines phasor-based and transient-based protection to improve protection speed and sensitivity. It is also dependent on the communication network. Unlike many protection methods dependent on communication lines to measure and transform signals, a communication-less PS is proposed in [70]. The strategy uses a hybrid tripping characteristic, combining IEEE standard inverse-time characteristic for OC relay [71] and IEC standard under-voltage relay characteristic [72] to differentiate between

overloading and low FC. Fixed grading for relays is used to avoid communication, and since the setting remains the same in both modes, the PS also becomes independent of the mode of operation. Though a fixed grading margin makes selecting relay settings easier and more suitable at high FCs, it may not be ideal for lower FCs where relay operating times are longer. Additionally, coordination cannot be achieved without relay-to-relay grading, a requirement in the modern power system [73, 74].

2.2.5 Fault Current Limiters

FC is fairly low in autonomous mode, but in grid-connected mode, the DG sources contribute to the FC that alters the SC levels, affecting the coordination of protective relays [75]. Fault current limiters (FCL) can overcome this problem and is considered one of the promising solutions for microgrid protection [76]. They are usually placed in series with DGs to vary impedance depending on the normal or faulty condition. They are also installed near PCC to limit FC contribution from the grid towards the microgrid, and vice versa [77]. FCLs can be inductive [78], solid-state [79], super- or non superconducting [80]. Also, unidirectional [79], and bidirectional [81] FCLs have been employed. Locations of placing FCL can impact the relay operation. Optimal settings for directional FCLs are projected in [82]. In contrast, various possible locations for FCL are analysed in [83]. The results show that the bus with DG is the optimal location to place FCL for efficient relay operation. On the other hand, [81] suggested placing it near PCC, as shown in Fig. 2.5.

FCL is a capable solution, but there are a few associated challenges. The relay settings must be optimised for optimal FCL location, different DGs, normal operation and fault conditions. For normal conditions, impedance settings should be such that losses are minimised, while for faults, it should be high enough to limit the FC [84]. Additionally, most FCLs limit current in both directions, which may affect adaptive OC relay operation and relay coordination [85]. Installing numerous FCLs is not financially viable, and most importantly, the optimal relay settings and FCL location need to be re-calculated for changes in a microgrid.

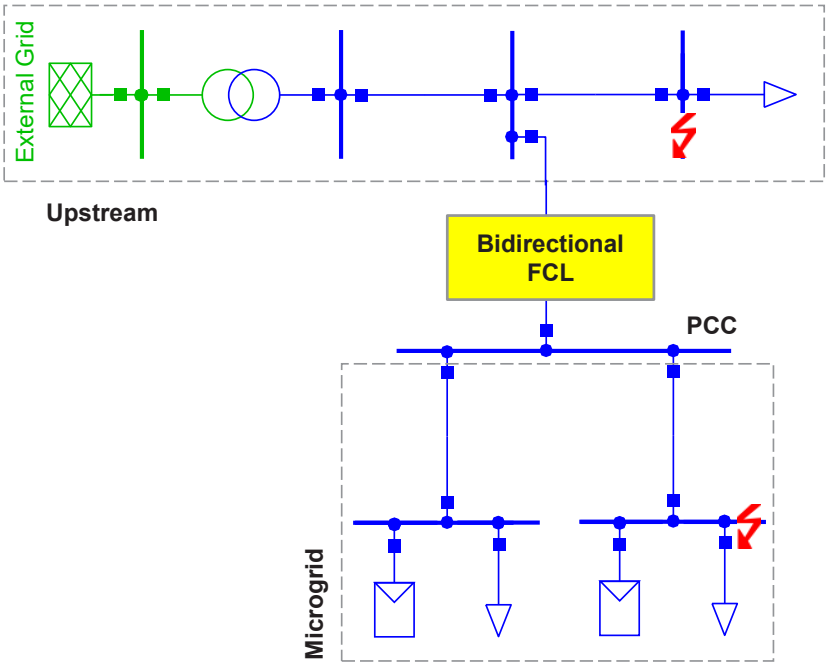

Figure 2.5: Bidirectional non-superconducting FCL location

2.2.6 Voltage Based Protection

A novel PS that converts the three-phase AC voltages into DC signals through the dq0 transformation to provide a disturbance signal for identifying the existence of SC fault is presented in [86]. Some major drawbacks of this method include insensitivity to grid-connected mode and the inability to detect high impedance and symmetrical faults. Likewise, a PS using a new voltage-based relay is presented in [87]. The pre- and post-fault active power difference and sensitivity calculations of voltage measurements are used for relay operation. Only resistive loads that do not consume any reactive power are considered in this work. Further investigation with inductive, capacitive and combination different load types is required to examine the performance of the PS.

2.2.7 Travelling Waves Based Protection

Transients are produced at a fault instance on a power line at the fault location (FL). They circulate along the line as travelling waves in both directions [88]. These travelling waves propagate at ultrafast speeds and can quickly offer information on FL. This is the basis for

travelling waves (TW) based methods, which are primarily used to locate the fault in power lines, commonly in transmission lines and recently in DN. There aren't many methods proposed to detect faults in an AC microgrid using TW-based methods.

TW-based FL can be mainly divided into single-terminal and two-terminal techniques. The single-terminal TW-based method identifies the location of the fault by comparing the time between the first TW and the reflected wave arriving at the selected terminal [89]. A technique using single-end data to locate the fault in a transmission line is proposed in [90]. The polarity of the voltage and current TW identifies the fault direction. Conversely, a PS for a microgrid with IIDGs based on the time features and polarity of the first current TW is developed in [91]. When a fault occurs on line AB, as shown in Fig. 2.6, the first two wavefronts have the same polarities, or else they are opposite. A limitation of this method is the uncertainty of the fault inception angle. Protection performance may be affected if the fault occurs when the voltage is not close to the peak. The major drawback of the single-terminal TW-based method is that it is difficult to differentiate the two wavefronts having similar energy levels, resulting in erroneous FL. Additionally, it becomes difficult to detect the reflected wave in the DN with multiple branches [92]. On the other hand, the main advantage is its lower cost as it doesn't require a communication line [93, 94].

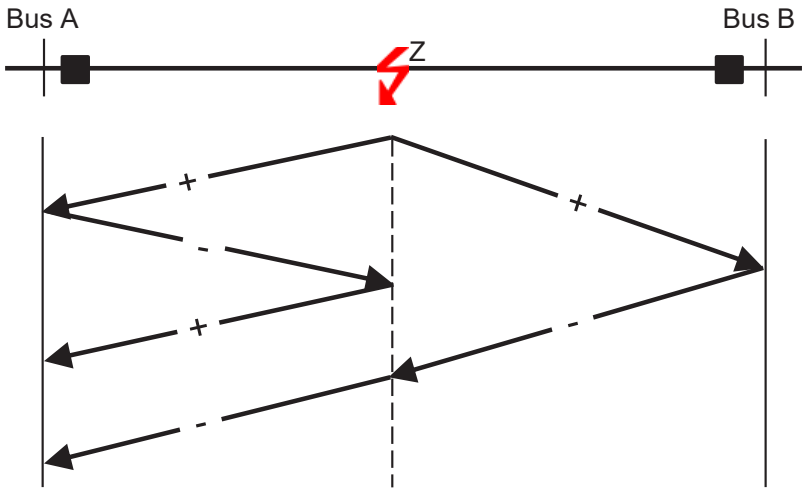

Figure 2.6: Lattice diagram of travelling waves

To address the above limitations, [95] proposed a modified mathematical morphology filter

technique using polarities of TW from both feeders' ends. A two-terminal TW-based method uses only the first arrival wavefront on either end. However, it costs significantly more compared to the single-terminal method due to the requirement of a communication channel [96, 97].

At present, most FL approaches using TW are significantly affected by errors in the arrival time. To remove this limitation, a multi-terminal TW-based FL technique using residual clustering is proposed in [98] for active DNs. In the same way, [99] has proposed a fault detection method using the frequency of TW reflections, contrary to most TW-based methods using the arrival time of TW reflections. Also, a TW-based fault detection and location method for DN using vertex cover and metric dimension is proposed in [100]. Likewise, an approach to locating the fault in a DN, based on calculating the reclosing superimposed TWs, is proposed in [101]. Differing from commonly used TW-based methods for FL, recently, a technique to identify unintentional islanding using TW reflection and refraction coefficient has been proposed in [102].

A primary consideration using the TW-based method is the signal processing method for high-frequency non-stationary TW signals. Various forms of Fourier transforms are not suitable [103]. WT is considered an appropriate technique [104] but is dependent on the selection of the mother wavelet [105]. Although TW-based protection functions well for long-distance transmission lines, it encompasses problems for short distribution lines [95] and requires further assessment in future research.

2.2.8 PMU Based Protection

A phasor measurement unit (PMU) provides real-time measurements of amplitude and phase angle of current and voltage, frequency and rate-of-change of frequency. These units are installed on both ends of a section to indicate changes in values above the threshold. A significant shift in phase angle and differences in current and voltage waveforms from the normal condition can exhibit a fault and its location. PMUs have been extensively used in power transmission networks for a long time and have also been deployed for power system protection control and monitoring [106]. A significant drawback of using the transmission system PMUs in microgrid

protection with many DG sources, lines and buses is the very high implementation cost due to the branched network. Even a small section of the network with one DG requires numerous PMUs, as shown in Fig. 2.7.

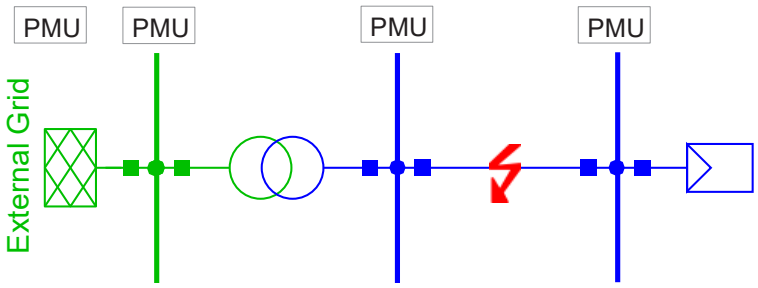

Figure 2.7: Simple network with multiple PMUs

A PS based on PMU for wide-area (WA) phase angle measurement is presented in [107]. The rate-of-change of phase angle difference between voltage phasors at PCC and the bus closest to the fault indicates the presence of a fault. Likewise, a PMU-based integrated impedance angle PS is proposed in [108]. WA positive sequence components of fault current and voltages are obtained by placing PMUs at both ends of the distribution line. The difference in values is used for FD.

Higher accuracy requirements and advancement in signal processing [109] have given way to the development of micro-PMU (μPMU) [110]. Besides lower costs, these are more accurate and have higher measurement resolution than PMUs used before [111]. Table 2.1 compares PMUs and μPMUs.

Table 2.1: Comparison between PMU and μPMU [1, 2, 3]

	PMUs	**μPMUs**
Application	Transmission network	Distribution network
Angle Accuracy	$\pm 1^{\circ}$	$\pm 0.01^{\circ}$
Angle Resolution	0.1°	0.001°
Total Vector Error	$\pm 0.1\%$	$\pm 0.01\%$
Readings/second	10–60	100–240
Cost	High	Low

An adaptive PS based on μPMUs for the microgrid is presented in [112]. It proposes installing multiple μPMUs within a microgrid to detect topology changes. Once any change is identified, primary and backup OC relay settings are reconfigured automatically by an online program. This centralised PS assumes a fast and reliable communication network. Similarly, a μPMU based modified WA protection is proposed in [113]. The revised approach uses the ratio of the sum of voltage phasors measured at each end of the line to the sum of the current phasors flowing in the line for FD. Furthermore, a method based on PMU measurements and modified revised state estimation for detecting FL in an active DN is proposed in [114]. After identifying the faulted zone, residual indices are computed to determine the actual FL. The accuracy decreases for the fault furthest away from the substation in a radial network. Another technique for FL in a microgrid based on μPMU measurements is proposed in [1]. Contrary to commonly used current and voltage signals, voltage phasor and magnitude measurements detect the FL.

A centralised protection scheme for fault detection and abnormal operation identification in a microgrid using μPMUs is proposed in [115]. Synchronised phasor measurements are sent to the central microgrid controller. Clarke transformation is then used to compute the fault coefficient index for fault detection, while abnormality coefficients are calculated to identify abnormal operations. This centralised protection scheme is dependent on the communication network. Network latency may add to processing time.

Similarly, a data-driven method to differentiate measurement anomalies from events in microgrids using μPMUs is proposed in [116]. The changes are detected by comparing the changes in voltage phasor measurements of a μPMU with other μPMUs. This method depends on the defined threshold values to differentiate measurement anomalies from events. On the other hand, to find the suitability of μPMUs for FL in a distribution system, authors of [117] analysed its behaviour by introducing noise to measurements. They found that the accuracy of the traditional impedance method for locating the fault is significantly impacted by μPMU noise. Additionally, the single-ended impedance method is less accurate than the double-ended impedance method under the influence of noise. They also suggested that angle error is critical when high accuracy is required.

PMU and μPMU based techniques are dependent on communication. For comparison, measurements across WA should also be collected in a time-synchronised manner using a common GPS time source [118]. Synchronised phasor measurements can also assist in the loss of mains or islanded mode detection.

2.2.9 Harmonic Content Based Protection

For identifying the FP and location, a methodology based on harmonic content is put forward in [119]. According to the authors, a noticeable variation in 50 Hz fundamental frequency amplitude will occur in the FP compared to unfaulty phases. To locate the fault, it is proposed to calculate total harmonics distortion (THD) of the faulted and un-faulted phase. Likewise, a PS for islanded microgrids with IIDGs based on injecting a percentage of the 5th harmonic to the FC is proposed in [120]. A microprocessor-based digital relay at each section extracts the real-time low-order harmonics employing Fast Fourier transform (FFT) algorithm to detect the fault. The proposed method doesn't require communication between devices, nor is it dependent on high FC magnitude, as long as the current is nearly sinusoidal under normal conditions and the system has only linear loads; otherwise, PS may misoperate.

On the contrary, [121] proposed to use a 3rd harmonic current component to detect high impedance faults regardless of location. The magnitude of the 3rd harmonic is not an adequate fault criterion since the ambient magnitude differs too much over a period of time. While [52] highlighted that the harmonic component-based PS is unable to detect some faults effectively besides introducing latencies due to filtering and algorithm computations. Furthermore, some harmonic component-based PS do not consider transformer connections, especially delta-wye, which can considerably affect the fault voltage and current waveforms.

2.2.10 Sequence Components Based Protection

Many researchers have proposed protection strategies using one or a combination of sequence components. A positive-sequence component-based FD method for radial and meshed DNs is proposed in [122]. It is claimed that this is a unique component, present during all kinds of

faults. When a fault occurs, there is a significant rise in the magnitude of positive-sequence current in the respective section of the microgrid, which can be detected by using PMUs on both ends of every line. The information is passed to a central processing unit that compares before and after fault magnitude for FD. To locate the fault, downstream and upstream Thevenin's equivalent positive-sequence impedances are compared before and after the fault occurrence. PMUs drastically increase the cost, while the centralised system increases processing time.

Conversely, [123] proposed a method to detect earth faults that are among the most frequent faults in any power system. Zero-sequence components are used as their structure in the network remains the same for both modes of microgrid operation. When a fault occurs, there is an apparent voltage dip. The instantaneous voltage is transformed to a DC signal using dq0 transformation and then compared to a set value for FD. Likewise, [124] suggested using zero-sequence components to detect LG faults and negative-sequence components to detect LL faults.

One of the main risks of using negative- and zero-sequence components-based protection methods is that due to the presence of single-phase or unbalanced three-phase loads, these components are also non-zero under normal microgrid operation, making it difficult to distinguish between unbalanced and faulty conditions, which can result in nuisance tripping. In addition, zero-sequence current can not pass distribution transformers with the delta-wye connection. Hence, alternate techniques for protecting balanced and unbalanced systems are required.

2.2.11 Wavelet Transform Protection

Wavelet transform (WT) can overcome the issues related to symmetrical components. It is a technique for analysing intermittent, noisy, aperiodic, transient, and non-stationary signals. In comparison to Fourier and short-time Fourier transform, WT has the benefit of being able to analyse signals in time-frequency domains [125]. For detailed analysis, WT extracts features from the signals. In the high-frequency region, discrete wavelet transform (DWT) has a comparatively low resolution that can be overcome by wavelet packet transform, which offers further decomposition of the signal, allowing it to separate the high-frequency transient com-

ponents [126]. For fault and islanding detection, WT-based techniques are proposed in [127] and [128]. Both approaches have used Daubechies (dB) as mother wavelet (MW). While the latter considered both the positive and zero-sequence components, dB10 and LLG faults, the former only detected LL faults using dB5 and negative-sequence components. DWT is used to decompose the signal once it has been extracted. It is claimed that power quality issues and islanded mode can be detected by identifying the difference in parameters before and after the fault and by comparing them with the threshold values.

FL can also be predicted by subtracting the pre-fault coefficients from post-fault coefficients [127]. Likewise, a method to detect symmetrical and asymmetrical faults in microgrids based on dq0 components is given in [129]. Using WT, one of the dq0 components is filtered, and the desired frequency band is separated. Differences between filtered signal samples are used for FTC. To synthesise and analyse the wavelet filter, a Haar wavelet is used as MW. The algorithm is limited to detecting low-impedance faults, as the variations in DC components of three-phase current make it difficult to detect high-impedance faults. Also, the results are only valid for low sample frequency.

The fundamental drawback of WT-based protection strategies is the selection of optimum MW function. Application of different MWs leads to different results [105, 130, 131] that may lead to misoperation of the protection system. Furthermore, DWT response is significantly influenced by the sampling rate and the fault inception angle. New FE approaches are thus necessary.

DWT response is significantly influenced by the fault inception angle and sampling rate. Hence, new FE techniques are required.

2.2.12 Multi-agent Based Protection

An agent in artificial intelligence (AI) is any software or hardware that is capable of making a decision and taking action autonomously [132]. A MAS is formed when multiple agents with unique goals interact with the environment and each other [133]. The distinctive characteristics of agents are very appropriate for protection operations in a microgrid. The distributed monitoring function is ideal for monitoring local parameters. The autonomous operation can aid

in reducing FD and segregation time. Interaction with other agents is suitable for protection coordination and fast service restoration, while adaptability to changes in the environment can enable the application of the AP scheme [134]. Characteristics of a typical agent are presented in Fig. 2.8.

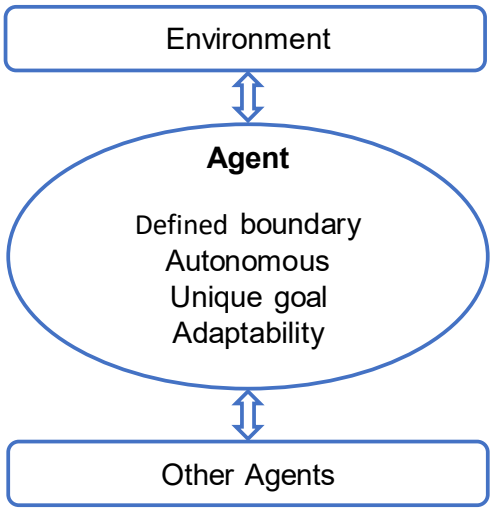

Figure 2.8: Characteristics of an agent

An initial MAS architecture for a large-scale transmission network was proposed in [135], comprising three layers, as shown in Fig. 2.9. Each layer includes various software agents interacting to detect faults. FD is achieved by comparing preset values with current and voltage signals. A trip command is issued to section CB for segregating the fault. Such a MAS for transmission systems is not feasible for microgrid operation due to its dynamic nature, which requires frequently changing preset values. To make the MAS proposed in [135] suitable for microgrids, the authors of [136] modified it and incorporated ML to detect and classify faults.

A modified, decentralised MAS-based PS with a communication network for FL, segregation and service restoration in a microgrid is presented in [137]. For FD, the phase angle of the current waveform is measured by PMU on each protected section. The section agent sends a trip signal to CBs on each side to isolate the fault if the threshold is exceeded after phase angle comparison. Service restoration is achieved by message exchange between the generator agent, restoration agent, load agent and DGs. Similarly, a decentralised MAS-based AP is presented in [138] for FD and protection coordination. Different agents continuously measure three-phase

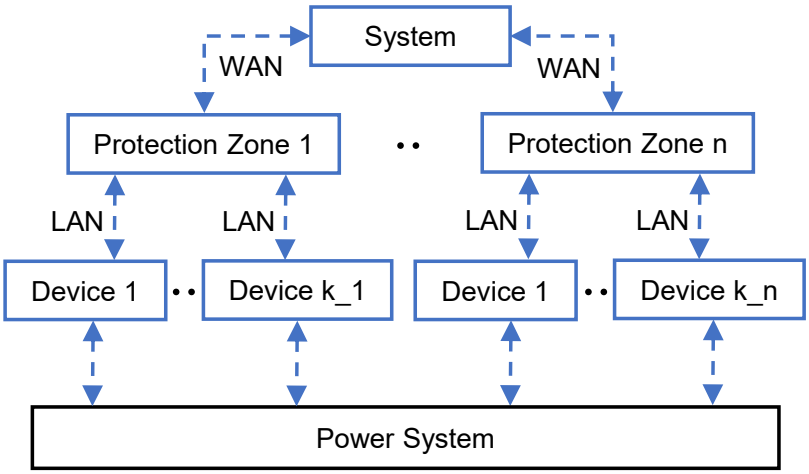

Figure 2.9: Initial three layered MAS

signals. A fault is detected when agents identify a difference in measurements before and after a fault event. Fig. 2.10 shows a bi-layered representation of a decentralised MAS, suggested in [139]. Moreover, decentralised MAS-based protection coordination schemes are given in [140, 141].

On the other hand, a centralised MAS-based AP is proposed in [142]. MAS is used for protection coordination. Digital relays transition to one of the three pre-calculated configurations for FD depending on changes in the microgrid. Another centralised MAS-based PS is proposed in [143]. The disparity of the current magnitude identified by agents is used for FD. AP, based on offline calculation for directional OC relays, is used as backup protection. Similarly, an AP method presented in [144] employs a tiered MAS for updating relay setting groups through coordination according to PCC status. Three pre-calculated settings are used, which are appropriate for a small-scale microgrid or static grid.

Alternatively, a MAS-based PS employing N-version programming is presented in [145]. Three N-version software units act as three protection agents. Each agent has a different FD technique. One agent uses Clark's transformation of three-phase current for FD, another uses OC protection, and the third agent uses the positive sequence phase differential method. A polling method aids in finalising the FD process. Also, a variable tripping time DP scheme based on MAS is projected in [146]. Various agents gather measurements, and then the tripping rule is applied if the threshold value is exceeded. It is claimed that the proposed scheme is not depen-

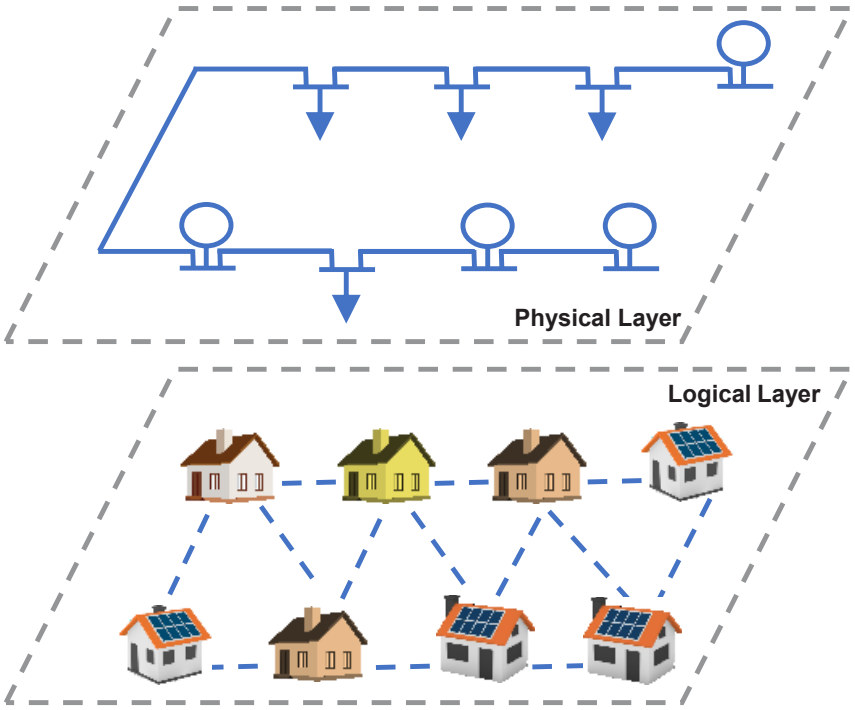

Figure 2.10: Physical and logical layers of a decentralised MAS

dent on the status of the microgrid, network topology or generation sources. Nevertheless, this may not be a financially feasible solution due to differential relays. Conversely, a MAS-based WA AP for backup relays is projected in [147].

2.3 Application of Artificial Intelligence in Microgrid Protection

With the development in AI techniques, the focus has shifted to using ML algorithms and DL for solving microgrid protection issues.

2.3.1 DT Based Protection Methods

A DT-based DP scheme is proposed in [148]. Discrete Fourier transform is used for FE. Seven differential features are computed by measuring the rate-of-change of voltage, frequency, power angle, negative sequence current and voltage, active and reactive power for both sides of the

feeder. Similarly, a microgrid FD and FTC method is presented in [149]. Current signals are processed using WT to compute features, including change in energy of the wavelet coefficients, standard deviation and entropy. Out of the six detail coefficients (d1-d6), it was observed that coefficient d3 was the most relevant as it contained important information during fault events. After obtaining the features for the fault and normal operation, a data set is constructed to train the Decision Tree (DT) for fault detection in the microgrid, as shown in Fig. 2.11.

Besides FD, faults are also classified using wavelet-based features derived from the current signal's negative- and zero-sequence components. Results showed that fault classification achieved high accuracy, while FD was reasonably accurate.

Correspondingly, a protection method based on DT is proposed in [150]. Only voltage signals are used for FE by short-time Fourier transform, which may result in nuisance tripping as three-phase voltage waveforms can fluctuate in case of transformer energising, heavy load and capacitor switching and motor starting. Nine features are used to classify symmetrical faults, and six features are used for asymmetrical fault classification. The main limitation of the transform used for FE is the fixed temporal resolution.

DT algorithms are fast learners but inherently have high variance and suffer from overfitting the training data samples [151, 152], which means that these models memorise the variations of the training data. A slight change in the data may result in a significant change in DT structure.

2.3.2 BT and RF Based Protection Methods

Bagged Trees (BT) and Random Forest (RF) are ensembles of DT. In BT, all features are available to choose from at each decision split. In RF, at each decision split, a subset of features is available to minimise correlation between individual trees [153, 154]. These algorithms can overcome the overfitting problem of DT by growing many DTs instead of just one. The predictions of each DT are aggregated to make the final prediction [155].

An RF-based fault event detection method for the autonomous microgrid is put forward in [156]. Training data preparation is initiated using a Monte Carlo-based simulation, and then

a dynamic response database of each of the four generators is prepared. Pre-defined features are extracted, and a dataset is built for training the RF classifier. The trained classifier is tested on new data to evaluate the proposed algorithm. The study has numerous limitations,

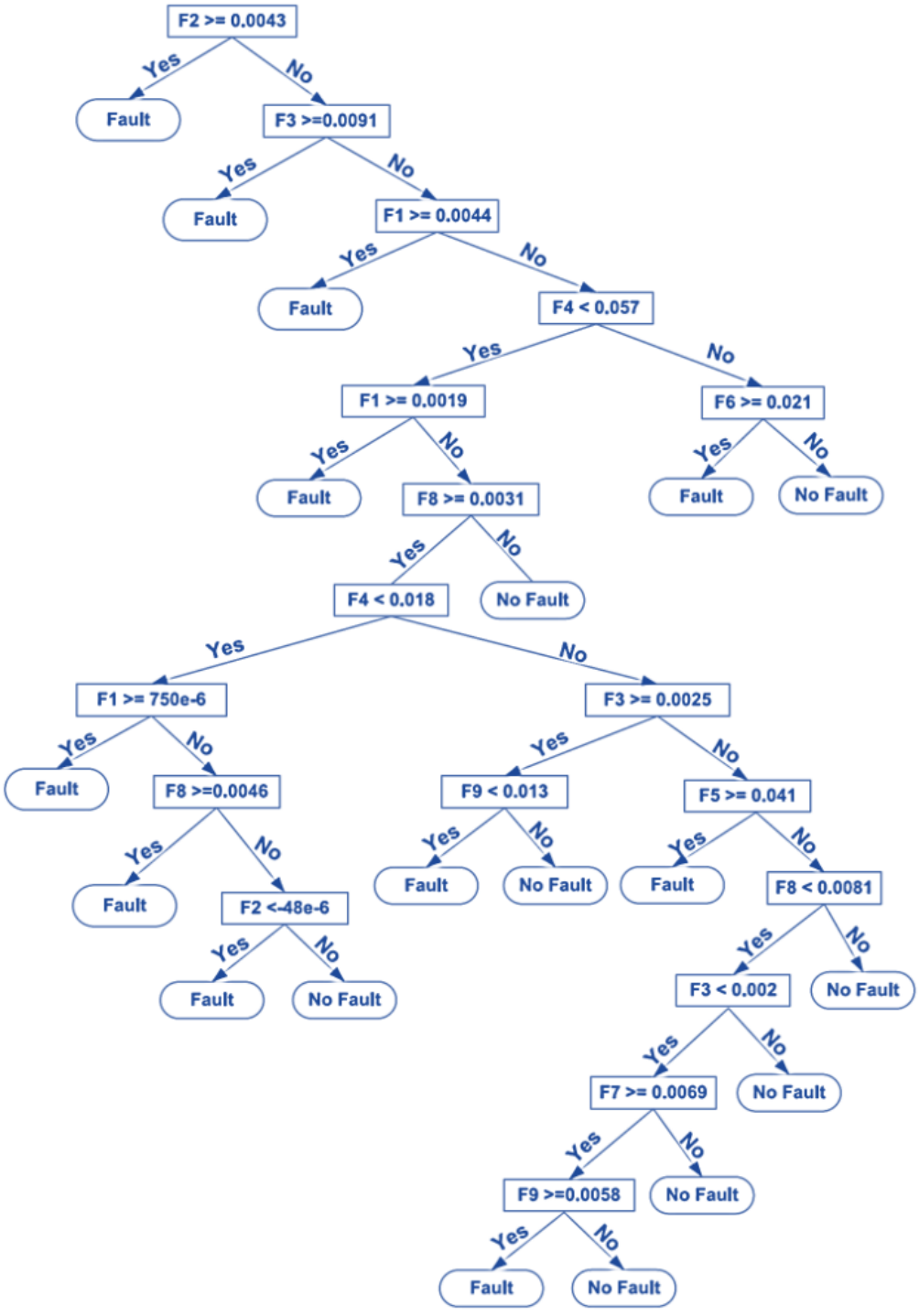

Figure 2.11: DT for FD

including disregard for missing data and incorrect classification due to time lag, short and biased data window selection during faults, constant load, and dispatchable generation from non-dispatchable sources. More importantly, only a single type of three-phase fault causing rotor angle instability was considered for detecting dynamic changes. On the other hand, a protection method for AC microgrids based on machine learning is developed in [157]. Besides detecting faults, they are also classified. Ten feature extraction techniques are applied to three-phase voltage, current, short-circuit current and frequency signals. These techniques include peaks metric, max factor, first and second principal components standard deviation, kurtosis, total harmonic distortion, skewness, shape factor and crest factor. Thirty-five classification learners are trained and tested. All other ML classifiers were outperformed by RF. The protection technique is superior to other approaches because of its higher accuracy in detecting and classifying faults besides identifying the faulted phase and high protection sensitivity for various operating situations. Similarly, RF-based methods for fault detection are put forward in [158, 159]. Multiresolution decomposition of WT and Wavelet Packet Transform are used to extract features from the voltage and current signals. Features include total harmonic distortion and negative sequence components. FE process presented in [158] is shown in Fig. 2.12.

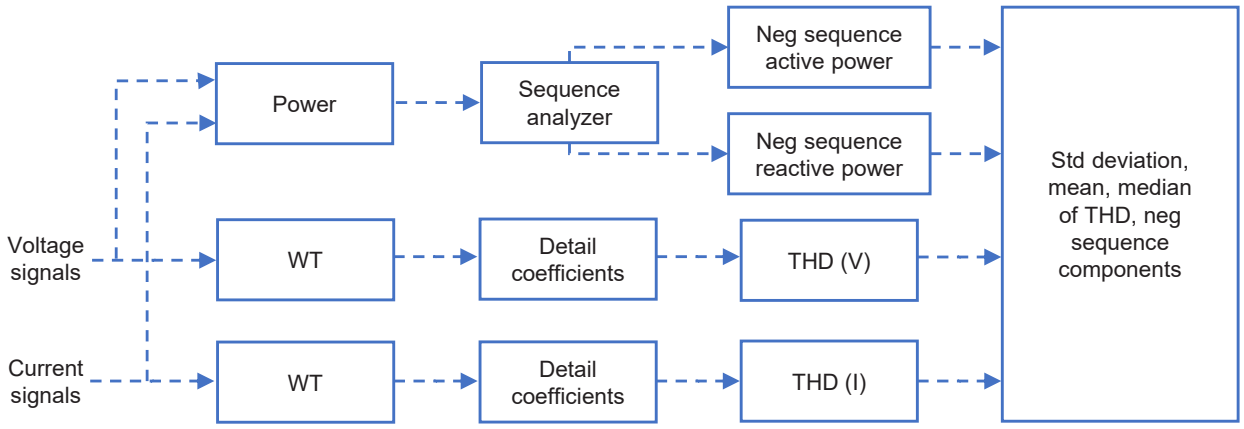

Figure 2.12: WT-based FE process

Conversely, an FD scheme based on BT is presented in [160]. Windowed FFT and WT are used for FE from voltage and current waveforms. Haar wavelet is used as MW. FE by FFT consists of a variation in the first harmonics' phase angles and harmonic components' magnitude of voltage

and current signals. In comparison, FE extracted by WT includes the change in wavelet energy and change in peak values of wavelet coefficients.

2.3.3 Semi-supervised Metric Learning

A technique to detect high impedance faults is presented in [161]. PMU placed at each bus collects high-resolution time-synchronised current and voltage samples. Discrete Fourier transform and Kalman filtering harmonics decomposition are used for FE. Features include angle between and magnitude of current and voltage sequence components and THD. Features are fed to information-theoretic semi-supervised metric learning [162], which is a self-training approach for FD. Probability ranking is applied to locate the fault.

2.3.4 Protection Based on Neural Networks

An FTC method based on Feedforward neural network (FNN) is presented in [163]. Discrete Fourier transform is used to compute RMS values of three-phase voltage and current signals which are input to FNN. There are 6 neurons in the input layer, 7 in the first and 5 neurons in the second hidden layer. FNN is the simplest of all neural networks and has been reported to be incapable of extrapolating [164]. Additionally, the performance of multi-layered FNN is affected by limited, sparse and noisy data [165].

In the same way, a PS for microgrids with double-fed induction generators-based wind turbines is put forward in [166]. DWT is used for FE from current and voltage signals to train Extreme learning machine (ELM) for FD and FTC. ELM algorithm is a single-hidden layer FNN. In ELM, the number of neurons are randomly chosen, and output weights are logically determined [167]. Even though ELM is a fast-learning method, it has two main limitations. The random allocation of neurons adds further uncertainty problems in learning and approximation. Moreover, it has been found that it has reduced generalisation ability [168]. Generalisation is the capacity of a model to do well on unseen data taken from the same distribution as the one used for training the model [169].

2.3.5 Multi-classifier Approach

A data mining approach to classifying fault and no faults in an isolated microgrid is given in [170]. Symmetrical components are used as features to train Naïve Bayes (NB) and DT models. Results show that DT outperformed NB for the given dataset. Only typical cases of load switching and a few faults are used for generating training data instead of a large dataset with numerous events over long periods. Also, both classifiers have limitations. NB does not require a large dataset for training, but this also limits learning. On the other hand, there is an overfitting problem with DT classifiers. Additionally, a protection method for low and medium-voltage AC microgrids based on supervised machine learning and principal component analysis is proposed in [171]. Bolted, low and high-impedance LG faults and faulted phases are identified. Three feature extraction techniques are applied to short-circuit current, phase voltage and line-to-line voltage for the three phases. The feature extraction techniques include the first and second principal components and standard deviation. SVM, KNN and BT performed better than other ML classifiers.

On the other hand, a novel method for detecting AC microgrid faults using wavelet functions and ML classifiers is proposed in [172]. In contrast to many researchers who have used a single wavelet function, they have used the optimal combination of wavelet functions identified by the particle swarm optimisation technique. After identification of wavelet combination, wavelet coefficients, calculated using DWT, are fed to various classification algorithms, including DT, k-nearest neighbours, Support vector machine (SVM) and NB. Statistical performance comparison shows that the k-nearest neighbours classifier shows the highest accuracy among all other classifiers. Numerous fault types, different FLs, resistance values and both modes of microgrid are used to simulate different conditions.

Another ML-based microgrid PS is proposed in [173]. Hilbert-Huang transform is used to extract useful differential features. Of the three ML techniques used, the ELM-based approach outperformed NB, which was better than SVM. A core shortcoming of the transform used is that in the low-frequency band, it generates unwanted components and is also inefficient in isolating some of the low-energy components of the signal [174].

In a different way, an adaptive OC and distance PS using ANN for fault classification and SVM for FL is presented in [175]. Relay settings are updated based on operating states. The limitations of the work include using a single-neuron ANN model and distance protection. Impedance-based protection is significantly affected by DG fault behaviour and is not suitable for short distribution lines.

2.3.6 DNN Based Protection Methods

Deep learning is a growing AI technique that overcomes the shortcomings of a typical artificial neural network (ANN). Not all neural networks are DNN. A DNN consists of three or more layers, including input and output layers, whereas other neural networks can comprise just one layer.

A PS based on deep neural network (DNN) is proposed in [176]. A gated recurrent unit, a recent variation of neural networks, is used to build the DNN. It overcomes some of the limitations of ANN by adding extra recurrent connections in the hidden [177]. Branch current is measured, and then DWT is used for FE. Features include standard deviation, skewness, energy, minimum, maximum, and mean value of the coefficients, input into DNN for FTC and FP identification. The proposed scheme can also predict FL. Fig. 2.13 illustrates the proposed methodology.

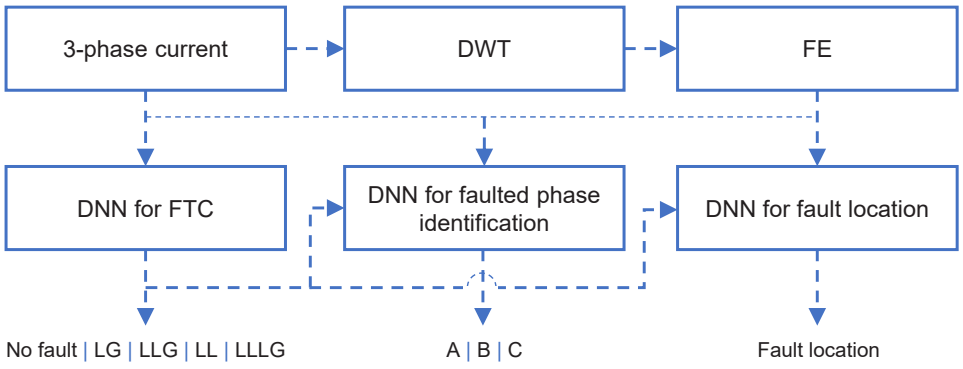

Figure 2.13: Schematic of DNN-based PS

Another DNN-based protection technique is presented in [178]. Three-phase current signals are input to DNN for FD. With only 3 input neurons, the first hidden layer uses 50 neurons,

while the second hidden layer uses 25 neurons. Using such a large number of neurons in the hidden layers has no advantage as it may result in overfitting [179]. Additionally, raw data is fed to the hidden layers without pre-processing, resulting in overfitting. On the other hand, an FD method for single-phase grid-connected photovoltaic Inverters using deep AlexNet CNN is projected in [180]. Voltage and current signals are normalised and equally segmented before converting them to 2D images as input to the CNN. Although this technique is suitable for offline pattern recognition and CNN performs better than other neural networks on image data, it has many practical limitations. Converting the signals to an image requires additional memory and processing time. Many other AI techniques can process the signals directly without needing image conversion. Layers of the general AlexNet CNN are shown in Fig. 2.14.

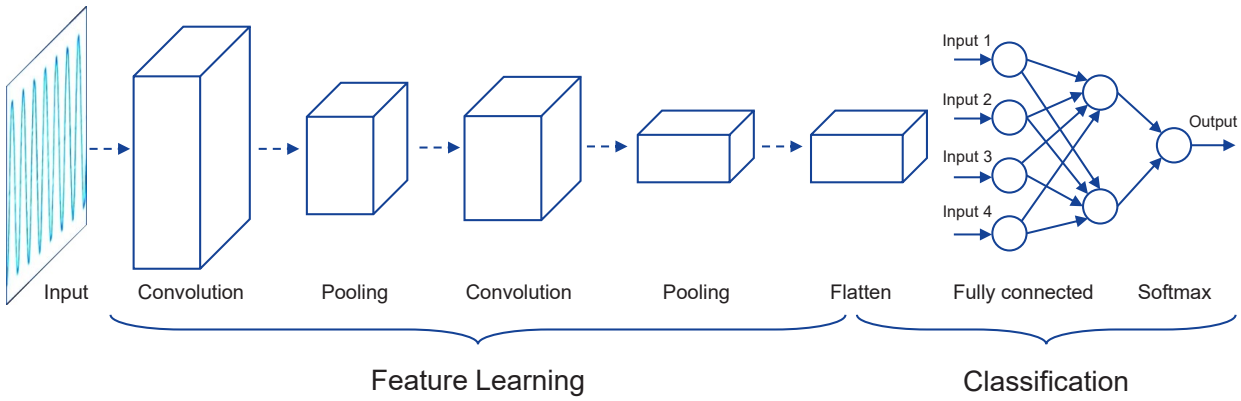

Figure 2.14: General AlexNet CNN architecture

2.4 Comparison of Protection Techniques for AC Microgrids and Related Characteristics

To summarise the methodology proposed by different authors and to highlight important characteristics, various comparisons are shown in tabular form. A comparison of AC microgrid protection techniques without Artificial Intelligence is shown in Table 2.2. The method used for fault detection, the benefits of the proposed scheme and the limitations of the work are presented. On the other hand, Table 2.3 shows a comparison of Artificial Intelligence-based microgrid protection techniques. Many different Supervised, Semi-supervised, Multi-classifier

and Deep learning-based methods with their advantages and limitations are presented. Additionally, the functional characteristics of protection systems are comprehensively compared in Table 2.4. This gives a complete picture of the most suitable protection method for various protection needs. Lastly, a novel comparison of FE techniques and features extracted for recently proposed AI-based PS is given in Table 2.5. This unique comparison table highlights the feature extraction techniques and the features extracted to train the machine learning algorithms applied recently. It shows that WT is the most common FE technique. On the contrary, the commonly used features are negative sequence components, THD, Standard deviation, the angle between and magnitude of current and voltage sequence components, entropy and change in energy of the wavelet coefficients of the current signals.

Table 2.2: Comparison of AC microgrid protection techniques without Artificial Intelligence

No.	Scheme	Method	Advantage	Limitations
1.	Directional OC [51, 54]	Current threshold	Simple and less expensive	Fixed settings not suitable for a dynamic network.
2.	Adaptive [58, 59, 60]	Current-based	Suitable for Dynamic network	Recalculations required when fixed setting groups are used.
3.	Differential [63, 64]	Difference between parameters on each side of protected zone	Very effective for DN with DG and both modes of microgrid operation	Financially not viable.
4.	Hybrid [68, 69, 70]	Current-based	Combines benefits of different PS	Real-time experimental investigation is needed to verify the feasibility.

5.	FCL-based [75, 84]	External device used with OC protection	Deals with FC variations in two modes of microgrid operation	Optimal relay settings and FCL location to be re-calculated for any changes. A trade-off has to be made between impedance settings during normal and fault conditions.
6.	Voltage-based [86, 87]	Transformation of voltage signal to provide a disturbance signal	Suitable for islanded mode.	Inability to detect high impedance and symmetrical faults
7.	Travelling waves [90, 94, 102]	Polarity and time features of initial current	Potential to be become an important PS	Complicated calculations. Not suitable for short distribution lines.
8.	PMU-based [107, 1, 116]	Measurement difference above the threshold	μPMUs have lower costs, are more accurate and have higher measurement resolution	Synchronisation problems.
9.	Harmonic content [120, 52]	Variation in fundamental frequency	Suitable for specific fault types.	Unable to detect some faults effectively. Some harmonic component-based PS do not consider transformer connections, especially delta-wye.

10.	Sequence components [122, 123]	Best suited to detect faults where delta-wye distribution transformers are not connected.	Variation in zero-, negative- or positive-sequence components	Single-phase or unbalanced three-phase loads may cause nuisance tripping.
11.	Wavelet transform [127, 128]	Signal transformation and differences between filtered signal samples	Best suited to identify patterns in signals	The main shortcoming of PS using WT is the selection of an optimal MW.
12.	Multi agent systems [137, 143]	Advanced signal processing and communication between agents	Offers a potential solution to incorporate internet of things (IoT) devices	Complicated, still evolving and requires real-time experimental investigation to verify the feasibility.

Table 2.3: Comparison of Artificial intelligence based microgrid protection techniques

No.	Scheme	Method	Advantage	Limitations
13.	MAS combined with ML [136]	Combines the benefit of communication by MAS and intelligence offered by ML.	Evolving and requires real-time experimental verification.	
14.	SML DT-based [150, 152]	Advanced signal processing. DT-based	Simple and fast learners	Suffers from high variance and overfitting issues.
15.	SML BT & RF-based [155, 158]	Advanced signal processing. Ensemble of DTs	Overcomes the overfitting problem of DT.	Results vary for Split criterion, the number of trees grown and predictors used.
16.	Semi-supervised metric learning [161, 162]	Advanced signal processing.	Self-training approach	Black-box model, still evolving.

17.	Neural networks [166, 163]	Advanced signal processing. Neuron connection in different layers	Tends to be more accurate when a large data set is used for training.	Limited, sparse and noisy data affects the outcome. A large number of neurons in the hidden layers result in overfitting.
18.	Multi-classifier [172, 175]	Advanced signal processing. Comparing the output of multiple classifiers	Makes it easy to compare models with the highest accuracy.	Same features may produce different accuracy for different ML models.
19.	Deep learning [176, 178]	Advanced signal processing. Computational models comprising multiple layers	Best suited for Big data applications	Black-box model. Requires large amounts of processing power.

Table 2.4: Comparison based on functional characteristics of protection systems

No.	Scheme	Speed	Sensitivity	Selectivity	Reliability	Cost
1.	Directional OC	Moderate	Moderate	Moderate	Low	Inexpensive
2.	Adaptive	Fast	High	High	High	Reasonable
3.	Differential	Fast	Very High	High	High	Very Expensive
4.	Hybrid	Fast	High	High	High	Expensive
5.	Fault current limiters	Fast	Moderate	Low	Moderate	Expensive
6.	Voltage based	Moderate	Low	Low	Low	Reasonable
7.	Travelling waves	Very Fast	High	High	Moderate	Reasonable
8.	PMU-based	Moderate	High	High	Moderate	Expensive
9.	Harmonic contents	Moderate	Moderate	Moderate	Moderate	Reasonable
10.	Sequence components	Moderate	Moderate	Moderate	Moderate	Reasonable
11.	Wavelet transform	Fast	High	High	Moderate	Expensive
12.	Multi-agent systems	Moderate	High	High	High	Expensive

13.	MAS with ML	High	High	High	High	Expensive
14.	SML DT-based	Fast	High	High	Moderate	Expensive
15.	SML BT & RF-based	Fast	High	High	High	Expensive
16.	Semi-supervised metric learning	Fast	High	High	Moderate	Expensive
17.	Neural networks	Fast	High	High	High	Expensive
18.	Multi-classifier approach	Fast	High	High	High	Expensive
19.	Deep learning	Fast	High	High	High	Expensive

Table 2.5: Comparison of FE techniques and features extracted for recently proposed AI-based PS

No.	Scheme	FE Technique	Features Extracted
1.	[148]	Discrete Fourier transform	Rate-of-change of voltage, frequency, power angle, negative sequence current and voltage, active and reactive power accuracy.
2.	[149]	Wavelet Transform	Standard deviation, entropy and change in energy of the wavelet coefficients of the current signals.
3.	[150]	Short-time Fourier transform	Linear combination of energy and entropy of three-phase voltages.
4.	[157]	Peaks metric, max factor, first and second principal components standard deviation, kurtosis, total harmonic distortion, skewness, shape factor and crest factor.	All ten feature extraction techniques are applied to three-phase voltage, current, short-circuit current and Frequency signals.
5.	[158]	Multiresolution decomposition of WT	Negative sequence components and THD of current and voltage signals.

6.	[159]	Wavelet Packet Transform	Negative sequence components and THD of current and voltage signals.
7.	[160]	Windowed Fast Fourier transform and Wavelet Transform	Variation in first harmonics' phase angles and harmonic components' magnitude of voltage and current signals. Also, change in wavelet energy and a change in peak values of wavelet coefficients.
8.	[161]	Discrete Fourier transform and Kalman filtering harmonics decomposition	The angle between and magnitude of current and voltage sequence components and THD.
9.	[163]	Discrete Fourier transform	RMS values of three-phase voltage and current signals
10.	[171]	Principal component Analysis	Standard deviation, first and second principal components of short-circuit current, phase voltage and line-to-line voltage for each phase.
11.	[176]	Discrete Wavelet Transform	Standard deviation, skewness, energy, minimum, maximum, and mean value of the coefficients obtained from current signals.
12.	[178]	Not Used	Three-phase current signals are directly fed to DNN.

2.5 Open Microgrid Protection Research Problems

Based on this review, future research can be directed towards hybrid protection to combine their benefits to solve microgrid protection issues. With the advancement in communication technologies, autonomous systems like multi-agents using computational intelligence with real-time data analysis and application of SML for adaptability seem to be the future trend in microgrid protection research. AP scheme using MAS incorporating SML and HDL will increase the sensitivity of detecting the faults, speed of segregation and reliability of coordination. Ideas for future research involving microgrid protection are presented below:

a. Protection of IIDG dominant microgrids, where inverters reveal non-linear behaviour with their impedance characteristics and fault ride-through transients when a fault occurs, requires further research.

b. Studies of DG sizing and allocation considering fault ride-through behaviour of different DG types and their impact on grid performance still have much research potential.

c. Development of a less expensive and more accurate FL method for all faults in an AC microgrid.

d. Development of less expensive IoT technologies and devices for microgrid protection and measurement. μPMUs have brought the cost down, but there is still room for new high-frequency IoT-based smart sensing and measuring devices for wide-area monitoring and to communicate with IEDs and other devices as agents.

e. Investigation of hybrid PS combining the advantages of multiple PS is also an overlooked research domain.

f. Primary relay settings are dynamically and automatically updated in adaptive, MAS and ML-based protection schemes to account for fault current variations. There is a need to investigate the possible miscoordination between the primary and backup relays as a result of different relay settings within the active distribution network.

g. With the gradual modification of the network, various relays, IEDs, and IoT devices

from multiple vendors will also be employed. New methods to transform protection settings into globally readable settings files will be necessary to achieve protection settings interoperability.

h. Development of intelligent relays, reclosers and new microprocessor-based current interrupter devices that can protect the system in centralised and decentralised schemes and are compatible with MAS, ML and DL.

i. The MAS-based protection scheme is a promising method. However, it has not been extensively investigated in the literature, and there is a significant research gap in this area.

j. Development of detailed simulation models of meshed microgrids, incorporating many different DG sources and types for different loads and fault conditions. Such detailed models will enable the collection of close-to-real-world synthetic data for ML and DL.

k. New feature extraction techniques are required to improve the speed, accuracy and robustness of ML and DL models for microgrid protection.

l. Applications of ML and DL offer promising solutions to most microgrid protection problems. However, not much research has been put into this area, providing many researchers with a massive opportunity.

m. Future grids will depend heavily on communication as most modern protection techniques, including adaptive, PMU, WT, MAS, and AI-based, require a communication network. Studying the effects of communication network latencies and noise on protection systems is an important research area.

n. With increased dependency on communication for sophisticated protection and control of microgrids and use of IoT devices, a significant cybersecurity threat may arise due to natural catastrophes, human mistakes or attacks by hackers and can cause wide-scale power outages. Additionally, these attacks may result in denial of service, unauthorised access and modification of IEDs and SCADA systems, invasion of customer privacy and data. Hence, designing resilient protection schemes to deal with cyberattacks is a critical

research domain.

o. There is also a need to develop decentralised backup protection to detect faults in both modes of microgrid operation in the event of communication or primary protection failure.

p. Real-time experimental investigation of numerous proposed techniques is also required to verify the feasibility.

2.6 Summary

This chapter encompasses the current status of DN protection, its limitation in active DN, significant protection challenges associated with AC microgrids, a wide-ranging critical review and classification of various methods that have been proposed to solve the protection challenges in microgrids and their shortcomings.

Directional OC and AP methods have been proposed to overcome the limitations of traditional overcurrent PS. However, with a fixed plug setting multiplier, time dial settings and pre-calculated setting groups, these techniques will be ineffective due to dynamic changes in fault levels within the microgrids. Therefore, high-speed communication infrastructure is required for online setting calculations, differential and hybrid protection methods, but financial viability, network latency and cyber security are crucial issues with such methods. FCL offers a possible solution but requires optimisation for FCL location with variations in operating conditions. Also, impedance settings require a trade-off to minimise losses during normal operation and limit current when a fault occurs.

On the other hand, WA PMU-based methods are expensive. Harmonic contents and sequence component-based techniques are affected by delta-wye transformer connections. Similarly, WT-based methods are limited by the selection of mother wavelets. ML and DL methods require a large dataset for various conditions to avoid overfitting.

Based on the literature review, it seems primary and backup protection based on hybrid protection, autonomous systems like multi-agents using computational intelligence with real-time data analysis and application of ML and DL for adaptability can offer promising microgrid

protection solutions. AP schemes using MAS incorporating ML and DL will increase the sensitivity of detecting the faults, segregating speed, and coordination reliability. Moreover, there is a need for FP identification, besides fault detection and classification, for accurate single- and double-pole tripping, which will increase system resilience and economic benefits. Extensive research regarding microgrid protection, particularly for autonomous mode, is still required.

Chapter 3

Classifying LG faults in an AC Microgrid using Supervised Machine Learning

3.1 Introduction

In recent years, the growing global demand for renewable energy sources has led to the rapid expansion of microgrids, which are small-scale, localised power distribution systems that can operate independently or in conjunction with the main grid. These microgrids offer numerous benefits, including enhanced energy efficiency, increased grid resilience, and a reduced carbon footprint. However, as microgrids become more prevalent, understanding and mitigating potential faults within these systems becomes of paramount importance to ensure their safe and reliable operation.

This chapter is based on the work reported in M. Uzair, L. Li, J. G. Zhu, "Identifying line-to-ground faulted phase in low and medium voltage ac microgrid using principal component analysis and supervised machine-learning", *Proc. IEEE 2018 AUPEC*, pp. 1–6, Nov 2018 and M. Uzair, M. Eskandari, L. Li, and J. Zhu, "Machine Learning Based Protection Scheme for Low Voltage AC Microgrids," *Energies*, vol. 15, no. 24, p. 9397, 2022.

Among the various faults that can occur in electrical systems, line-to-ground faults are the most common and particularly significant due to their potential to disrupt power flow, compromise system stability, and pose safety hazards [27]. Line-to-ground faults are categorised based on their resistance: bolted, low-resistance, and high-resistance faults. Each type of fault has its unique characteristics and implications.

Bolted line-to-ground faults represent one of the most severe fault conditions in electrical systems. These faults occur when a conductor comes into direct contact with the ground or another conducting surface, resulting in extremely low fault resistance and extremely high short-circuit currents, which can lead to catastrophic failure if not addressed promptly. On the other hand, low-resistance line-to-ground faults exhibit slightly higher fault resistances compared to bolted faults. While the fault currents in such scenarios may be lower, they can persist for longer durations, making them a critical concern for microgrid stability.

Similarly, High-resistance line-to-ground faults represent a unique challenge in electrical systems, especially in microgrids with distributed energy resources. These faults exhibit significantly higher resistances and may go unnoticed in traditional fault detection schemes, leading to prolonged fault durations and potential safety hazards. Moreover, high resistance faults can result in voltage fluctuations and power quality issues.

Detecting line-to-ground faults in microgrids using traditional protection methods can be challenging for several reasons, including fault resistance, distributed energy resources (DERs), and bidirectional power flow. Traditional fault detection schemes, which are primarily designed for large centralised power systems, may not be directly applicable to microgrids. The development of innovative fault detection techniques for microgrid systems, such as using Supervised ML, considering the dynamic nature and operational modes, is required.

3.2 Supervised Machine Learning

Supervised machine learning (SML) is a powerful subfield of artificial intelligence that involves the training of algorithms to make predictions based on labelled data. The primary goal of

supervised machine learning is to develop a model that can accurately map input data (features) to the corresponding output labels. Features, also known as input variables or attributes or predictors, play a critical role in this process. They represent the measurable characteristics of the data, which the algorithm utilises to identify patterns and relationships between the inputs and outputs.

Selecting appropriate features is a fundamental step in supervised learning as they significantly impact the model's performance and generalisation ability. Well-chosen features provide meaningful information and help the model distinguish relevant patterns, leading to better predictive capabilities.

3.3 Shortcomings of Wavelet Transform Based Feature Extraction

A common tool for analyzing non-stationary, noisy, aperiodic, transient, and intermittent signals is wavelet transform (WT). While it has been a popular choice for feature extraction in ML-based microgrid protection schemes, it has certain limitations. As mentioned in Chapter 2, the main shortcoming of protection schemes using WT for feature extraction for ML is selecting an optimal mother wavelet basis function. The choice of mother wavelet can significantly impact the results of feature extraction, potentially causing protection system misoperation.

Additionally, the effectiveness of discrete wavelet transform (DWT) based feature extraction can be affected by the fault inception angle and the sampling rate of the data acquisition system, leading to inconsistencies in the extracted features and impacting the ML model's generalizability. Consequently, most DWT-based protection techniques or derived features are efficient for specific fault types and operating conditions. However, applying such models to unseen data with different characteristics can result in misclassifications and inaccurate protection operations [157]. Furthermore, depending on the chosen wavelet function and decomposition level, WT can be computationally complex and expensive, especially for real-time applications with high data volumes.

Approximate and detail coefficients of a current signal for a low resistance LG fault on phase A using Symlets 2 (Sym2) as MW are shown in Fig. 3.1.

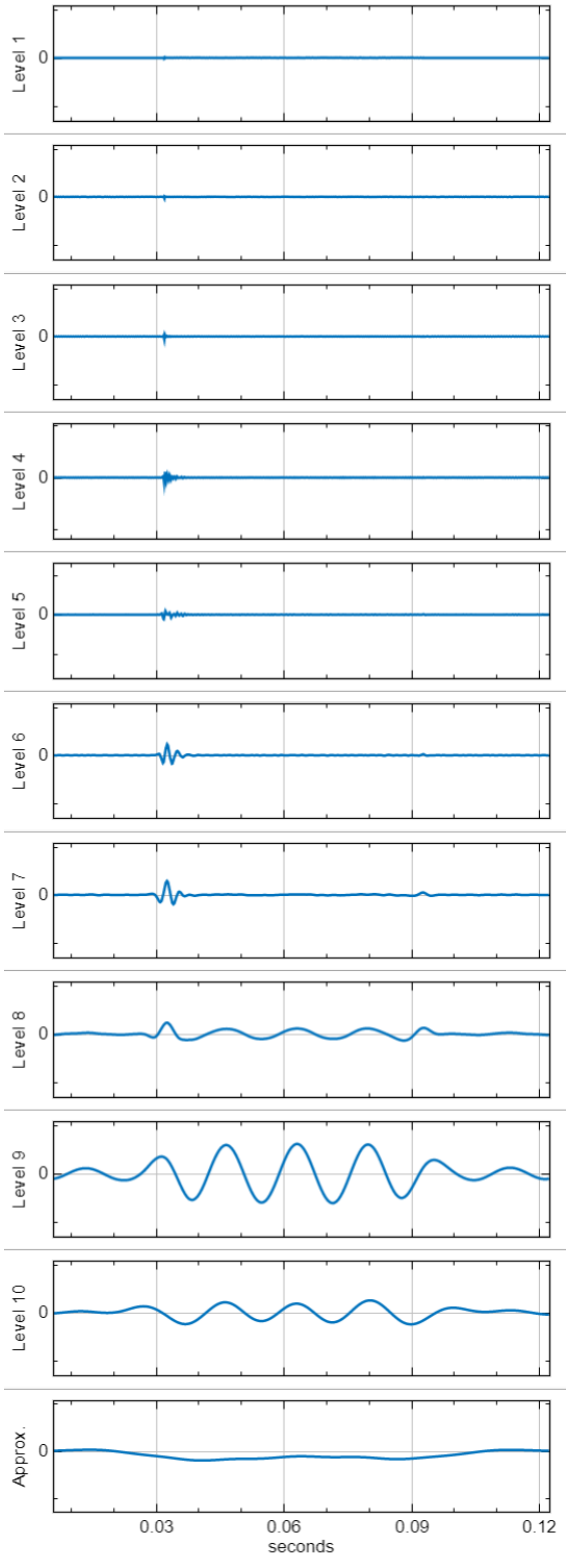

Figure 3.1: Sym2 approximate and detail coefficients for a low resistance LG fault on phase A

WT shortcoming is demonstrated by comparing the root-mean-square error (RMSE) for the reconstructed current signals using all the approximate and detail coefficients of a few wavelets for a low-resistance LG fault on phase A in Fig. 3.2. The RMSE seems to be negligible when all the approximate and detail coefficients are used to reconstruct the signal, but it is not feasible to use all the coefficients.

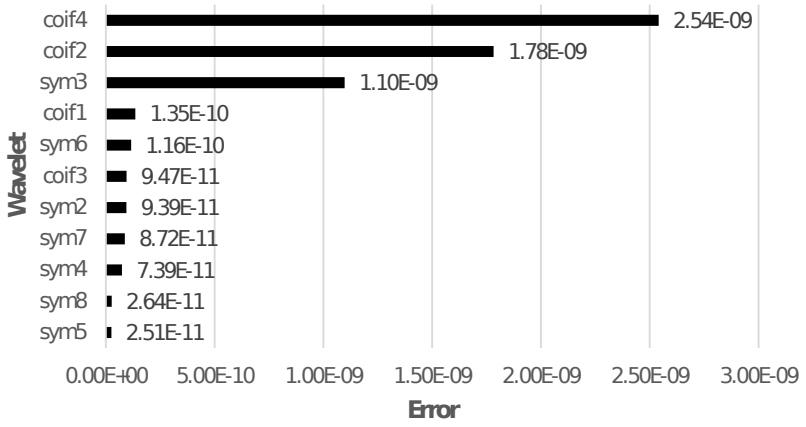

Figure 3.2: RMSE for the reconstructed signals using all the coefficients of different wavelets

In contrast, when the detail level coefficient corresponding to maximum relative energy is used to reconstruct the signal, there is a significant change in RMSE for different wavelets. A comparison of Level 9 detail coefficient of a current signal Iph_A and reconstructed signal for a low resistance LG fault on phase A using Symlets 5 ($Sym5$) as MW is shown in Fig. 3.3.

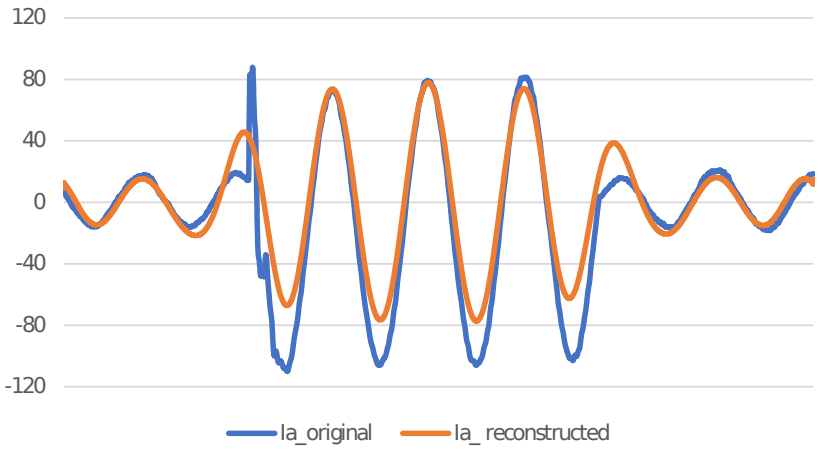

Figure 3.3: Iph_A and $Sym5$ reconstructed signal using Level 9 detail coefficient for a low resistance LG fault on phase A

RMSE comparison for the reconstructed current signals using only the Level 9 detail coefficient corresponding to the maximum relative energy of different wavelets is depicted in Fig. 3.4.

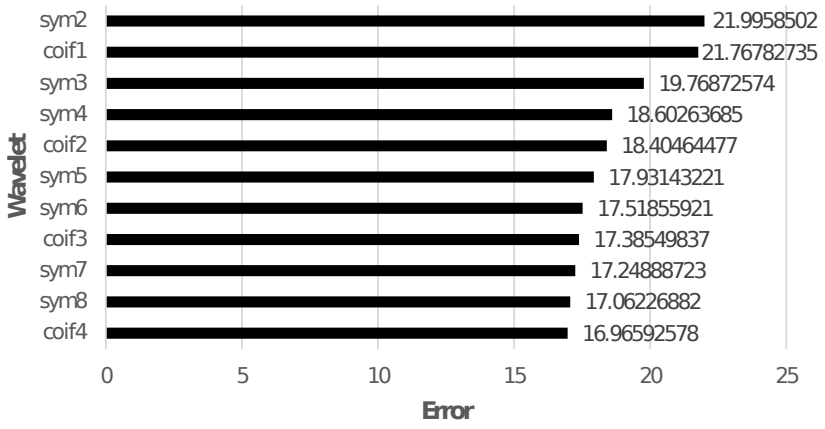

Figure 3.4: RMSE for the reconstructed signals using Level 9 detail coefficient of different wavelets

Due to the above-mentioned limitations of WT, this research proposes exploring alternative feature extraction techniques. Specifically, we investigate the application of Principal Component Analysis (PCA) to obtain predictors for machine learning-based microgrid protection.

3.4 Application of PCA to Obtain Predictors for Supervised ML

PCA has the potential to overcome the shortcomings of WT in the selection of an optimal mother wavelet basis function. It is a multivariate analytical method, and its primary objective is to reduce dimensionality. The goal is to find latent features that drive the patterns instead of using raw signals that will increase processing time and overfitting. This extraction involves transforming the original variables into a new set of orthogonal variables known as principal components [181]. In this study, PCA identifies the composite features or principal components of the three fault signals, line-to-line voltage ($u1$), phase voltage (u) and short-circuit current (Ish), for each phase. The fault is applied at different instances and for different spans to have a variety of data for training the ML classifier.

3.4.1 EMT Simulations for Data Collection

The test microgrid shown in Fig. 3.5 is used for simulations to collect fault and NF data. Three different types of loads are used. These include a 68% dynamic industrial load connected to 11 kV Bus, the unbalanced commercial load connected to Bus 3, and the unbalanced residential load connected to Bus 4. The DG sources include PV units, wind, and synchronous generators.

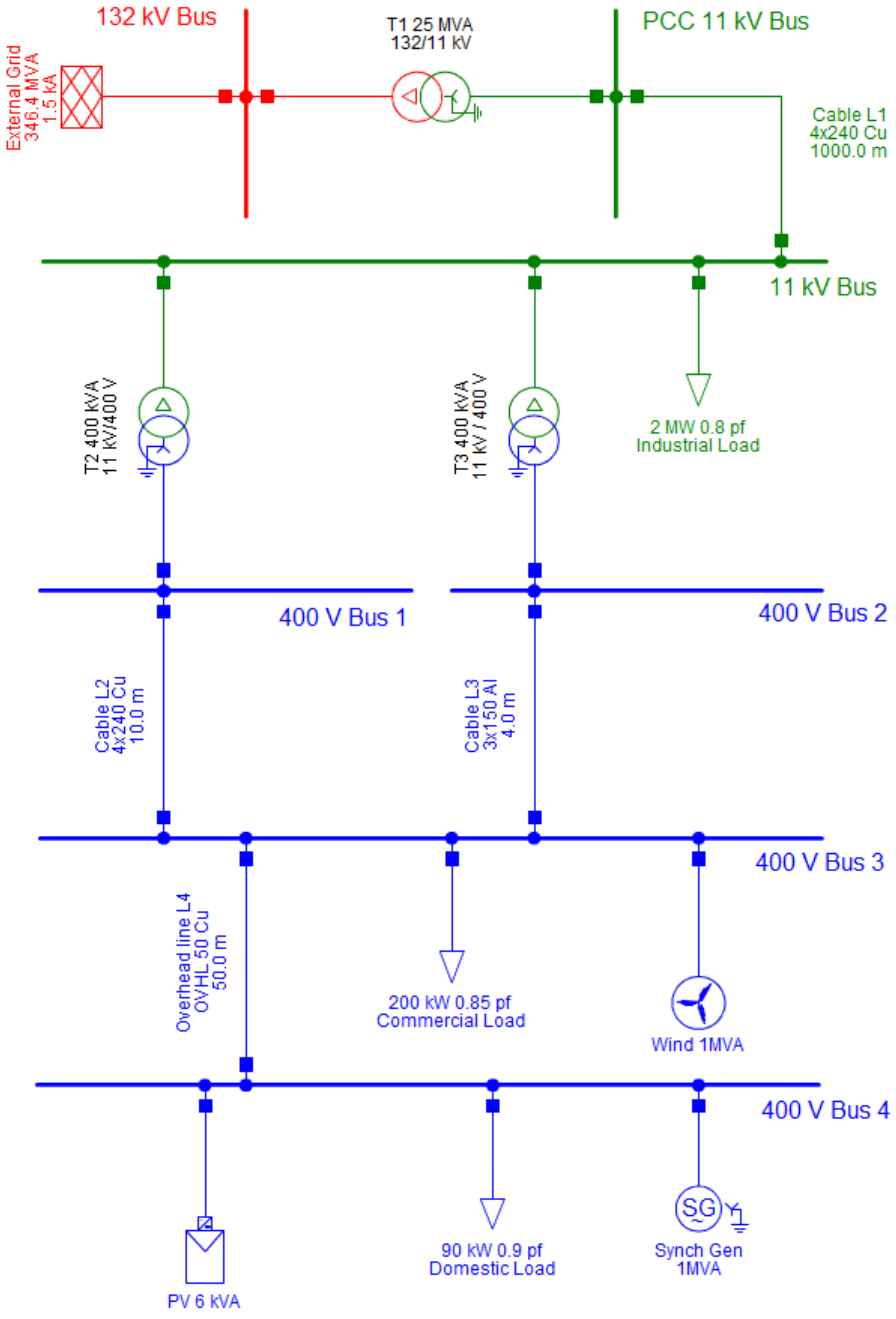

Figure 3.5: Test Microgrid

Data for the 0.1-sec window is recorded through EMT simulations for each case. A step size of 0.0001 sec is used to obtain more than 1000 samples for each scenario. This data is then pre-processed and labelled for supervised ML. Using raw signal with 1000 samples for training ML will increase processing time and introduce overfitting. In contrast, manual inspection to obtain combinations that give the largest variations when the fault occurs compared to the normal operation is impossible. Moreover, using multi-dimensional data on a complex classification algorithm can result in very high variance and prolonged processing time. To overcome these issues, the application of PCA is proposed to reduce the dimensionality of input features that will optimise the performance of the classification algorithm. Three different cases are used, including high impedance ground fault with 400Ω fault resistance, bolted ground fault, which has 0Ω fault resistance, and low impedance with ground fault 5Ω fault resistance were simulated for five different fault inception instances and duration at 400 V Bus 4. Symbols $u1$, u and Ish are defined in section 3.4.

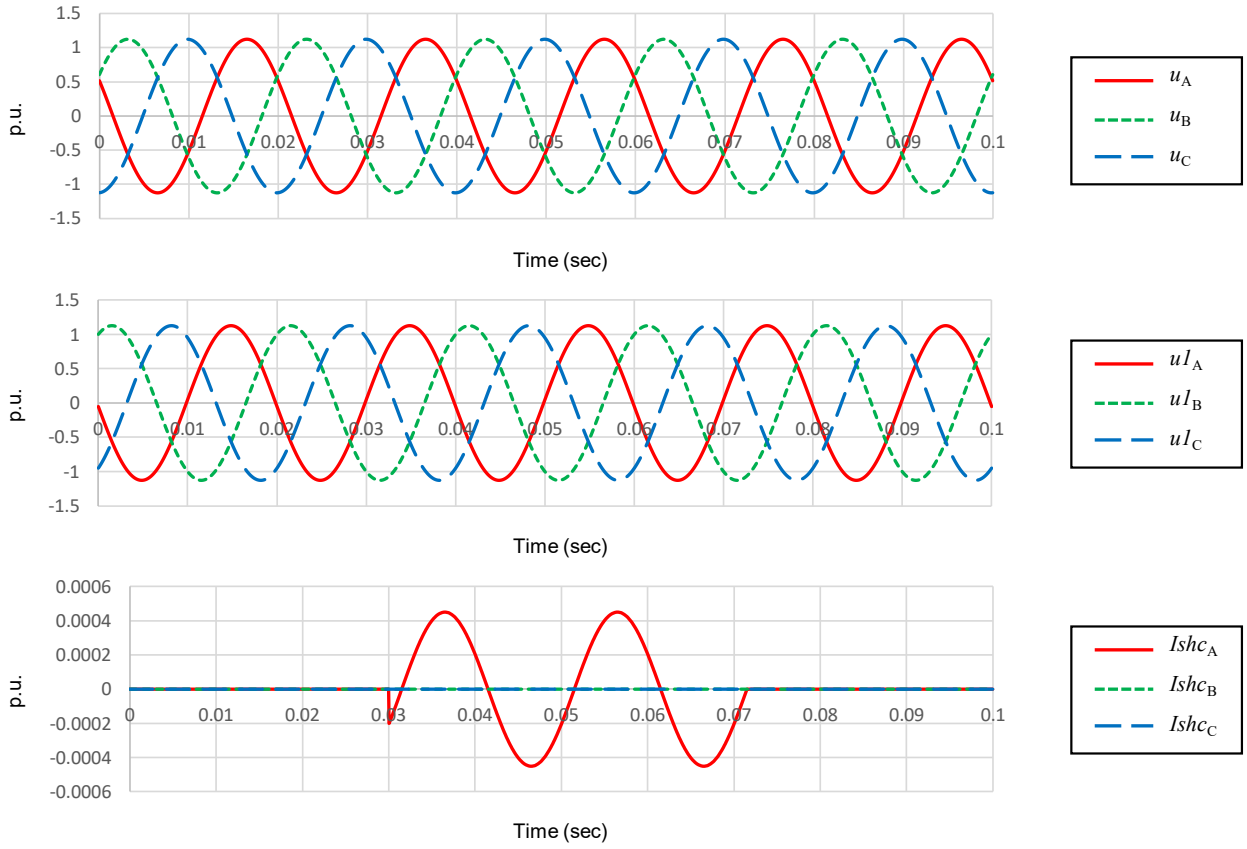

Figure 3.6: High impedance ground fault on phase A at 0.03 - 0.07 sec on Bus 4

As illustrated in Fig. 3.6, a high-impedance ground fault event presents minimal line-to-line ($u1$) and phase voltage (u) deviations. Furthermore, the measured fault current magnitude falls below the detection threshold of conventional OC protection relays. This observation underscores the limitations of traditional OC relays in identifying high-impedance ground faults due to their inherent reliance on significant current surges for fault detection. In contrast, it is visible in Fig. 3.7 that the voltage for FP collapses to zero, signifying a direct short circuit to the ground. This characteristic behaviour aligns with the low fault impedance of bolted faults, essentially creating a near-perfect connection between the phase conductor and the grounding system.

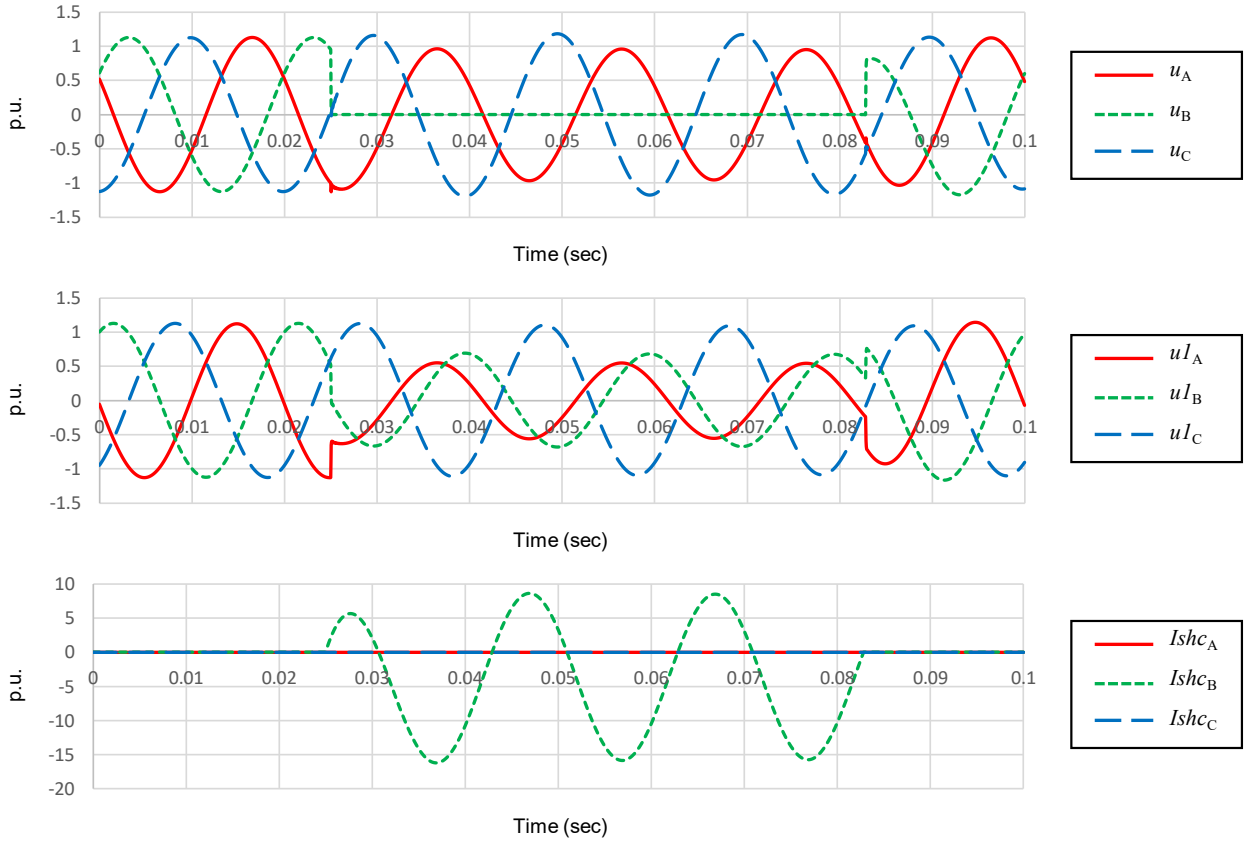

Figure 3.7: Bolted ground fault on phase B at 0.025 - 0.075 sec on Bus 4

In contrast to the zero phase voltage, the line-to-line voltages demonstrate noticeable deviations. This observed imbalance can be attributed to the effective shorting of one phase to the ground by the bolted fault. Consequently, the voltage readings between the remaining non-faulted phases become unbalanced, reflected in the significant departures from the nominal line-to-line

voltage levels typically observed during normal operating conditions. Furthermore, the current spikes directly result from the low impedance path established by the bolted fault, enabling a substantial current flow from the source to the grounded phase. The magnitude of this fault current can significantly exceed the normal current levels within the microgrid.

Fig. 3.8. shows variations in voltage and current waveforms for a low impedance ground fault. These faults have an impedance higher than bolted faults but much lower than high-impedance faults. The fault current magnitude is significant, lower than a bolted fault, but still exceeding normal operating currents. The voltage on the faulted phase decreases compared to normal conditions but does not drop to zero like in a bolted fault. Line-to-line voltages also show variations.

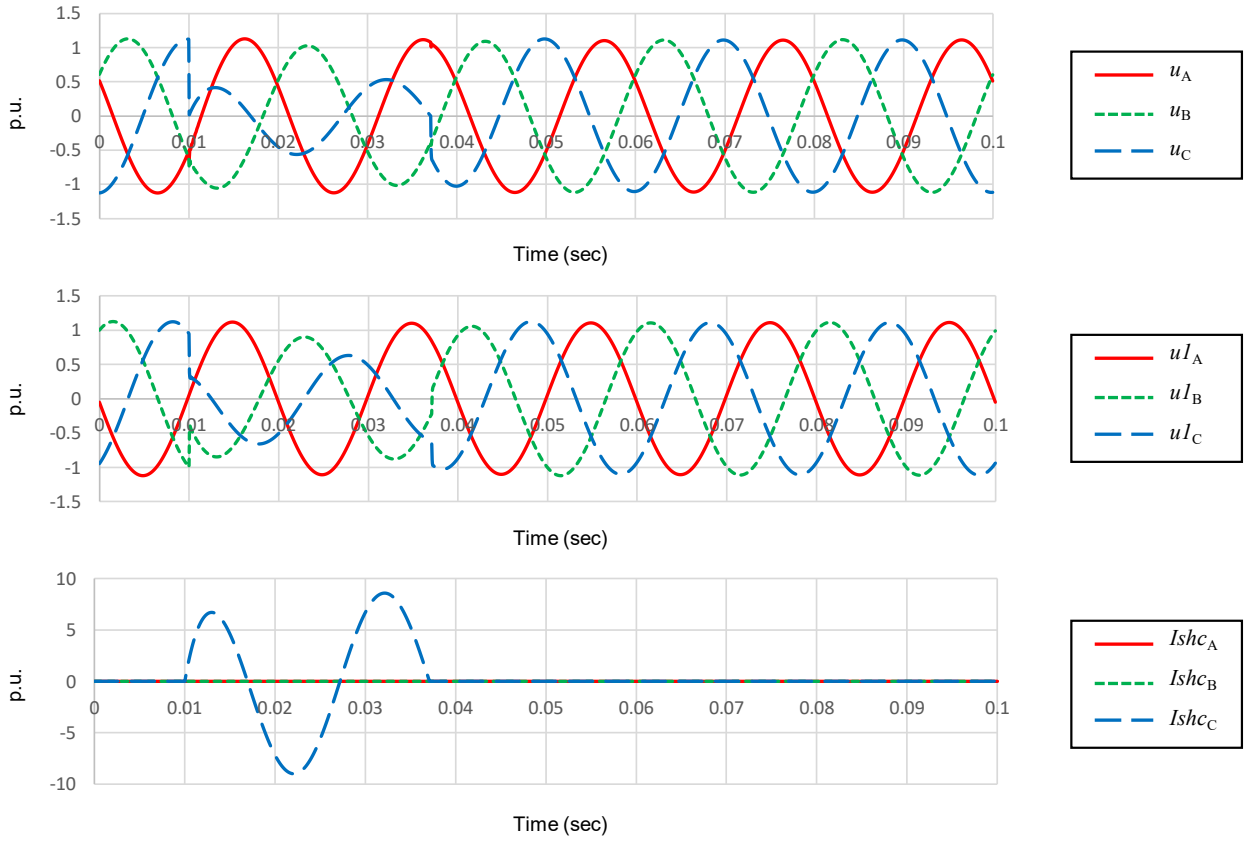

Figure 3.8: Low impedance ground fault on phase C at 0.01 - 0.03 sec on Bus 4

3.4.2 Principal Component Analysis for FE

The first step in PCA is to calculate the covariance matrix. The covariance matrix (C_M) of any two variables x and y, is the matrix of pairwise covariance (cov) calculations between each variable.

$$C_M = \begin{bmatrix} \text{cov}(x,x) & \text{cov}(x,y) \\ \text{cov}(y,x) & \text{cov}(y,y) \end{bmatrix} \tag{3.1}$$

where,

$$cov(x,y) = \frac{\sum_{i=1}^{N} (x_i - \bar{x})^* (y_i - \bar{y})}{N-1} \tag{3.2}$$

$\bar{x}$ and $\bar{y}$ are the mean values of x and y, respectively and $*$ denote the complex conjugate. Eigenvalues are used to calculate the eigenvectors for the covariance matrix, which are then used to extract patterns. The first eigenvector represents the eigenvalue that has the highest variance $e\vec{v}_1$. For the eigenvalue, which has the next highest variance, the second eigenvector corresponds to it, and so on. The matrix that results is as follows:

$$E = \begin{bmatrix} e\vec{v}_1 & e\vec{v}_2 & . & . & e\vec{v}_p \end{bmatrix} \tag{3.3}$$

Only the first and second eigenvectors are selected to obtain the first (pc_1) and second principal components (pc_2) that capture most of the variations in the data are used. Smaller principal components are ignored, which represent the noisy variations of those patterns. Variation for each principal component is demonstrated in Pareto charts of phase voltage (PV) and short circuit current (SC) of phase A, shown in Fig. 3.9 and Fig. 3.10.

$$E' = \begin{bmatrix} e\vec{v}_1 & e\vec{v}_2 \end{bmatrix} \tag{3.4}$$

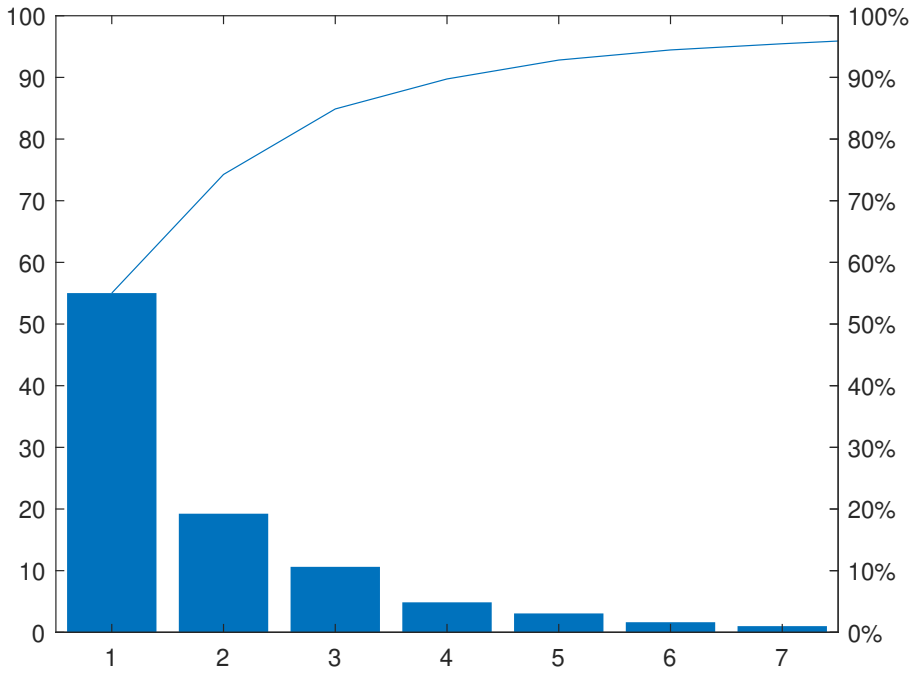

Figure 3.9: Pareto PV (phase A)

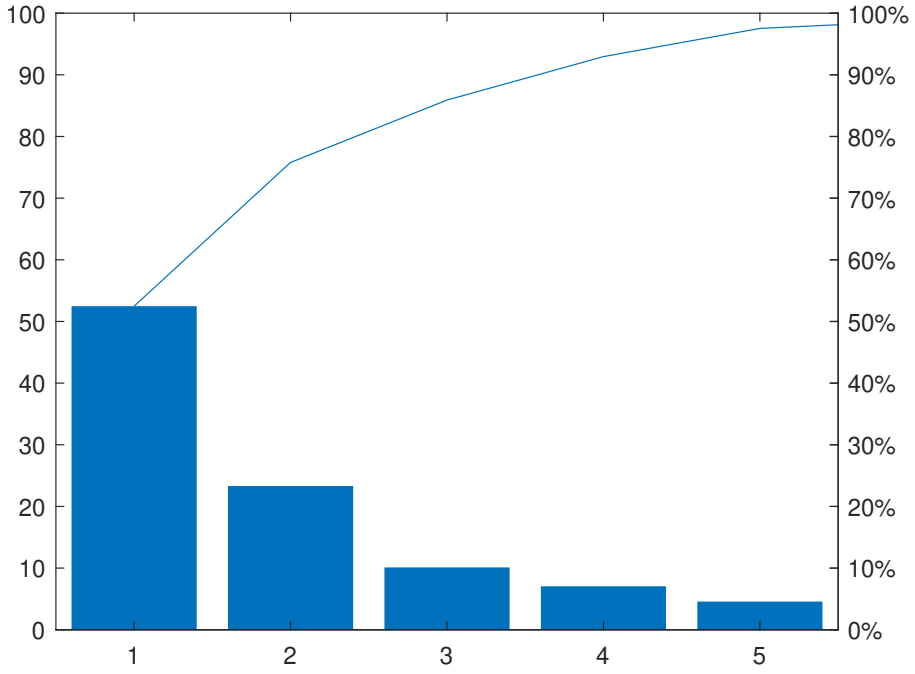

Figure 3.10: Pareto SC (phase A)

The new features are represented as the projection of the vectors on the new base consistent with the pc_1 and pc_2.

$$pc_{1,2} = E' \cdot [x_i - \bar{x}]^T \tag{3.5}$$

where x_i and $\bar{x}$ respectively represent the variable and the mean vector of the original data, whereas $pc_{1,2}$ represents new features.

3.4.3 Additional Predictor

Besides obtaining features by applying PCA, the standard deviation is also used to increase the set of predictors for the ML classifier to identify FP. For a variable vector x made up of N scalar observations, the standard deviation (STD) is defined as

$$STD(x) = \sqrt{\frac{\sum_{i=1}^{N} (x_i - \bar{x})^2}{(N-1)}} \tag{3.6}$$

where $\bar{x}$ is the mean of x :

$$\bar{x} = \frac{1}{N} \sum_{i=1}^{N} x_i \tag{3.7}$$

3.5 Evaluating the Accuracy of LG Faults Classification

The obtained various predictors are fed to three different classifiers to compare the prediction precision. These include SVM, KNN, and BT. An iterative process is then applied to obtain the most accurate models. After trying different kernel functions for SVM, varying the number of neighbours, distance metric, and weight for KNN, and changing the number of learners and the maximum number of splits for BT, models with high accuracy are obtained. Once the models are trained, test data is applied to check the accuracy of predictions. 15-fold cross-validation has been applied to the training dataset to test the accuracy of the classifiers. With the increase in the number of folds, the variance of the resulting estimation decreases.

A total of 27 predictors are obtained, including 9 for standard deviation, 9 for the first principal component, and 9 for the second principal component of 3 signals for 3 phases during fault. Using the 27 predictors, all three ML classifiers identified the FP with high accuracy. Different combinations of predictors are then used in the classification model to identify and remove features with low predictive power to reduce the vital processing time in fault identification. Results for the three fault types with different numbers of predictors for 3 Ml classifiers are shown in Tables 3.1, 3.2, and 3.3.

Table 3.1: Accuracy of ML models for bolted LG faults

Bolted LG faults at Bus 4	ML Classifiers		
Predictors Used	*SVM*	*KNN*	*BT*
All 27 predictors	100%	100%	100%
Different combination of 18 predictors	100%	100%	100%
Different combination of 12 predictors	100%	100%	100%
Different combination of 12 predictors	93.3%	100%	93.3%
Different combination of 9 predictors	100%	100%	100%
Different combination of 9 predictors	60%	86.7%	86.7%
Different combination of 9 predictors	100%	100%	93.3%

For less than 9 predictors, large inaccuracy was observed. Therefore, for further scenarios a combination of 9 to 18 predictors with highest accuracy are presented.

Table 3.2: Accuracy of ML models for Low Impedance LG faults

Low Impedance LG faults at Bus 4	ML Classifiers		
Predictors Used	*SVM*	*KNN*	*BT*
18 predictors	100%	100%	100%
Different combination of 12 predictors	100%	100%	100%
Different combination of 9 predictors	100%	100%	100%

Table 3.3: Accuracy of ML models for High Impedance LG faults

High Impedance LG faults at Bus 4	ML Classifiers		
Predictors Used	*SVM*	*KNN*	*BT*
18 predictors	100%	100%	93.3%
Different combination of 12 predictors	100%	100%	100%
Different combination of 9 predictors	93.3%	100%	100%

These results show that using standard deviation and PCA for extracting predictors yields accurate identification of the FP for bolted, low- and high-impedance LG faults. It is also visible that KNN shows the highest overall accuracy for various scenarios and a combination of predictors for this study.

3.6 Summary

This chapter starts with the shortcomings of Wavelet transform-based feature extraction, and then the application of PCAs for FE from voltage and short circuit current signals is proposed. The main focus of the chapter is the classification of bolted, low- and high-impedance LG faults in AC microgrids using Supervised Machine Learning. DIgSILENT PowerFactory is used to simulate the underlying microgrid to obtain fault-related data, while MATLAB is used to apply machine learning. 15-fold cross-validation is applied to the training dataset to evaluate different machine learning models. Among the three classifiers used, KNN has demonstrated the highest overall accuracy.

Chapter 4

Detecting and Classifying All Faults in a Radial AC Microgrid using Supervised Machine Learning

4.1 Introduction

Supervised machine learning algorithms heavily rely on labeled training data to learn patterns and make accurate predictions. The significance and representation of features, which serve as input variables, play a crucial role in determining the performance of these algorithms. The process of feature extraction is a fundamental step in preprocessing, aiming to transform raw data into a concise, informative, and discriminative feature set, optimising the learning process and enhancing the model's generalisation capabilities.

In Chapter 3, different types of LG faults were classified for faulted phase identification. Signals included line-to-line voltage, phase voltage and short-circuit currents for phases A,B and C. Although these signals were enough to classify LG faults but would be not enough for FD.

This chapter is based on the work reported in M. Uzair, M. Eskandari, L. Li, and J. Zhu, "Machine Learning Based Protection Scheme for Low Voltage AC Microgrids," *Energies*, vol. 15, no. 24, p. 9397, 2022.

Moreover, a small dataset was used with manual parameter tuning, which can not match the automated optimisation, using every possible variation in order to improve performance. Additionally, features were selected using an iterative process instead of using FS techniques.

New feature extraction methods are proposed in this chapter. Additionally, dimensionality reduction techniques, statistical tools, impulsive and signal processing metrics to extract unique features for ML classifiers are examined. Various FS techniques are used and then supervised machine learning is used to detect and classify faults in a radial AC microgrid.

4.2 Test Microgrid and EMT Simulations for Data collection

The low voltage AC test microgrid simulated in DIgSILENT PowerFactory shown in Fig. 4.1, is part of a radial distribution system operating at 415 V, 50 Hz. It is connected to the main grid through an 11 kV/415 V transformer. There are three DG sources, two photovoltaic (PV) systems, which are inverter-interfaced distributed generators (IIDGs) and a synchronous generator-based microturbine to maintain microgrid stability in AUTO mode by providing sufficient damping component and rotational inertia. All have a rating of 1MVA and are connected to 415V buses. A commercial load is connected to Bus 1, and domestic loads are connected to Bus 2 and 3. Bus 2 is the point of common coupling (PCC). The circuit breaker after the transformer is used for switching between the two microgrid operational modes.

Data is recorded through EMT simulations for 400 cases. For every case, simulations are carried out for 0.05 seconds with a step size of 0.0001 sec to obtain 500 observations for each of the 10 signals. The signals include three phase voltage (Vph_{ABC}) in kV, three phase current (Iph_{ABC}) and short-circuit current (Ish_{ABC}) in kA and frequency ($Freq$) in Hz.

Simulations are carried out for ten faults to collect data for fault detection (FD) and FTC with FP. Besides variations in fault resistance, reactance, inception angles, number of cycles and locations, all faults are simulated for grid-connected (GC) and AUTO mode to identify the variations in fault current level and other signals. Three cases are used for the LG faults: bolted

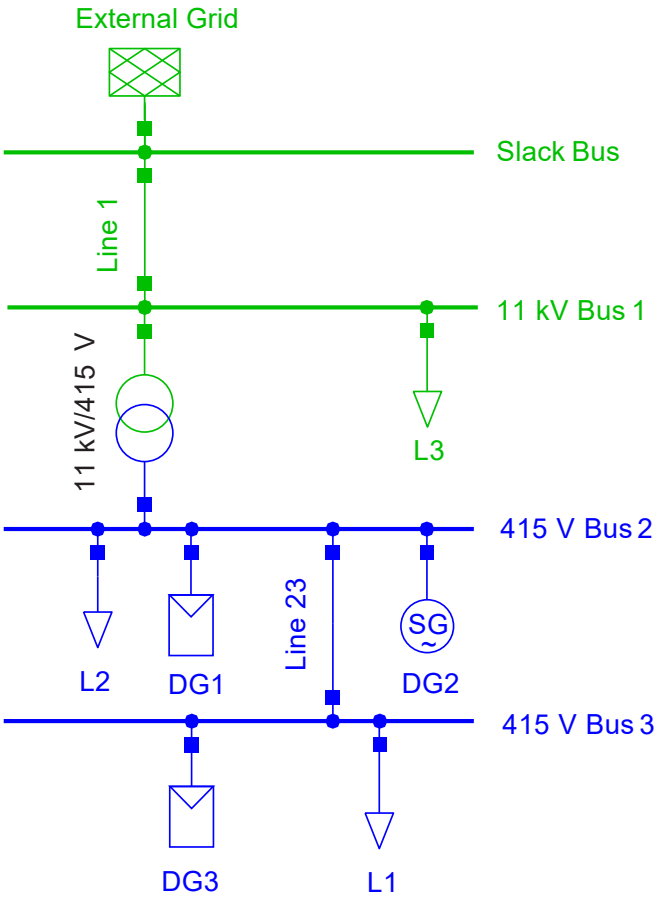

Figure 4.1: Test Microgrid

fault with 0Ω resistance, low resistance ground fault with 5Ω resistance, and high resistance fault with a value of 400Ω. For all other faults, the first case (C1) has no fault resistance or reactance. The second case (C2) has a resistance of 0.1Ω and a 0.001Ω reactance. The third and last case (C3) has a resistance of 0.1Ω and a comparatively greater reactance of 1Ω.

Waveforms of 10 signals: Vph_{ABC}, Iph_{ABC}, Ish_{ABC} and $Freq$ for LL-AB fault for case C3 in GC mode is shown in Fig. 4.2. NF case of loads switching on and off in AUTO mode is shown in Fig. 4.3. Similarly, NF case of load switching off in GC mode is shown in Fig. Fig. 4.4. Lastly, NF case of MG switching from AUTO to GC mode is shown in Fig. 4.5.

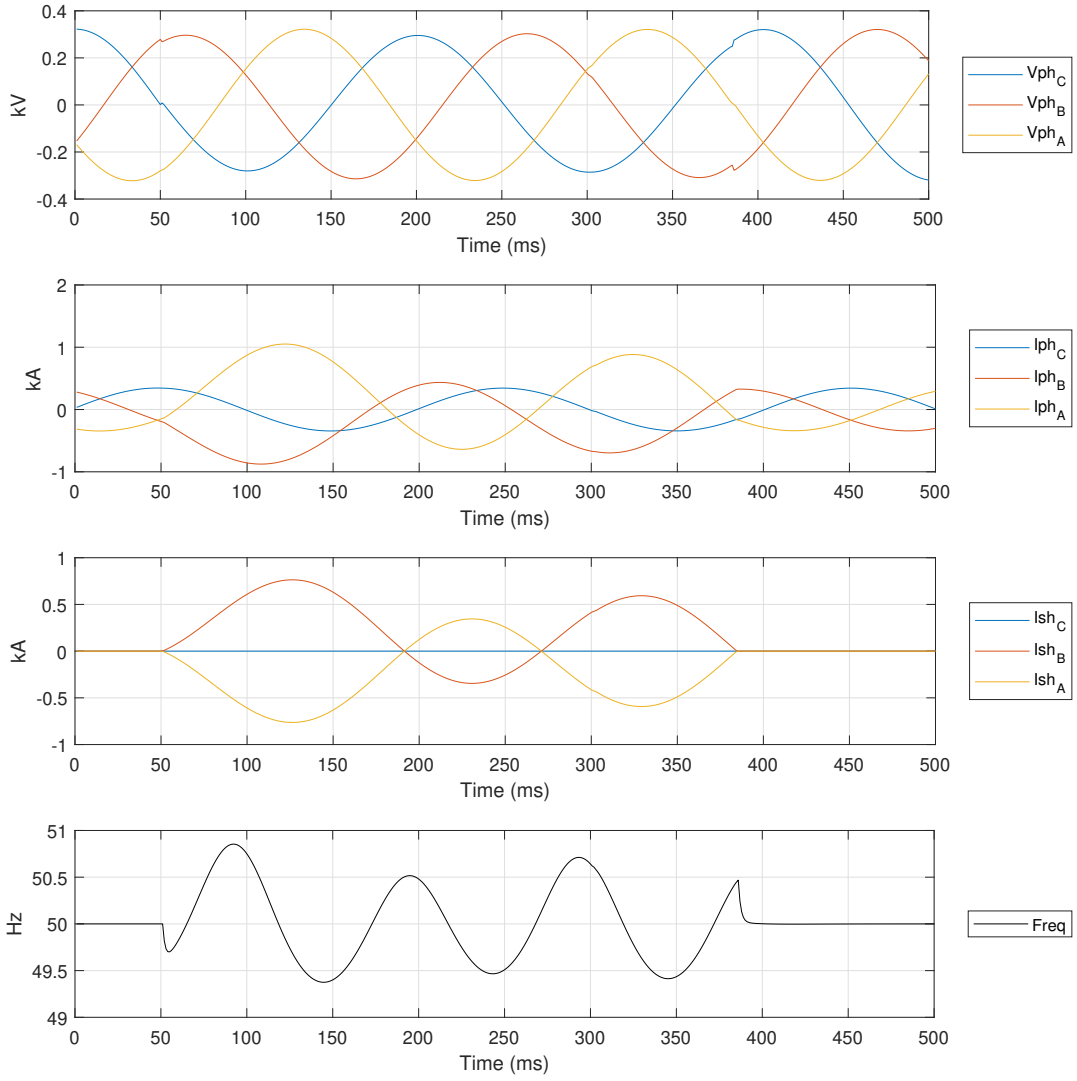

Figure 4.2: LL-AB fault for C3 in GC mode

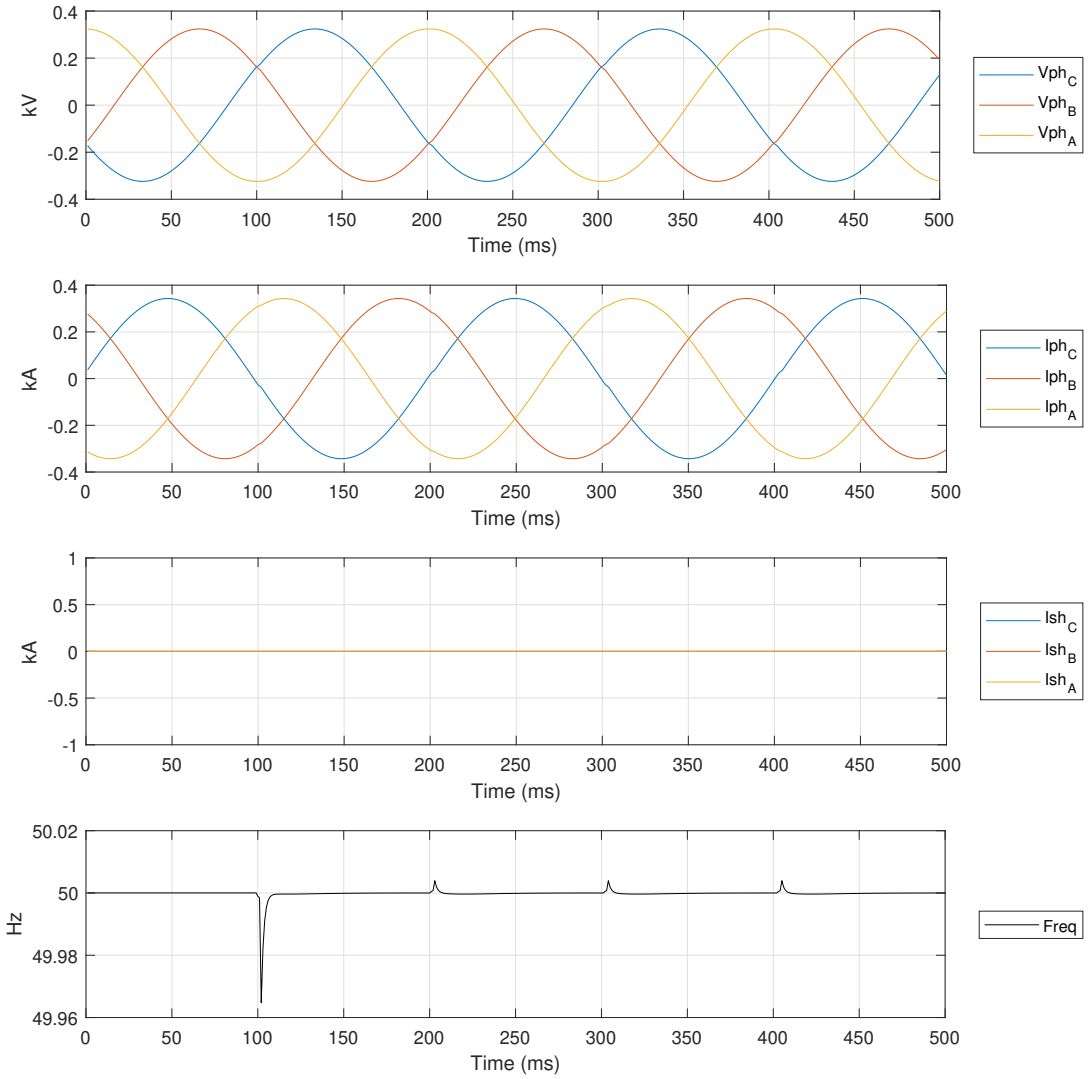

Figure 4.3: NF, Load switching in AUTO mode

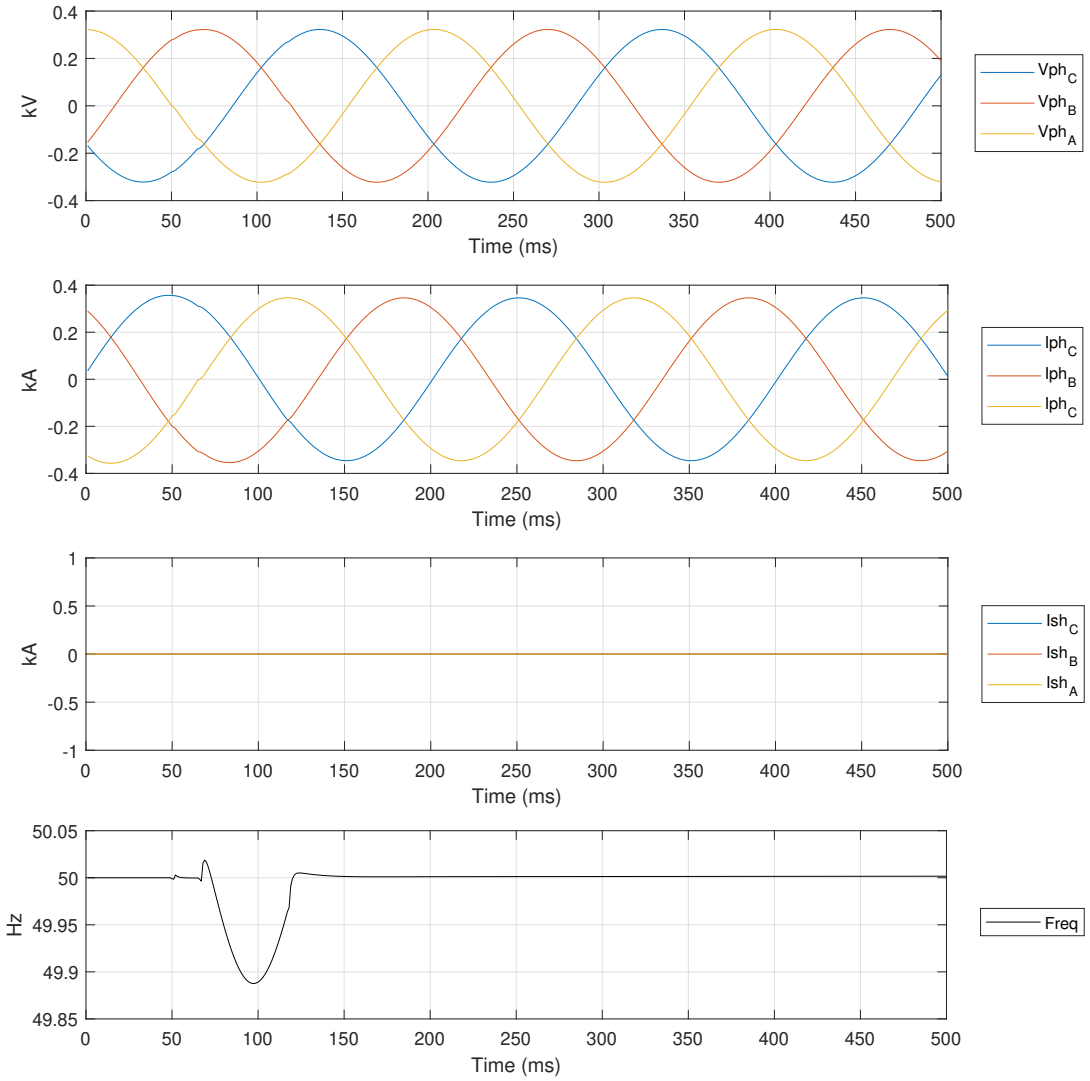

Figure 4.4: NF, Load switching in GC mode

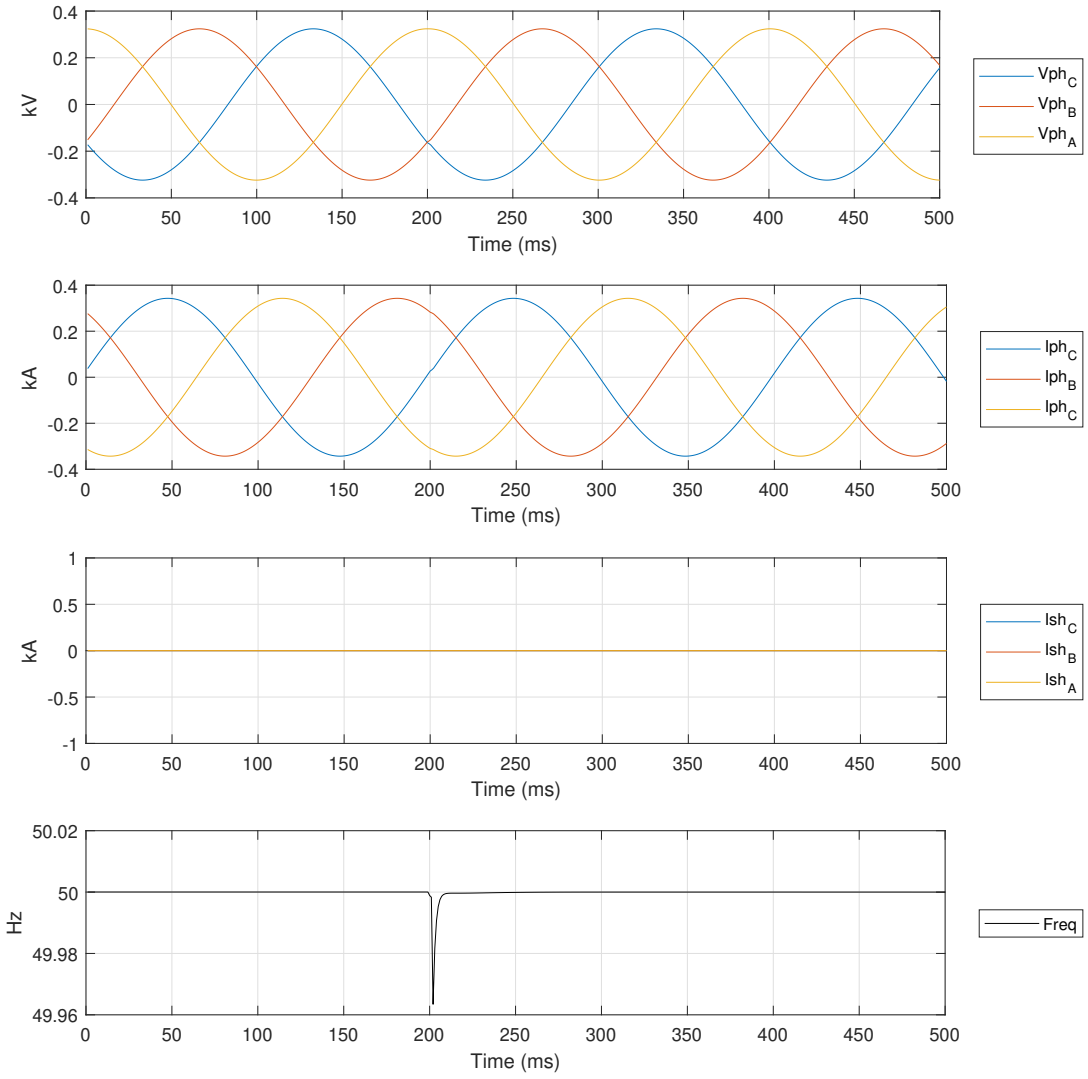

Figure 4.5: AUTO to GC mode switching

For FD, equal sets for different faults are categorised as Fault, while various cases of normal operation, load switching and grig switching are classified as No Fault (NF). On the other hand, FTC data has been organised to classify the fault type and FP. Data for the NF conditions include simulations of connecting and disconnecting 5 kW, 50 kW and 200 kW load in both modes, switching from GC to AUTO and vice-versa with and without load switching. Additionally, simulations without any fault, load or grid switching are also included to differentiate between a fault and NF conditions.

Data collected for symmetrical faults include LLL, LLLN and LLLNG faults. Due to close similarity in collected signals, all cases of symmetrical faults were categorised as LLL. Model misclassification due to high similarity in different symmetrical fault signals is shown in Fig. 4.29.

4.3 Feature Extraction

Feature extraction is a data transformation process that involves selecting or generating a subset of relevant and significant features from the original data. It aims to reduce dimensionality, eliminate noise, enhance the model's robustness against overfitting and retain the most relevant information for model training, leading to more efficient and accurate predictions [182].

4.4 Features Extracted and Techniques Used Including Proposed Novel Techniques

Two novel FE techniques, Peaks Metric and Max Factor are proposed and applied in this research. Additionally, the suitability of using Standard Deviation, First and Second Principal Components [171], Total Harmonic Distortion [158], Kurtosis, Crest Factor, Shape Factor and Skewness [183, 184] to extract useful features is investigated. A total of 100 unique features are obtained.

Kurtosis, Crest Factor, Shape Factor and Skewness are commonly used FE techniques for bearing fault diagnosis but have not been applied before to detect and classify faults in an AC microgrid to the best of the author's knowledge. Moreover, using Principal Component Analysis to detect and classify AC microgrid faults is also not common and was also proposed by the author of this thesis [171].

4.4.1 Standard Deviation

The standard deviation (STD), for a variable vector x composed of N scalar observations is defined as

$$STD(x) = \sqrt{\frac{\sum_{i=1}^{N} (x_i - \bar{x})^2}{(N-1)}} \tag{4.1}$$

where $\bar{x}$ is the mean of x :

$$\bar{x} = \frac{1}{N} \sum_{i=1}^{N} x_i \tag{4.2}$$

Variation in STD of Vph_B for random cases of NF and LL-AB fault is shown in Fig. 4.6. There is a notable difference between fault and NF features, which is desired for training ML classifiers. If the features also called predictors are very closely distributed, the probability of misclassification increases.

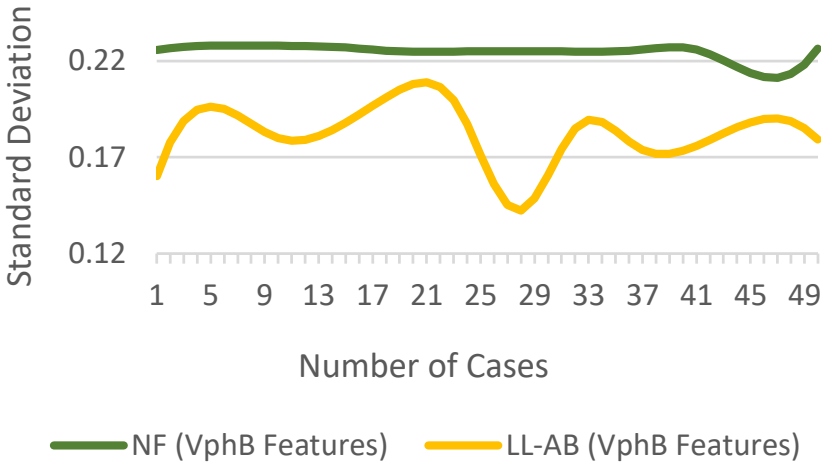

Figure 4.6: STD of Vph_B for NF and fault cases

4.4.2 Peaks Metric

Peaks Metric (PM) is a novel metric proposed in this research and is defined as the ratio of the mean of the peak values $\bar{x}_{peaks}$ in the signal to the mean $\bar{x}$ of the signal. It is a simple yet potentially useful feature extraction technique for analysing signals.

$$PM(x) = \frac{\bar{x}_{peaks}}{\bar{x}} \tag{4.3}$$

where

$$\bar{x}_{peaks} = \frac{1}{N} \sum_{i=1}^{N} x_{peaks_i} \tag{4.4}$$

For C3, LL-AB fault in GC mode, the deviation in $freq$ is shown in Fig. 4.7.

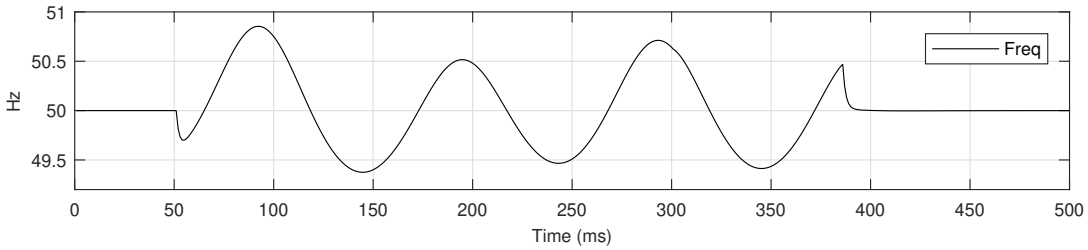

Figure 4.7: $Freq$ deviation for C3, LL-AB fault in GC mode

For the above observation, there are four peaks with values 50.8540, 50.5164, 50.7120 and 50.4684. The $\bar{x}_{peaks}$ is 50.6377, while $\bar{x}$ is 50.0130. For the above case, the value of PM is 1.0125. The difference in PM of $Freq$ for LL-AB fault and NF conditions is shown in Fig. 4.8.

The proposed PM considers all the peaks and takes their mean to represent the signal better, instead of just using the max value.

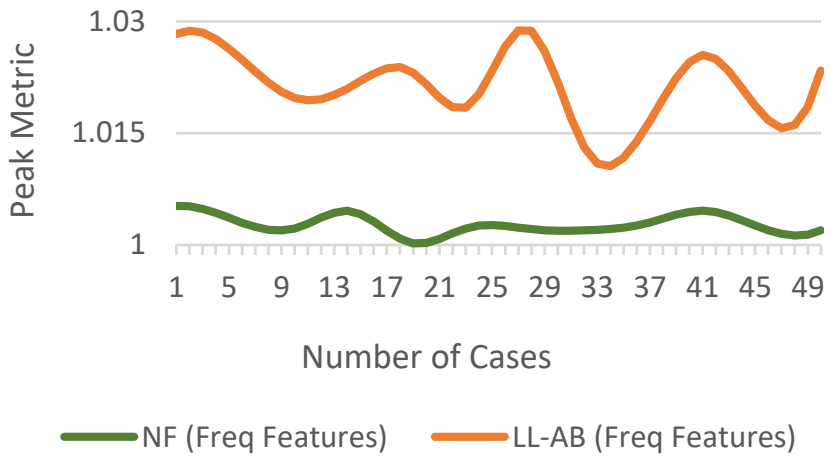

Figure 4.8: PM of $Freq$ for fault and NF conditions

4.4.3 Benefits of Peaks Metric

a. Simplicity and Computationally Efficient: The Peaks Metric is straightforward to compute since it involves only calculating the mean of peak values and the mean of the entire signal. The simplicity of the method makes it easy to implement and computationally efficient, which is especially important when dealing with large datasets or real-time signal processing to detect faults.

b. Detection of Faults and Anomalies: In electrical systems, when a fault occurs, the peaks of the waveform change before there is any significant change in the signal's energy. By extracting the Peaks Metric from the post-fault signal, faults can be detected. A significant deviation in the Peaks Metric from its expected value can indicate the occurrence of a fault.

c. Amplitude-independent Metric: The ratio nature of the Peaks Metric makes it amplitude-independent. This means that the technique normalises the signal's peak characteristics with respect to the signal's overall magnitude. Consequently, it can be more robust when dealing with signals with varying amplitudes, making it suitable for analysing signals from different sources and different fault scenarios.

d. Insensitivity to Noise: While no signal processing technique is entirely immune to noise,

the Peaks Metric exhibits some level of robustness to noise. By calculating the mean of the peak values, the technique is indirectly prioritising the significant components of the signal, which might reduce the impact of noise on the final result.

e. Complementing Existing Techniques: The Peaks Metric can be used in conjunction with other feature extraction methods to enhance the overall performance and accuracy of the predictions.

4.4.4 Max Factor

Max Factor (MF) is the second novel metric proposed in this research and is the ratio of maximum value x_{max} to the absolute value of mean $|\bar{x}|$ of the signal.

$$MF(x) = \frac{x_{max}}{|\bar{x}|} \tag{4.5}$$

For a bolted LG fault on phase B in AUTO mode, three-phase current signals Iph_{ABC} are shown in Fig. 4.9, and the signal for Iph_B is shown separately in Fig. 4.10 to demonstrate the application of proposed metric MF.

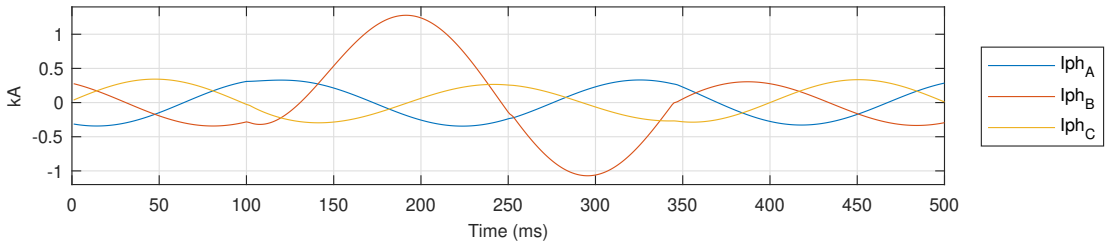

Figure 4.9: Iph_{ABC} for a bolted LG fault on phase B in AUTO mode

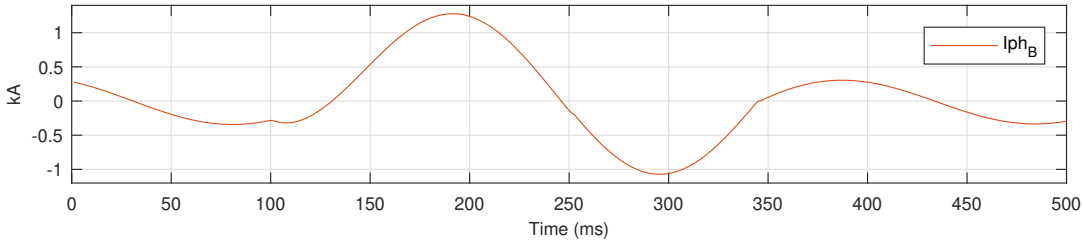

Figure 4.10: Iph_B for a bolted LG fault on phase B in AUTO mode

In Fig. 4.10, the max value of the Iph_B is 1.2775, while $|\bar{x}|$ is 0.0108. For the above case, the value of MF is 117.7036. For the NF case, the max value of the Iph_B is 0.343, while $|\bar{x}|$ is 0.026, resulting in MF of 13.273. The difference in MF of Iph_B for NF and LG-B fault cases is shown in Fig. 4.11.

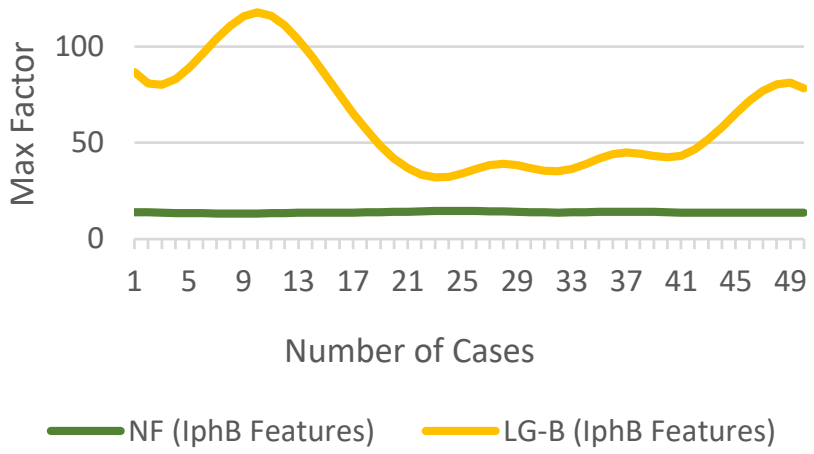

Figure 4.11: MF of Iph_B for NF and fault conditions

4.4.5 Benefits of Max Factor

a. Sensitivity to Fault Magnitude: By calculating the MF of the signal such as for the current signal of a phase, a numerical value that represents how large the maximum current peak is compared to the mean value can be obtained. During a fault, the current waveform can exhibit significant deviations from its normal behaviour. The MF will be high if the fault causes a substantial increase in the maximum current value, indicating the fault magnitude is significant. This sensitivity can help in detecting and assessing the severity of the fault.

b. Identification of Fault Duration: When an LG fault occurs, the fault duration can vary depending on the system characteristics and the fault location. Since the MF considers both the maximum value and the mean of the current signal, it can also provide insights into the duration of the fault. If the fault persists for an extended period, it will result in a higher MF value, while a shorter fault duration might lead to a lower MF value.

c. Differentiation from Normal Operation: During normal system operation, the MF value of the current signal is expected to be relatively stable. When a fault occurs, the MF can act as an indicator of abnormal behaviour, allowing for a clear differentiation between fault conditions and normal operation.

d. Reduced Data Dimensionality: MF can be useful for reducing the dimensionality of data. In electrical systems, signals are often continuous and sampled at high frequencies. By calculating the MF for each fault instance, the behaviour of the signal can be summarised with a single numerical value, making it easier to process and analyse.

e. Simplicity and Computational Efficiency: The MF technique involves basic arithmetic operations (division and mean calculation) and doesn't require complex mathematical modelling or extensive computational resources. This simplicity makes it easy to implement and computationally efficient, making it suitable for real-time fault detection and analysis.

f. Complementing Other Techniques: The MF technique can be used in conjunction with other fault detection and classification methods.

4.4.6 Principal Component Analysis

Principal component analysis (PCA) is a linear dimensionality reduction technique that projects the original features onto a new orthogonal basis, maximising the variance of the projected data. It identifies the principal components, which are linear combinations of the original features that capture most of the data's variability. By selecting a subset of principal components, PCA reduces the dimensionality while retaining the essential information [185], which improves processing time for ML and avoids overfitting the model.

Related equations have been presented in Chapter 3. The difference in pc_1 for Vph_A for NF and LLG-AB fault scenarios is shown in Fig. 4.12.

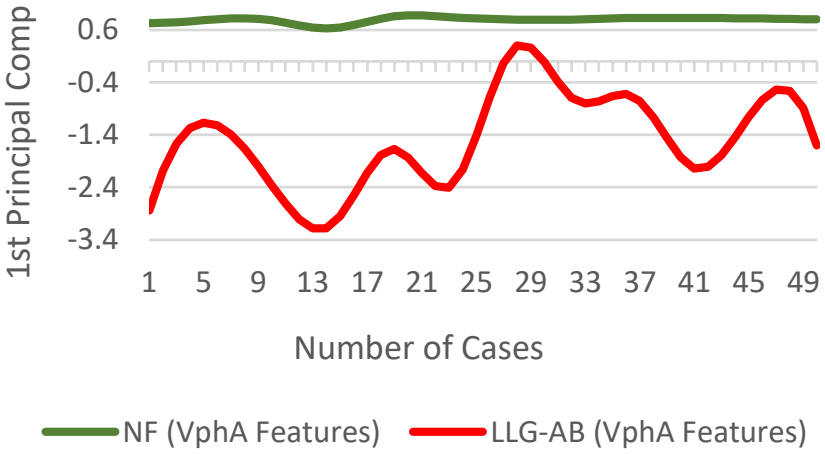

Figure 4.12: pc_1 of Vph_A for NF and fault scenarios

4.4.7 Kurtosis

The Kurtosis ($Kurt$) of a signal x is defined in (12) [184].

$$Kurt(x) = \frac{\frac{1}{N}\sum_{i=1}^{N}(x_i - \bar{x})^4}{\left[\frac{1}{N}\sum_{i=1}^{N}(x_i - \bar{x})^2\right]^2} \tag{4.6}$$

The $Kurt$ of the normal distribution is 3. A fault in the system will change the value, greater than or less than 3. The difference in $Kurt$ for Iph_B for NF and LLL fault cases is shown in Fig. 4.13.

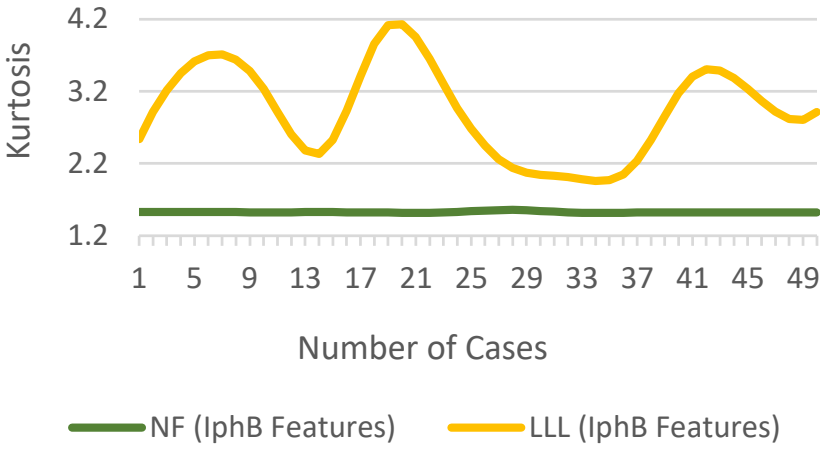

Figure 4.13: $Kurt$ of Iph_B for NF and fault cases

4.4.8 Crest Factor

Crest Factor ($CRES$) is the ratio of the maximum absolute value to the RMS [184].

$$CRES(x) = \frac{x_m}{x_{rms}} \tag{4.7}$$

where x_m is the maximum absolute value of the signal:

$$x_m = \max_i |x_i| \tag{4.8}$$

and x_{rms} is:

$$x_{rms} = \sqrt{\frac{1}{N}\sum_{i=1}^{N} |x_i|^2} \tag{4.9}$$

The $CRES$ of a sinusoidal current waveform for purely resistive load is 1.414. Fig. 4.14 show the difference in $CRES$ of Iph_A for NF and LLL fault condition.

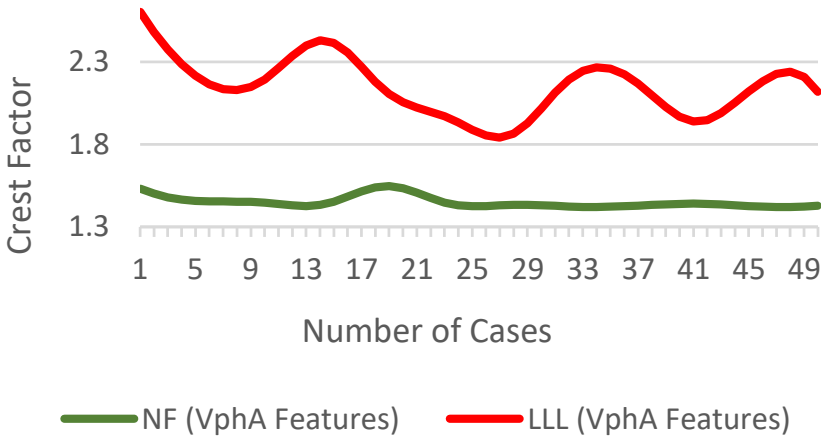

Figure 4.14: $CRES$ of Iph_A for NF and fault conditions

4.4.9 Shape Factor

Shape Factor (SF) is the ratio of RMS to the mean of the absolute value [183]. The SF is independent of the signal dimensions, but it relies on the signal shape.

$$SF(x) = \frac{x_{rms}}{\frac{1}{N}\sum_{i=1}^{N}|x_i|} \tag{4.10}$$

Fig. 4.15 shows the difference in SF of Vph_C for NF and LL-CA fault cases.

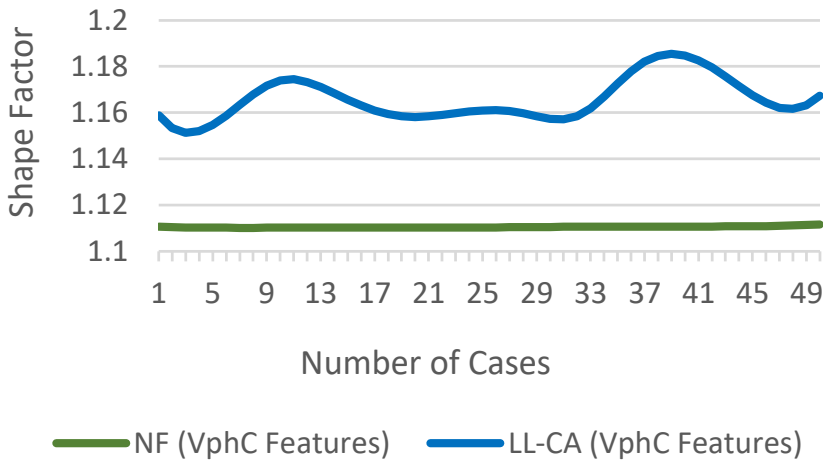

Figure 4.15: SF of Vph_C for NF and fault cases

4.4.10 Total Harmonics Distortion

The THD is the amount of distortion in the signal compared to the undistorted signal. It is defined as the ratio of the square root of the summation of all harmonics squared (from second harmonic) over the fundamental component [158]. THD is an essential measure in power systems. A lower value gives lower peak currents, higher power factor and system efficiency.

$$THD(x) = \frac{\sqrt{\sum_{n=2}^{\infty} x_n^2}}{x_1} \tag{4.11}$$

where x_n is the n-th harmonic of x and x_1 is the fundamental component. THD difference of Vph_C for NF and LG(C) fault cases is shown in Fig. 4.16.

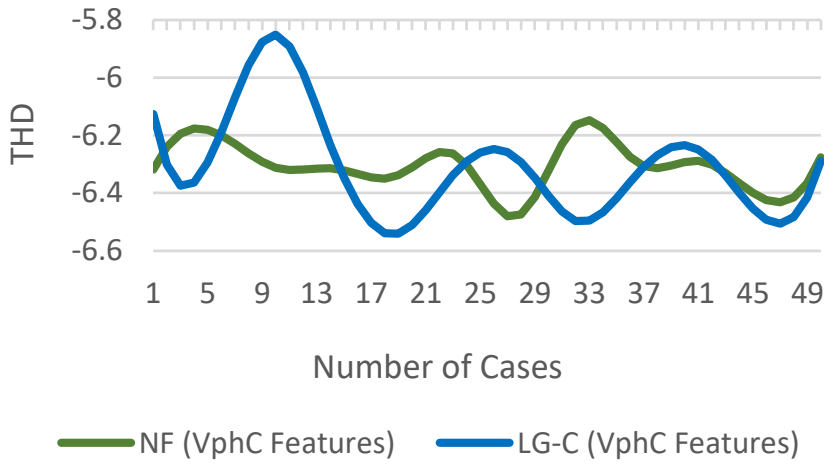

Figure 4.16: THD of Vph_C for NF and fault cases

4.4.11 Skewness

The skewness ($Skew$) shows the irregularity of signal distribution [184]. Distribution symmetry can be impacted by faults resulting in an increased level of skewness.

$$Skew(x) = \frac{\frac{1}{N}\sum_{i=1}^{N}(x_i - \bar{x})^3}{\left[\frac{1}{N}\sum_{i=1}^{N}(x_i - \bar{x})^2\right]^{3/2}} \tag{4.12}$$

The difference in $Skew$ of phase C for NF and LLG(CA) fault conditions is shown in Fig. 4.17.

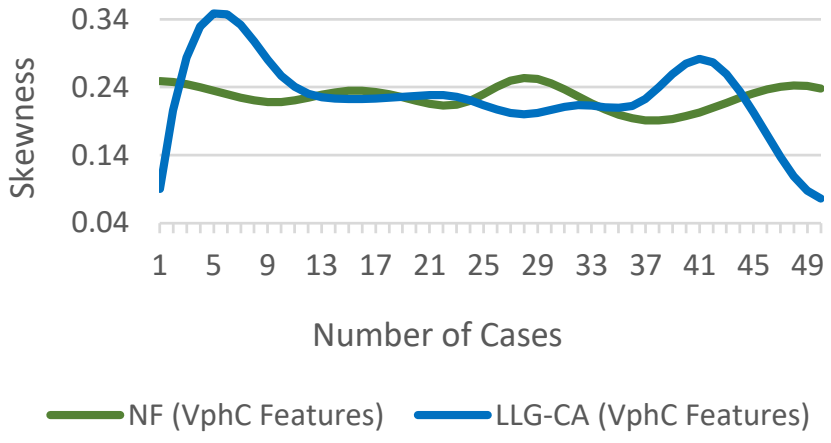

Figure 4.17: $Skew$ of Vph_C for NF and fault scenarios

4.5 Feature Selection

Feature selection (FS) is the process of reducing features or predictors to provide the best predictive power in modelling a set of data, as not all features are useful. The goal is to find the fewest possible features with the highest possible accuracy. Finding the best features essentially remains an iterative process and requires deep domain knowledge. Feature selection aids in improving the speed and accuracy of prediction [182] as it:

a. Prevents overfitting: modelling with many features can make the model more susceptible to specific observations in training data.

b. Reduces model size: fewer features increase computational performance and

c. Improves accuracy: reduced possibility of overfitting and fast processing improves predictive accuracy of ML model.

4.5.1 Parallel Coordinates Plot

Firstly Parallel Coordinates plot (PCP) [186, 187] is used to explore the features to be included. PCP is a powerful visualisation technique commonly used in feature selection and data analysis. It allows comparing the behaviour of multiple variables simultaneously, making it easier to identify patterns, relationships, and potential feature importance.

For a dataset with N samples and M features. Each sample is represented by a vector of M feature values:

$X_i = (x_{i1}, x_{i2}, \ldots, x_{iM})$

Each x_{ij} is a real-valued feature for the i-th sample and the j-th feature, where $i = 1, 2, \ldots, N$ denotes the sample index and $j = 1, 2, \ldots, M$ denotes the feature index.

To normalise the values of each feature to fit within the same range, min-max scaling is used. The min-max scaling equation for a specific feature j is given by:

$$x'_{ij} = \frac{x_{ij} - \min(x_j)}{\max(x_j) - \min(x_j)} \tag{4.13}$$

where x'_{ij} is the scaled and x_{ij} is the original value of the j-th feature for the i-th sample, min (x_j) and max (x_j) are the minimum and maximum values of the j-th feature across all samples. After getting the scaled values, the Parallel Coordinates plot is obtained. The misclassified points and respective predictors are also visible on the PCP as shown in Fig. 4.18.

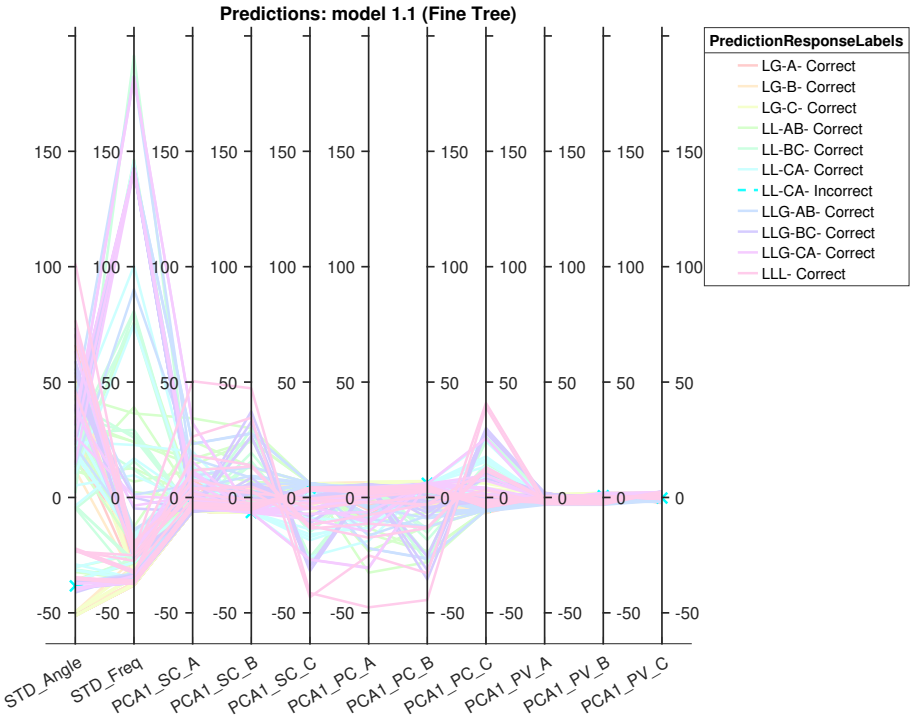

Figure 4.18: Parallel Coordinates Plot for Fine Tree

4.5.2 Kruskal-Wallis H-Test

After shortlisting features using PCP, features are ranked using the Kruskal-Wallis H-Test (KW) [188]. The Kruskal-Wallis H-Test is a non-parametric statistical test used for feature selection when dealing with multiple groups or categories. It allows the comparison of the distributions of multiple independent groups to determine if there are significant differences among them. The test statistic for the Kruskal-Wallis H-Test is given by:

$$H = \frac{12}{n(n+1)} \sum_{i=1}^{k} \frac{R_i^2}{N_i} - 3(n+1) \tag{4.14}$$

where N_i is the number of observations, while R_i is sum of ranks of observations in group i and is given by:

$$R_i = 1 + \sum_{j=1}^{N_i - 1} t_j \tag{4.15}$$

T_i is the Tie correction factor for group i and is given by:

$$T_i = \frac{(N_i^3 - N_i)}{12} \tag{4.16}$$

t_j = number of tied observations in the j-th tied group

The Kruskal-Wallis H-Test is based on the ranks of the values of the predictor variable X within each group. It computes the sum of squared ranks for each group, adjusts for tied ranks, and then combines them to obtain the test statistic H, which follows a chi-squared distribution with degrees of freedom equal to $k - 1$ ($df = k - 1$).

The top 18 features for FD ranked using the Kruskal-Wallis H-Test are shown in Fig. 4.19.

Figure 4.19: Feature ranking for FD using KW

Additionally, estimates of predictor importance for the classification ensemble methods are

also computed by summing the estimates over weak learners in the ensemble for each input predictor. A high value indicates that this predictor is important. Predictor importance for FD using Bagged Trees (BT) ensemble, where bagging is short for bootstrap aggregation [189] is shown in Fig. 4.20.

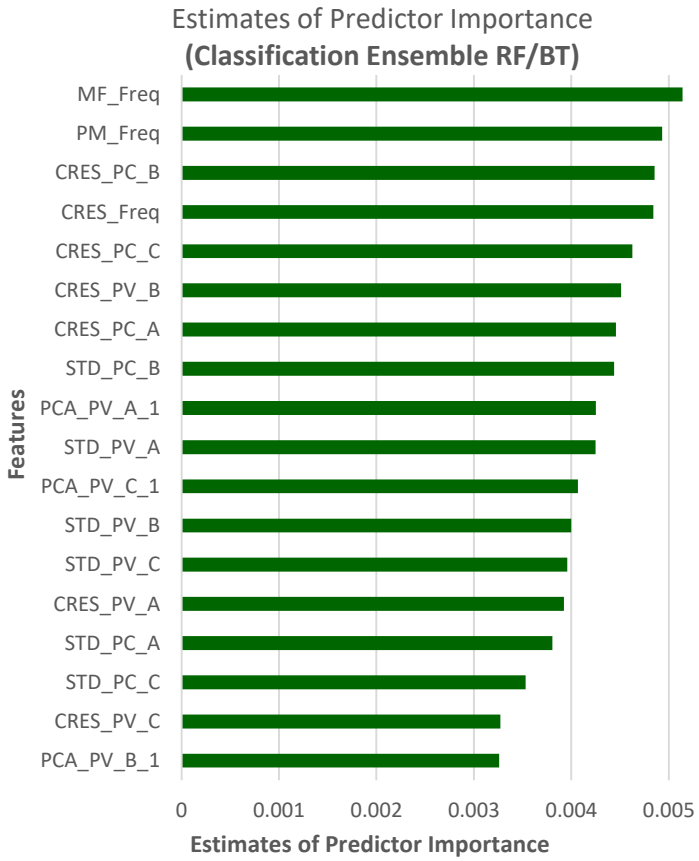

Figure 4.20: Predictor importance for FD using BT/RF

4.6 Application of Machine learning

The signals are pre-processed and labelled, before extracting latent features by applying standard deviation, principal component analysis, peaks metric and max factor. Only the first and second principal components are used to capture the patterns in the data. A separate set of features are obtained for FD and FTC with FP identification.

The top 25 features were initially selected to train 35 classification learners for FD and FTC with FP. These include Classification Ensembles, Naive Bayes, Neural Networks, Discriminant

Analysis, Support Vector Machine (SVM), Classification Trees and k-nearest neighbours (KNN) [190]. 10-fold cross-validation (CV) is applied to the training dataset to protect against over-fitting. Hyperparameter tuning of all models was performed to improve accuracy. Predictions were made using unseen data.

The obtained predictors are fed to different SML classifiers, followed by hyperparameter tuning to obtain the best performing models. The trained models are then tested on new data. The complete process of training and testing is illustrated in Fig. 4.21.

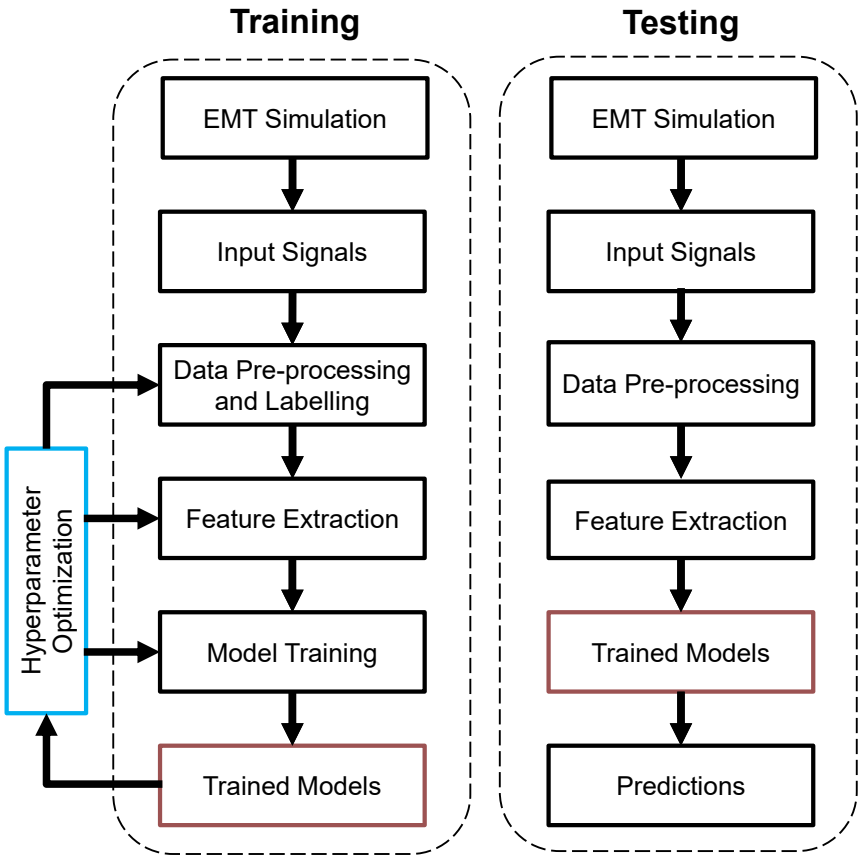

Figure 4.21: Training and testing process of ML Models

Amongst other learners, neural networks with a varying number of layers and neurons are also applied. Model and plot of a bi-layered feed-forward network (FNN), with 10 sigmoid hidden and 2 softmax output neurons are shown in Fig. 4.22 and Fig. 4.23.

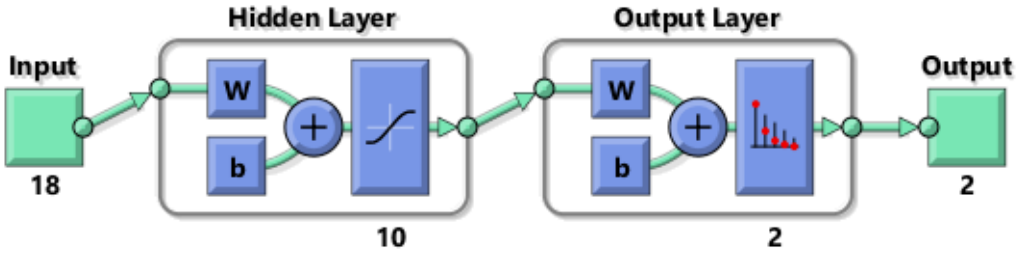

Figure 4.22: Bi-layered FNN model

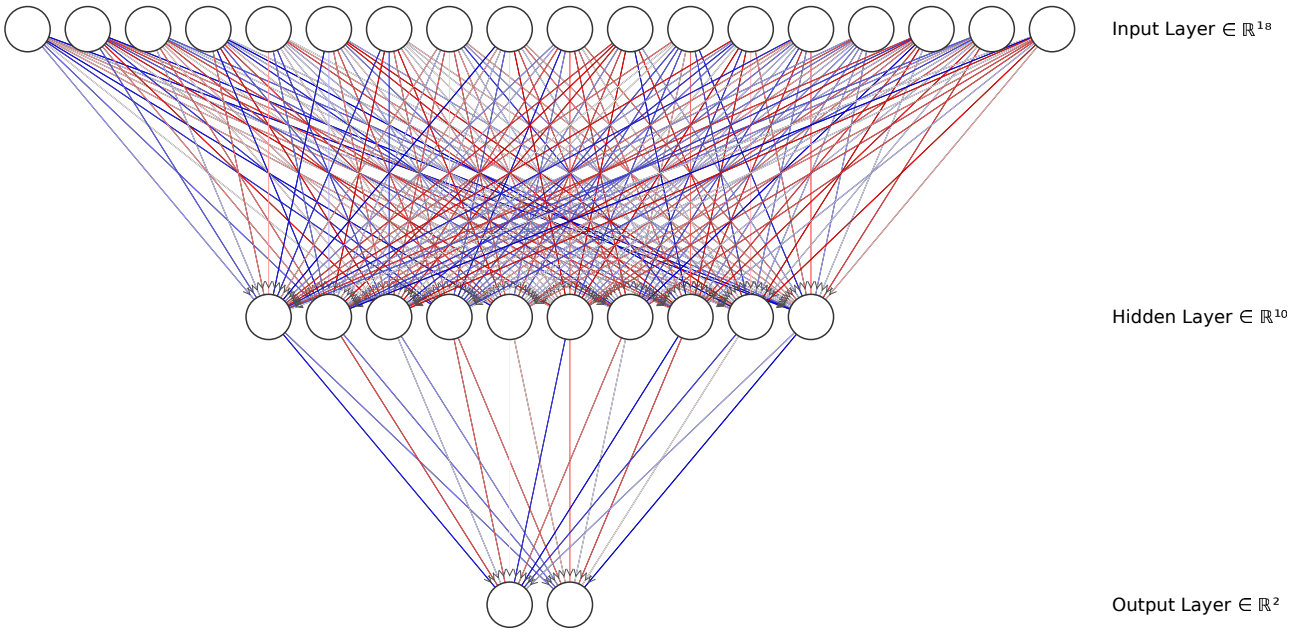

Figure 4.23: Bi-layered FNN plot

4.6.1 Training and Testing ML Models for FD

The top 5 models with CV and test accuracy for FD are shown in Table 4.1.

Table 4.1: Accuracy of ML models with 25 features for FD

Model	CV accuracy	Test accuracy
BT	100%	99%
Gaussian Naive Bayes	100%	98%
KNN (Euclidean)	96%	94%
Neural Network (Bilayered)	95%	91%
Decision tree (Fine)	94%	90%

BT outperformed all other ML classifiers. For FD, the BT model with optimal hyperparameters grows 488 individual trees. The view of one of the trees with randomly selected features is shown in Fig. 4.24.

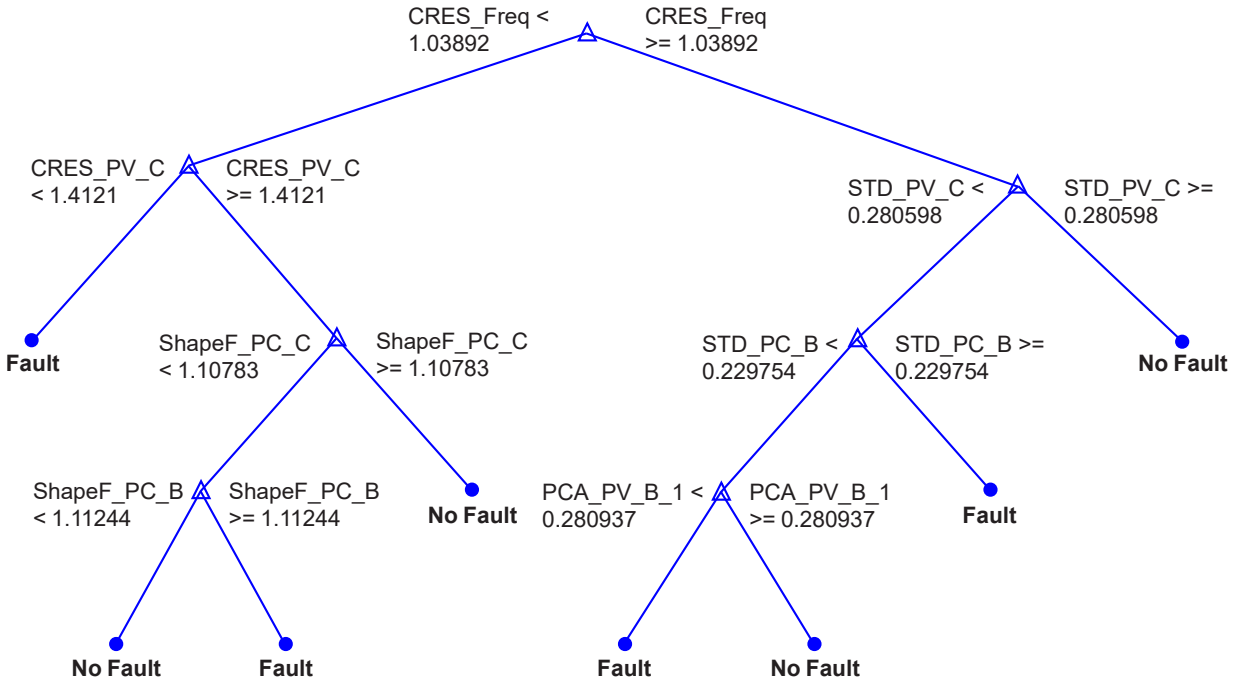

Figure 4.24: View of 4th Tree with 7 branches and 15 nodes

The accuracy of ML models with further reduction in the number of features for FD and FTC with FP was also investigated. Model accuracy dropped sharply for less than 18 predictors. The best combination of 18 predictors for FD include 3 predictors obtained by STD of Vph_{ABC}, 9 using pc_1 of Ish_{ABC}, Iph_{ABC} and Vph_{ABC}. The remaining 6 include $CRES$ of Ish_{ABC}, MF of

the $Angle_{VI}$ and MF and PM of $Freq$. The accuracy for the top 5 models with 18 predictors is presented in Table 4.2.

Table 4.2: Accuracy of ML models with 18 features for FD

Optimized BT	100%	100%
Optimized GB	100%	99%
Gaussian Naive Bayes	100%	98%
Optimized KNN (Cosine)	98%	96%
Neural Network (Bilayered)	96%	93%

With 18 features, BT displayed the highest test accuracy, while the second-best was optimised GentleBoost (GB) [191], which only misclassified 1 out of 90 observations, where a NF was classified as a fault, resulting in a false alarm. GB Test confusion matrix (CM) for FD is shown in Fig. 4.25.

4.6.2 Training and Testing ML Models for FTC with FP identification

Likewise, for FTC with FP identification, to begin with, 25 predictors were used. The top 5 models with 10-fold cross-validation and test accuracy are shown in Table 4.3.

Table 4.3: Accuracy of ML models with 25 features for FTC with FP

Bagged Trees	100%	100%
Decision Tree (Fine)	99%	98%
Optimized SVM (Linear)	97%	95%
Neural Network (Wide)	97%	92%
Linear Discriminant	95%	90%

The BT Test CM for FTC with FP is shown in Fig. 4.26.

More reduction of features to 18 for FTC was also explored. These included 6 obtained by STD of Vph_{ABC} and Iph_{ABC}, 9 using pc_1 of Ish_{ABC}, Iph_{ABC} and Vph_{ABC}. The remaining 3 include $CRES$ of Ish_{ABC}. Test accuracy for top 5 models is shown in Table 4.4.

For FTC, the optimised BT model has 271 trees. The view of one of the trees for this model is shown in Fig. 4.27.

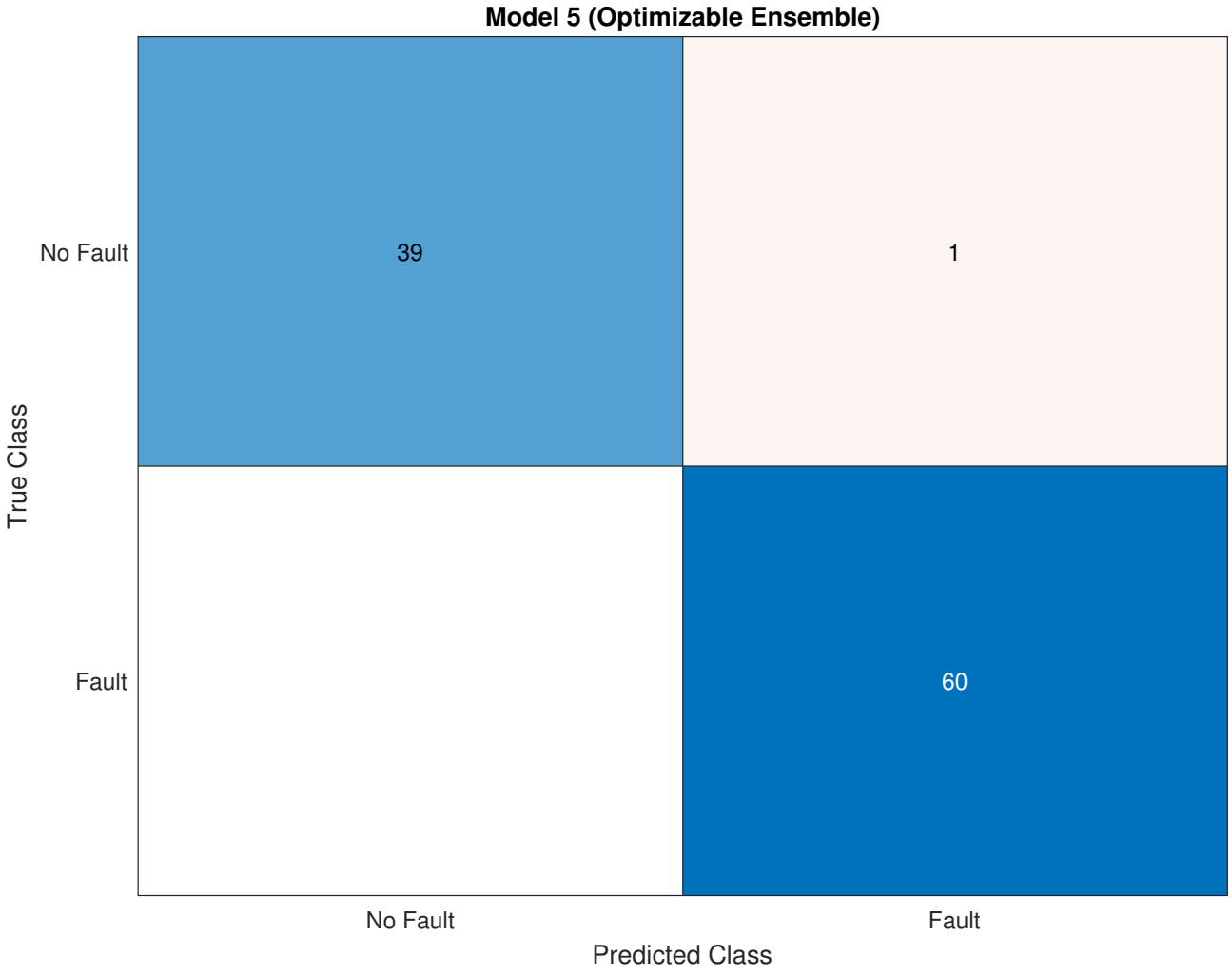

Figure 4.25: GB Test CM for FD

Table 4.4: Test accuracy of ML models with 18 features for FTC with FP

Optimized BT	100%	99%
Decision Tree (Fine)	99%	98%
Optimized SVM (Gaussian)	97%	95%
Neural Network (Wide)	95%	91%
Linear Discriminant	94%	89%

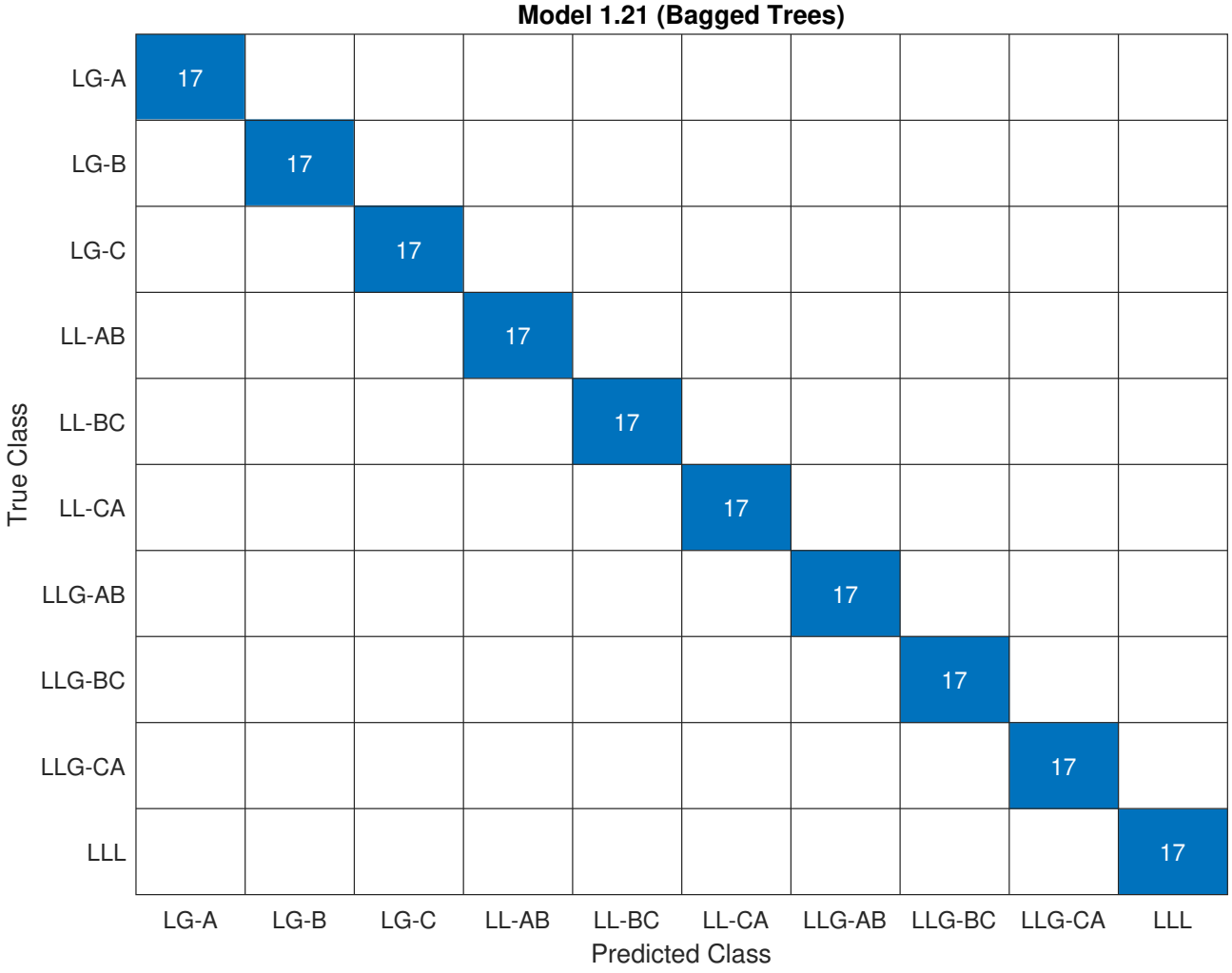

Figure 4.26: BT Test CM for FTC with FP

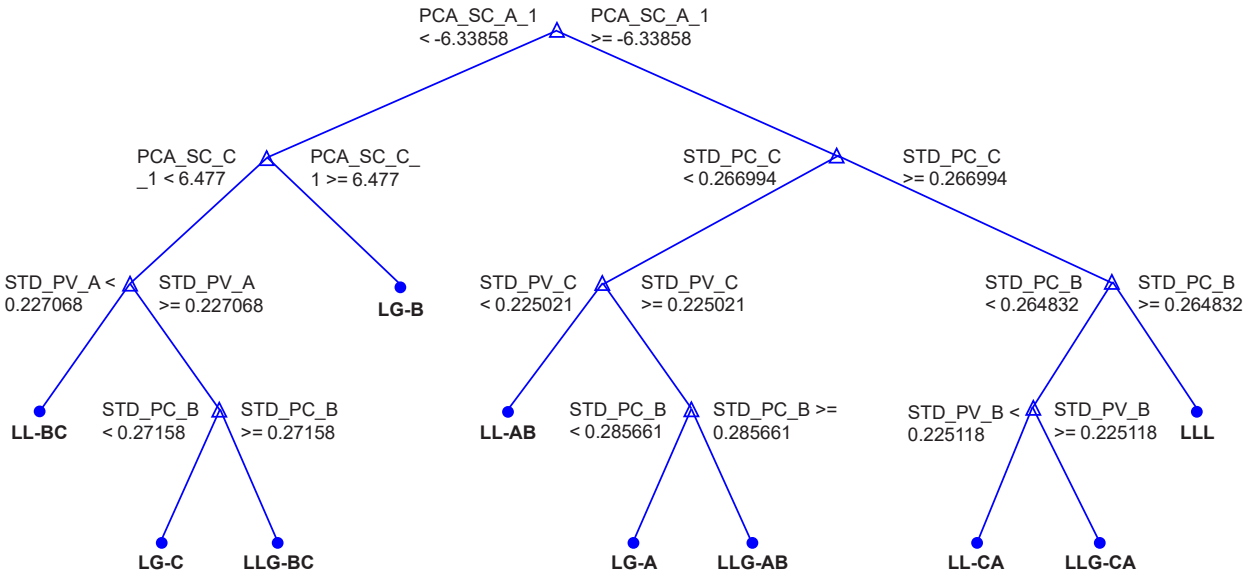

Figure 4.27: View of 20th Tree with 9 braches and 19 nodes

Hyperparameter tuning of SVM model with 18 predictors is shown in Fig. 4.28.

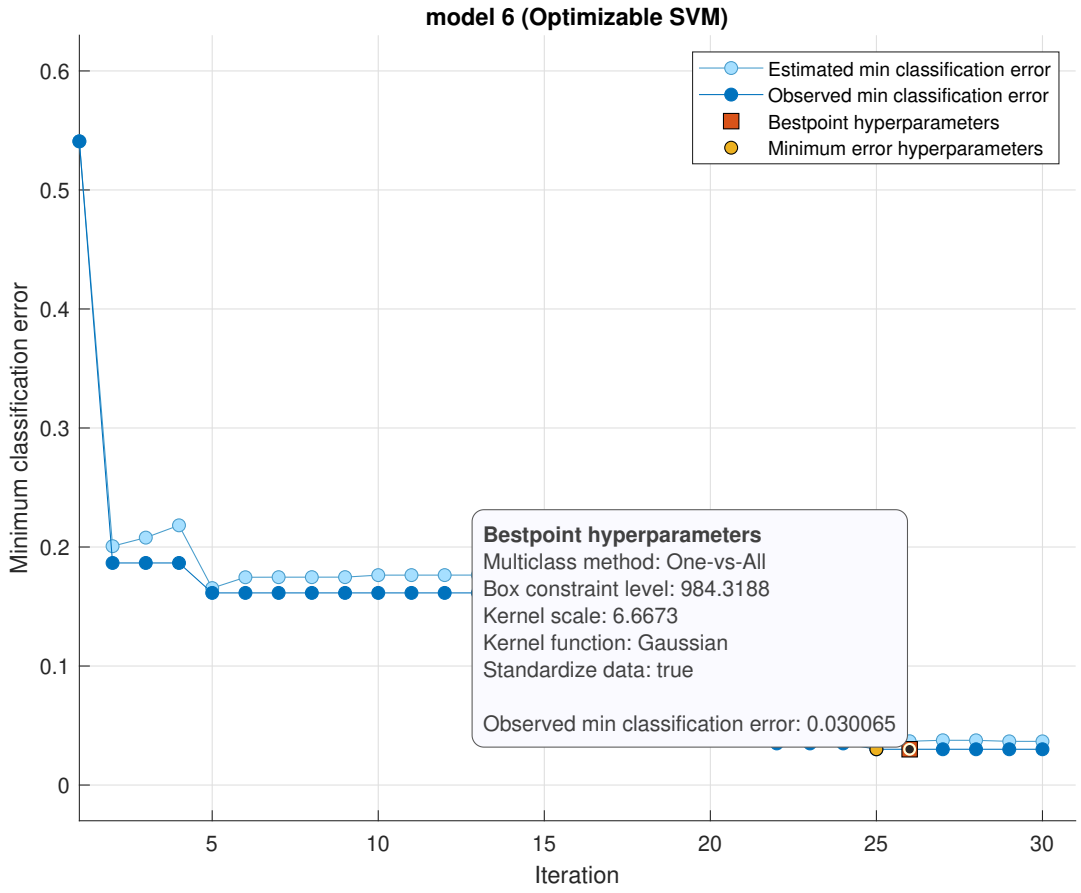

Figure 4.28: Minimum classification error plot for Optimizable SVM with 18 predictors

As mentioned in Sec. 4.2, data collected for symmetrical faults include LLL, LLLN and LLLNG faults and is very similar. The models missclassified them due to high similarity as shown in Fig. 4.29. Therefore all cases of symmetrical faults are categorised as LLL in further classification.

4.6.3 Detail Levels of Classification

The ML models were tested for level 4 and level 5 classification. The testing process began by first detecting faults, then identifying the fault type, and then determining the faulted phase. The models were also used to categorise test cases involving faults with varying resistance and reactance values. Test results of accurate detail classification of LG and LLG fault cases are shown in Fig. 4.30 and Fig. 4.31.

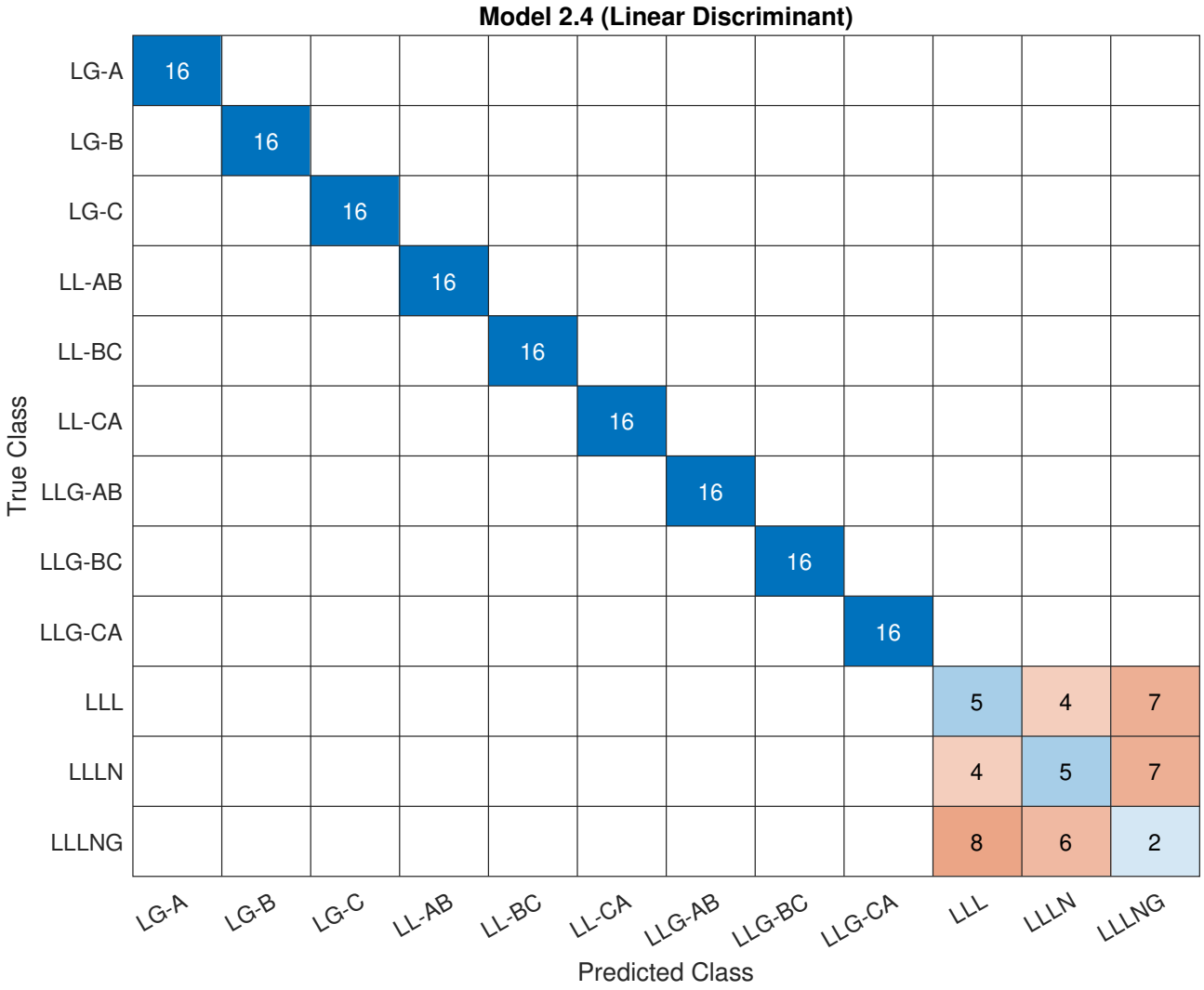

Figure 4.29: Misclassification of symmetrical faults

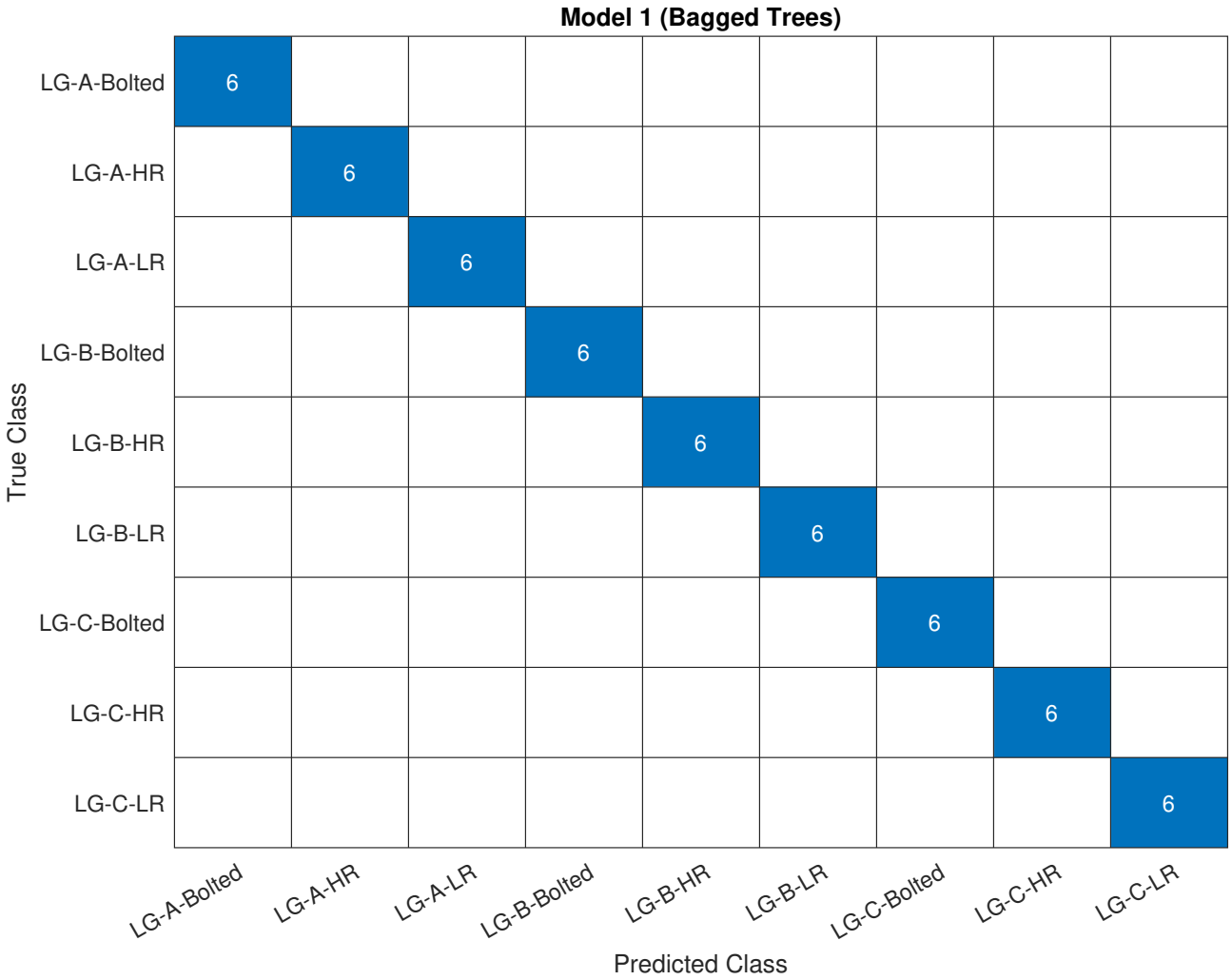

Figure 4.30: Classification of LG faults cases

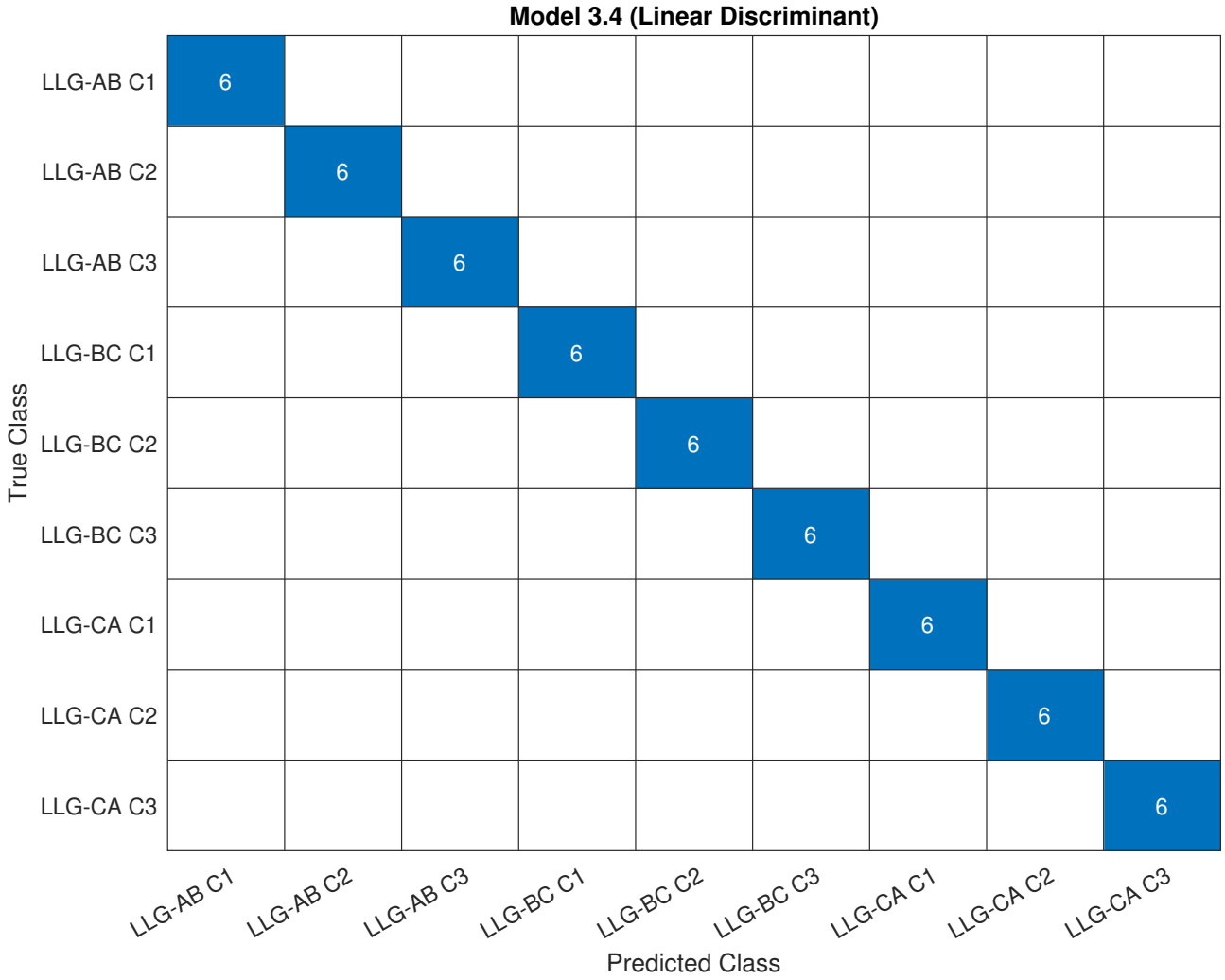

Figure 4.31: Classification of LLG faults cases

Detail classification also included identifying the mode of microgrid operation when a fault occurs, with reasonable accuracy, as shown in Fig. 4.32. Such detail and accurate classification will be helpful in future grids as well as in rectifying and repairing permanent faults quickly

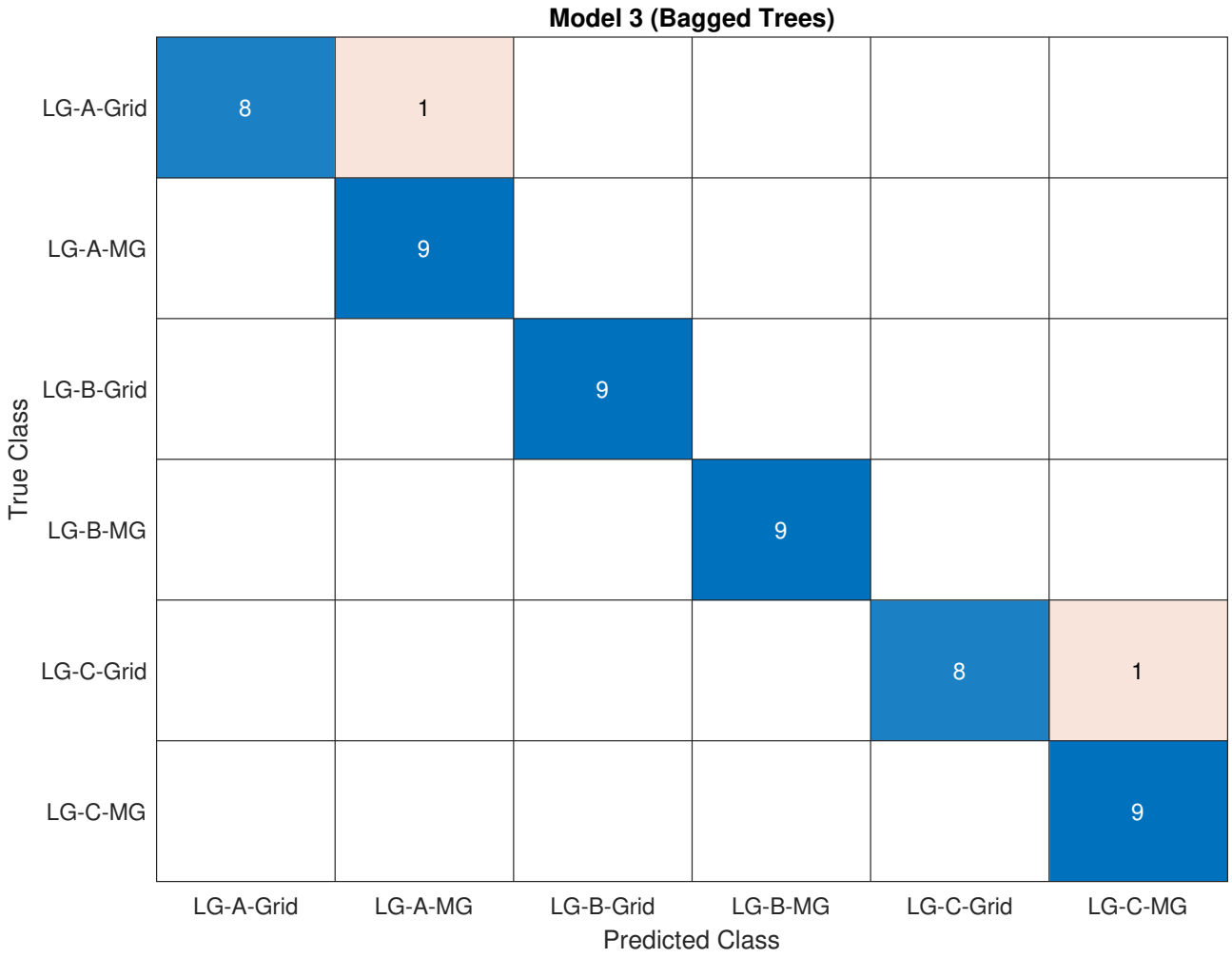

Figure 4.32: Classification based on mode of operation

4.7 Summary

In this chapter, datasets of various fault signals and features for FD and FTC are built and presented. Different signals for fault and no-fault data in grid-connected and autonomous modes of a microgrid for wide variations in operating conditions are obtained through EMT simulations for radial topology. After retrieving and pre-processing the signals, different feature extraction techniques, including new factors, Peaks Metric, and Max Factor, are applied. They are reduced using PCP, then ranked using the Kruskal-Wallis H-Test to identify the best-performing features, besides estimating predictor importance for ensemble ML classification. A new dataset is built using the best-performing features for FD and FTC with FP identification. These reduced features are input to training and testing 35 classification learners for FD and FTC with FP identification. These include Classification Ensembles, Naive Bayes, Neural Networks, Discriminant Analysis, Support Vector Machine (SVM), Classification Trees and k-nearest neighbours (KNN). 10-fold cross-validation is applied to the training dataset to protect against overfitting. Hyperparameter tuning of all models was performed to improve accuracy. Trained ML models are tested on an unseen dataset to check the accuracy of predictions. The Bagged Trees ensemble classifier outperformed all other ML classifiers for FD and FTC.

Chapter 5

Fault Detection and Classification in Radial and Meshed Microgrid using Hybrid Deep Learning

5.1 Introduction

A promising approach to solving protection challenges in microgrids is to use deep learning (DL) techniques. DL uses artificial neural networks to learn from the data. Techniques based on DL can be used to develop more accurate and robust protection systems for AC microgrids. DL models can learn to identify the spatial and temporal features from fault signals, which can be used to detect and distinguish between different types of faults.

DL has several advantages over other SML methods. DL algorithms can automatically extract features from data without human supervision, which most SML methods require. Additionally, it has the ability to handle large and complex datasets and often performs better compared to other SML.

Preparing to submit the contents of this chapter in M. Uzair, L. Li, J. G. Zhu, "Hybrid deep learning based microgrid protection", *IEEE Transactions on Power Delivery*.

Syed Basit Ali Bukhari, Assistant Professor at Department of Electrical Engineering, The University of Azad Jammu & Kashmir, Muzaffarabad Pakistan has helped in collecting fault and no-fault data.

5.2 Fault Detection Using Artificial Intelligence

Numerous studies have explored the application of AI for FD in power systems. In [192] a DNN is used to identify faults in the power system. Active, reactive power, three-phase voltage and current signals are collected, processed and sent to auto-encoders, which prepare and train a DNN. Similarly, a deep learning-based FD method for DN is proposed in [193]. The fault signal is decomposed using Daubechies 3 wavelet, and then normalized sub-band energy is fed to the self-encoding neural network to classify faults.

Moreover, LSTM and SVM are used for FD in [194]. Signals used as input include current, voltage and active power. Likewise, an LSTM-based method to protect a meshed DN is proposed in [195]. Various time-series signals are used as input, including three-phase RMS current and voltage and sequence components for current and voltage.

A CNN-based fault protection strategy is proposed in [196]. It integrates the feature extraction and classification processes by directly applying three-phase current signals as inputs to three CNNs. Different CNN architectures are proposed for fault detection, fault-type classification, and estimating location. On the other hand, in [197] a time-time transform is employed to extract features from post-fault current samples, which are used to train a deep belief network.

On the contrary, a protection strategy to distinguish between symmetrical line and PV array faults based on DNN and sparse autoencoder is presented in [198]. Current and voltage signals are transformed into images and used as input to the sparse autoencoder. While fault location in a radial distribution system was determined using μPMU measurements and stack auto-encoder in [199]. Notably, only single line-to-ground faults were considered in this research work. In a different study, an adaptive CNN was employed to locate and classify the fault using data from PMUs in [200]. Likewise, the fault classification in the modified IEEE 13-bus radial distribution feeder was carried out using CNN and LSTM in [201].

Conversely, a method for islanding detection in microgrids is proposed in [202]. The method uses a multi-layer LSTM network to learn the patterns of harmonic distortion in the voltage and current signals at the PCC. The LSTM network is able to detect islanding events with

high accuracy, even in the presence of distorted grid voltage. The proposed multi-layer LSTM network should be investigated for fault detection.

5.3 Methodology

A hybrid deep learning-based protection system (HDLBPS) is proposed in this chapter. Deep CNN (DCNN) is used to extract the spatial features from the fault signals, while deep LSTM (DLSTM) is used to extract the temporal features. Rectified linear unit activation function and dropout layers are used to prevent overfitting.

5.3.1 Microgrid Test System

In order to validate the efficacy of the developed protection method, a standard IEC microgrid, as depicted in Fig. 5.1, is modelled. The parameters for the network and load are taken from [196]. The microgrid operates at 25 kV. There are two synchronous DERs and two inverter-interfaced DERs connected through step-up transformers. The control scheme implemented for I inverter-interfaced DERs is taken from [203]. The microgrid can transition between meshed and radial configurations through circuit breakers CB-Loop-1 and CB-Loop-2. Moreover, the microgrid can switch to islanded or grid-connected modes through the CB before PCC Bus-1.

Table 5.1: DER and Transformer Data for IEC Test Microgrid

Equipment	**Rating**	**Voltage**
TR1	20MVA	120/25 kV
TR2, TR3	5MVA	25/2.4 kV
TR4, TR5	4MVA	25/0.575 kV
DER-1, DER-2	4MVA	99.62%
DER-3, DER-4	3MVA	0.575 kV

5.3.2 Data Collection

A large number of fault and NF cases have been simulated to evaluate the efficacy of the proposed HDLBPS. The evaluation encompasses fault detection and classification of fault types with faulted phases. Three-phase current signals are obtained for fault and NF cases.

Fault Data

To generate the necessary fault data, simulations are carried out using a standard IEC microgrid model, depicted in Fig. 5.1. The simulations incorporated ten different types of faults with variations in fault location, resistances, loads, distribution lines, operating modes, and topology.

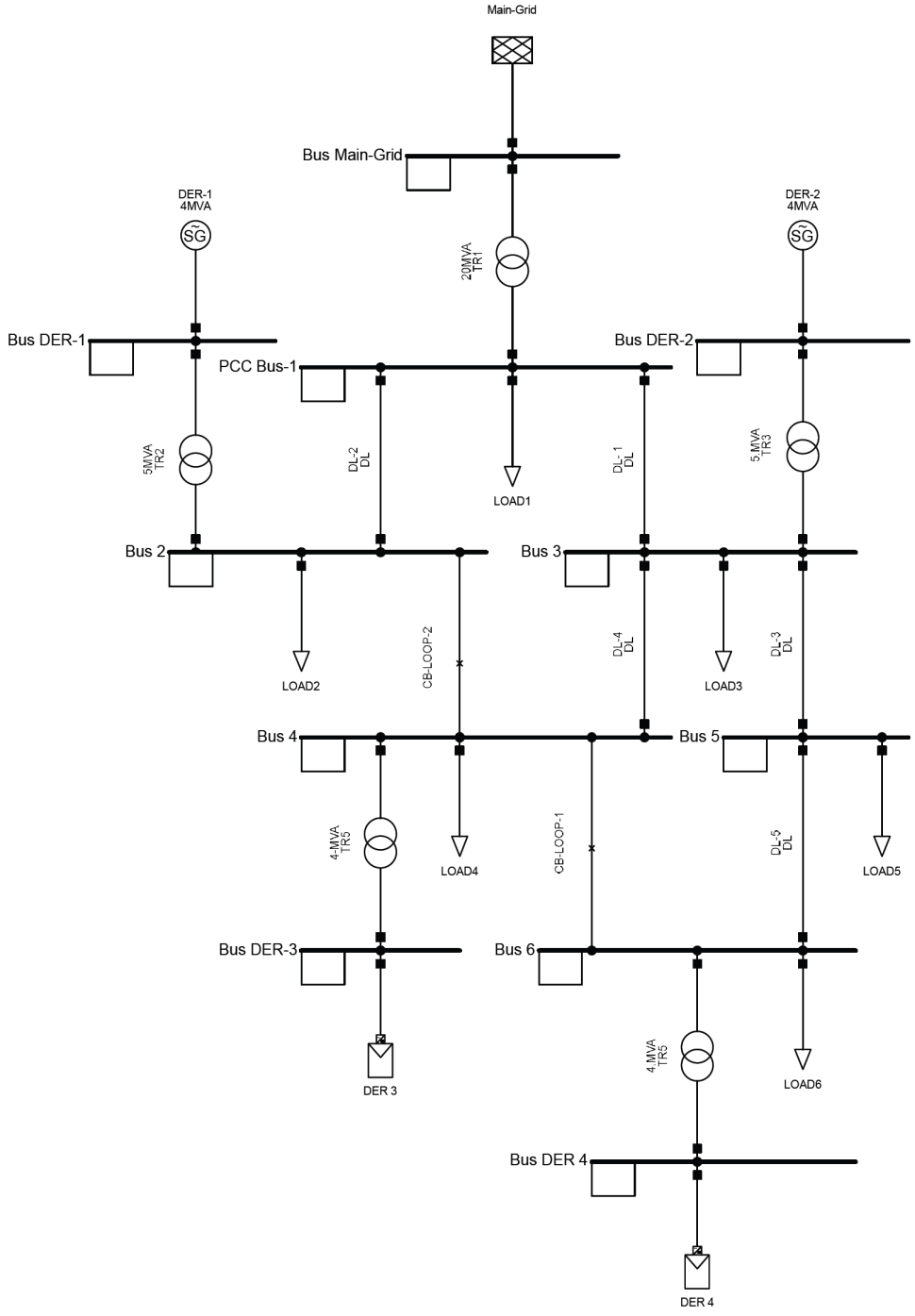

Figure 5.1: IEC Microgrid

A total of 16,000 fault cases are simulated. DER and transformer data is presented in Table 5.1, while the description of the simulated fault is presented in Table 5.2.

Table 5.2: Fault Cases

Parameters	**Count**
Fault on different lines (DL1-DL5)	5
Fault location (10, 25, 50, 75 and 95%)	5
Fault resistance (0.01, 10, 50 and 80 Ω)	4
Fault inception angle (0, 45, 90 and 180°)	4
Operational mode (GC/AUTO)	2
Topology (Radial/Meshed)	2
Fault types (LG, LL, LLG, LLL)	10
Total simulated Fault cases	**16000**

Fig. 5.2 - Fig. 5.5 shows three-phase current signals for some of the fault cases, while Fig. 5.6 demonstrates the 64 samples used for training the HDL model.

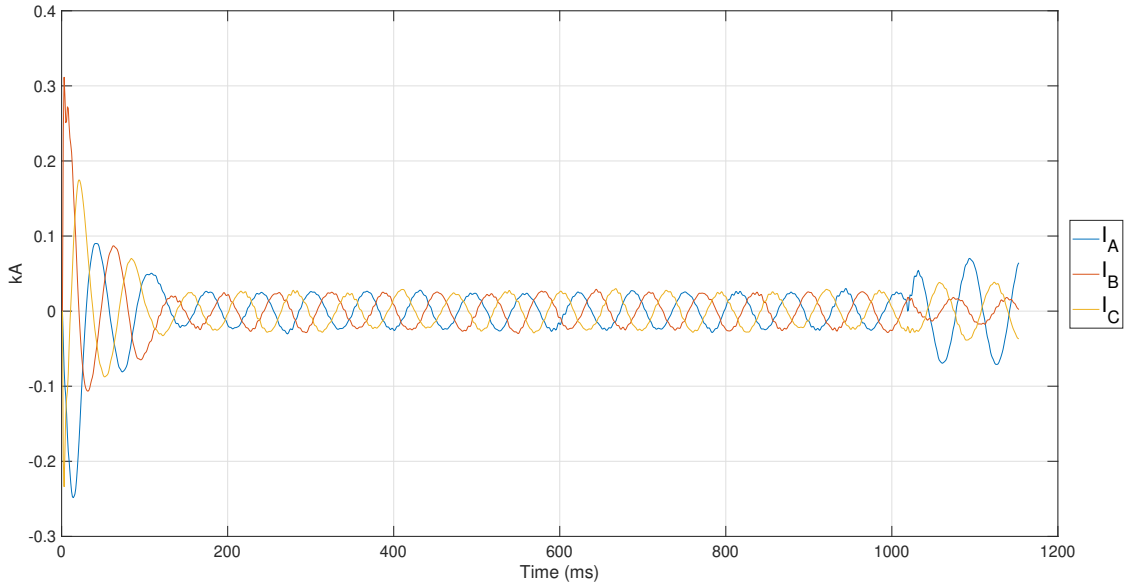

Figure 5.2: I_{ABC} before and during AG fault in AUTO mode on DL1

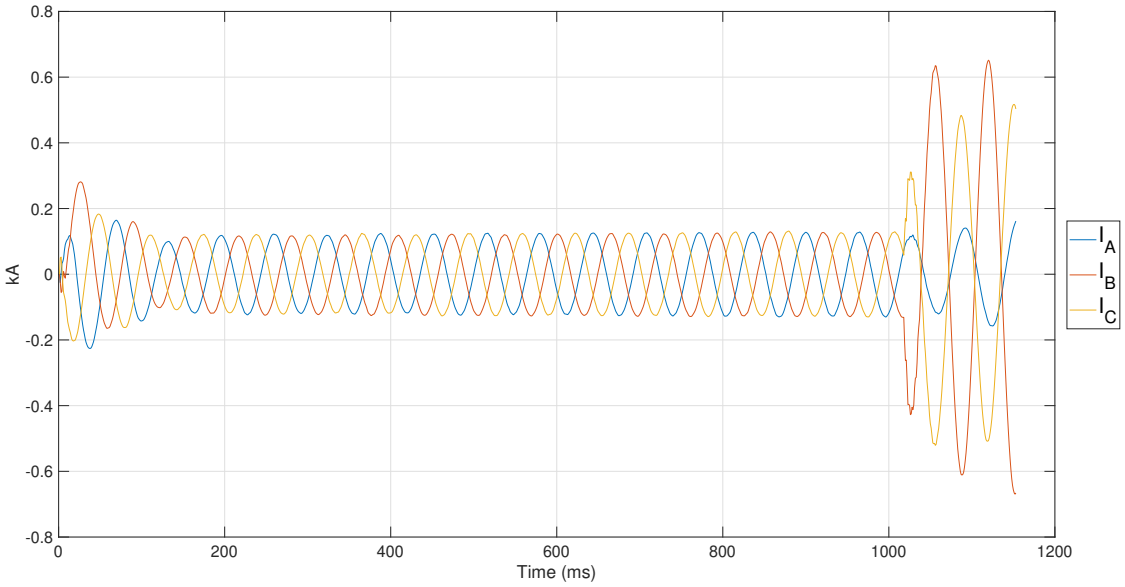

Figure 5.3: I_{ABC} before and during BC fault in GC mode on DL3

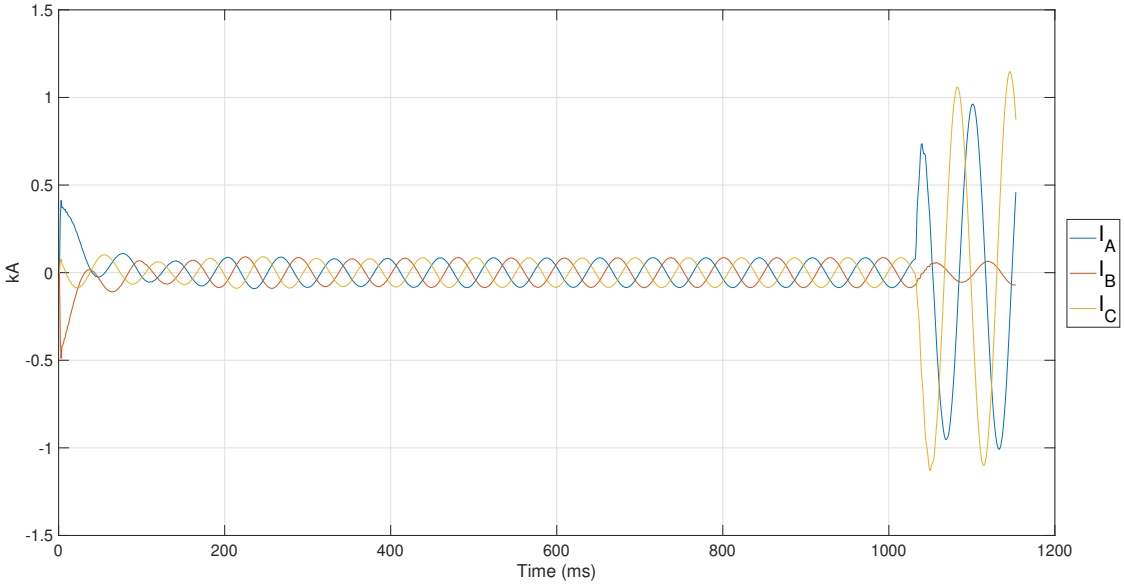

Figure 5.4: I_{ABC} before and during CAG fault in AUTO mode on DL5

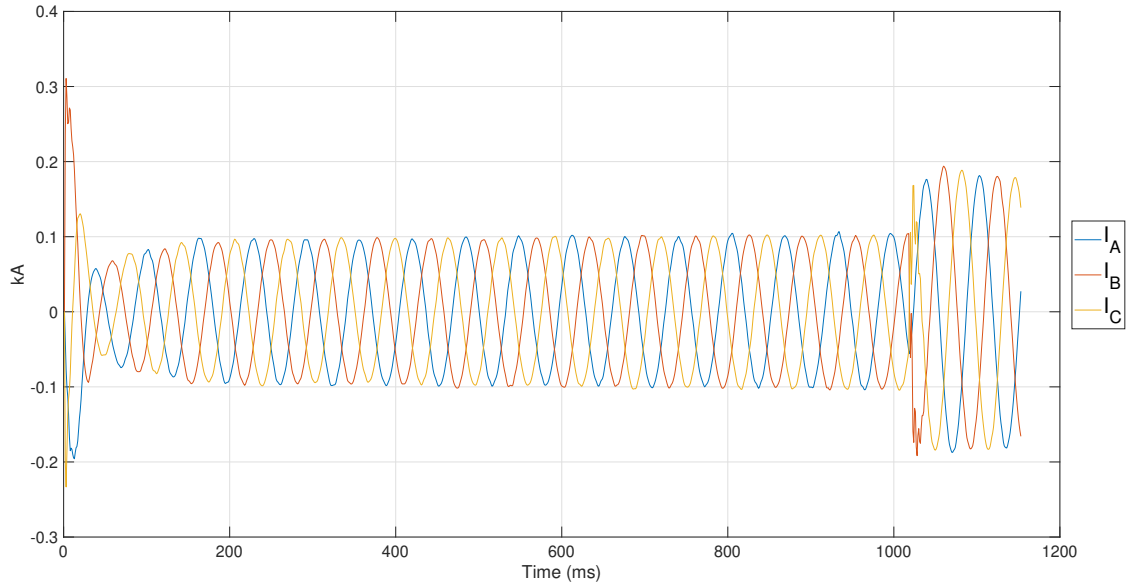

Figure 5.5: I_{ABC} before and during ABC fault in GC mode on DL1

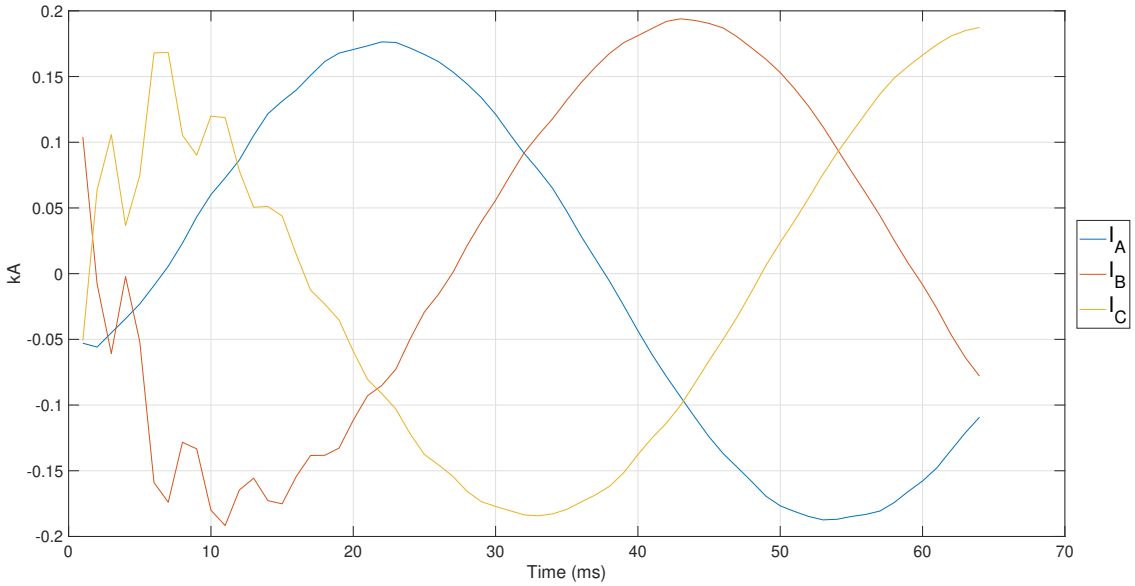

Figure 5.6: 64 samples Fault Data from Fig. 5.5

NF Data

Furthermore, the study considered multiple cases of NF under constant and varying load conditions. For the AUTO mode, load adjustments were made to maintain the generation-load balance. A total of 432 NF cases are simulated. A description of the simulated NF conditions can be found in Table 5.3.

Table 5.3: NF Cases

Parameters	**Count**
Load variations	6
Operational mode	2
Topology	2
Capacitor switching at PCC and load buses	6
Levels of DER penetration	3
Total simulated NF cases	**432**

Fig. 5.7 - Fig. 5.10 shows three-phase current signals for random NF conditions.

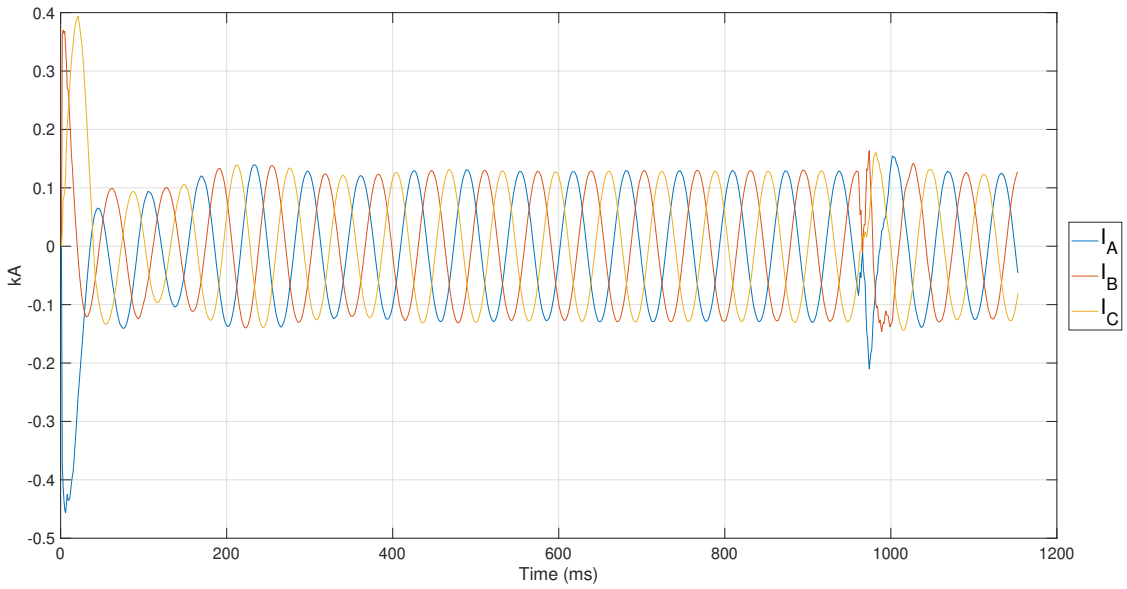

Figure 5.7: I_{ABC} during load switching - NF case

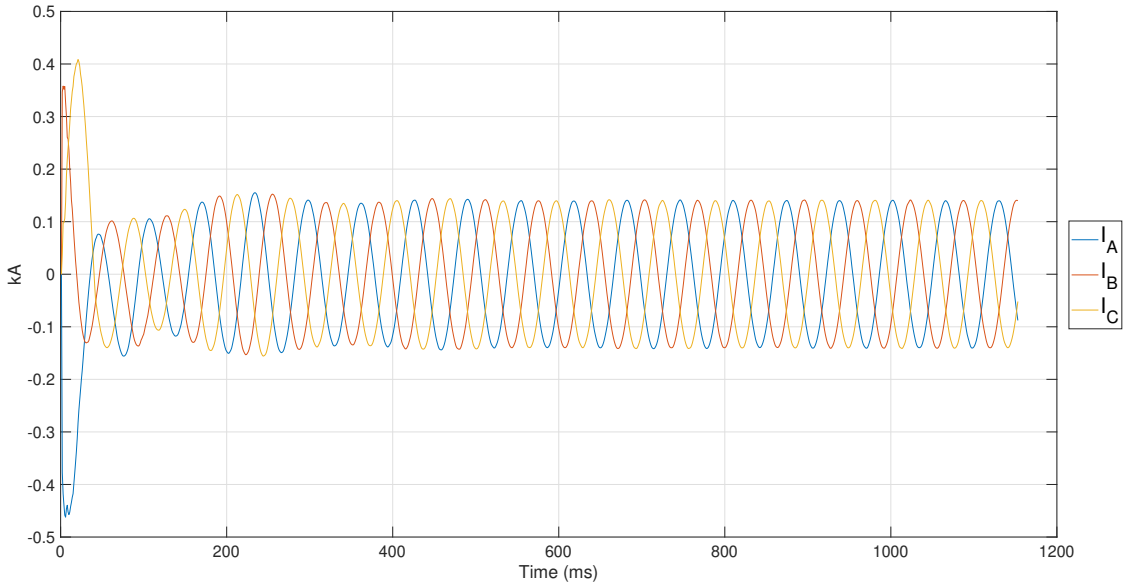

Figure 5.8: I_{ABC} during normal operation - NF case

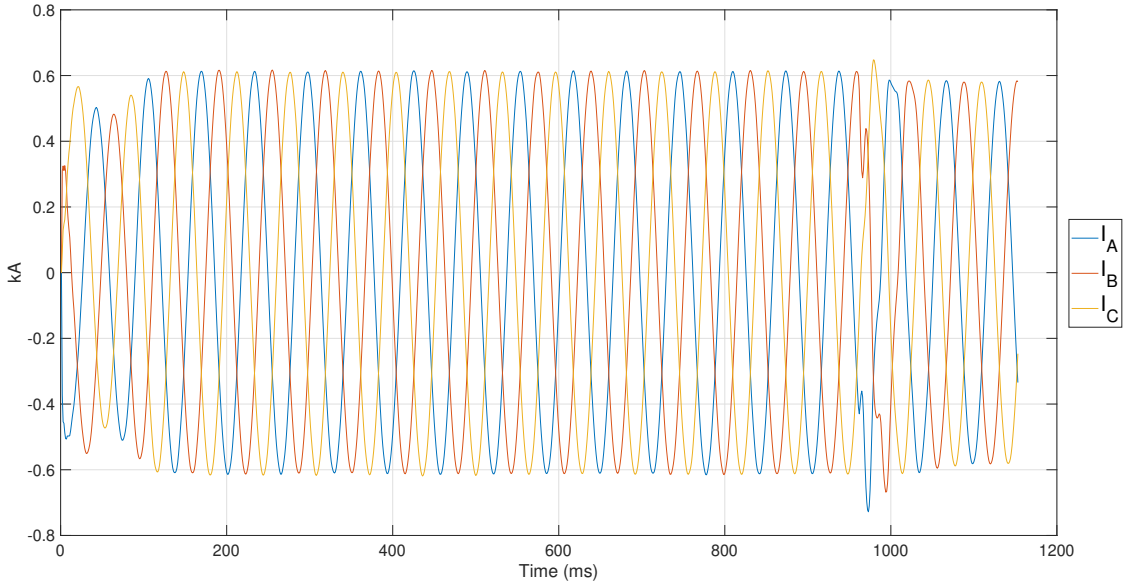

Figure 5.9: I_{ABC} during grid switching - NF case

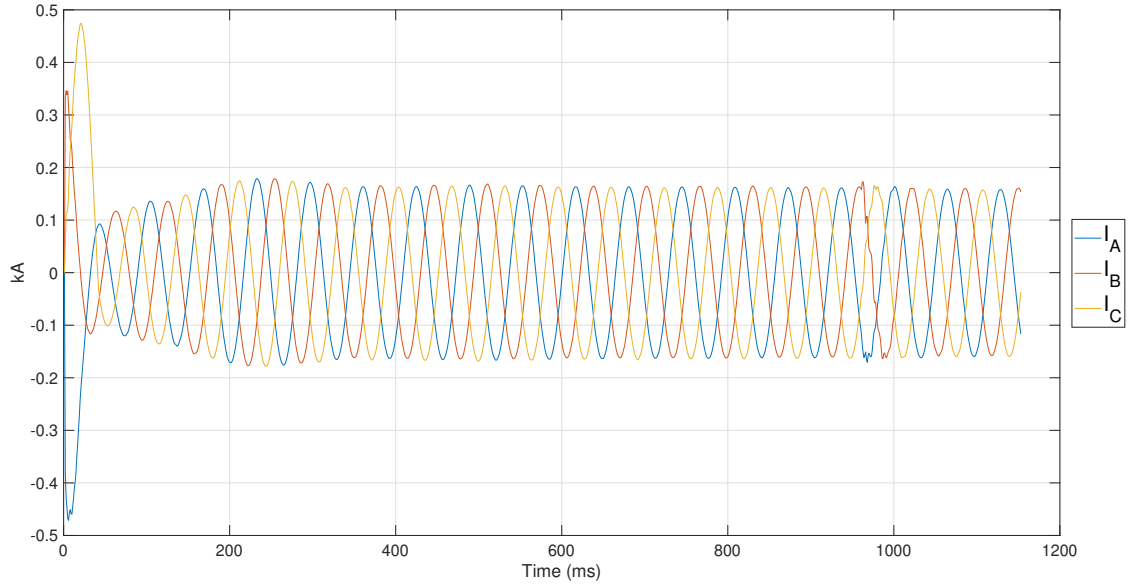

Figure 5.10: I_{ABC} during capacitor switching - NF case

Training Dataset

Fault and NF datasets are partitioned into 70% Training and 30% Testing data sets. The 16000 fault cases data set is divided into 320 cases for ten faults for each of the five distribution lines. To match the number of individual fault cases for NF, a data set of randomly selected 320 cases is prepared.

5.3.3 Model Architecture

The proposed HDLBPS combines DCNN and DLSTM to capitalize on their complementary strengths in spatial and temporal feature extraction, respectively. The DCNN excels in capturing spatial patterns within the three-phase current signals, while the DLSTM effectively captures temporal dependencies among consecutive signal samples.

5.3.4 Convolutional Neural Network

A Convolutional Neural Network (CNN) is a prevalent deep learning architecture comprising two fundamental components: convolution and pooling. For the convolution operation, linear filters are employed by the convolution layer, yielding spatial features. The weights and biases

are core training parameters of the convolution layer [204]. After convolution, a non-linear activation function commonly $ReLU$ is applied to generate a feature map, which is input to the subsequent layer [205]. The mathematical expression for the convolution layer with the activation function is given by:

$$Z = ReLU\left(\sum_{i}^{p\times q} W_i X_i + b\right) \tag{5.1}$$

W represents the weights, X is the input data, b is the bias, and p and q represent the dimensions of the input data matrix. Lastly, $ReLU$ is:

$$ReLU\left(z_i\right) = \max\left(0, z_i\right) \tag{5.2}$$

The feature map is sensitive to feature position changes. To address this, a pooling layer is introduced, which further reduces feature map dimensionality, leading to reduced computational complexity and achieving translation invariance. Maximum pooling is a commonly used pooling scheme due to its remarkable performance [206]. It selects the maximum value from specific regions of the feature map. $MaxPooling$ can be represented by:

$$P(i,j) = \max(I(i,j), I(i,j+1), I(i+1,j), I(i+1,j+1), \ldots) \tag{5.3}$$

where $P(i,j)$ represents the pooled value at position (i,j) after applying the maximum pooling operation to the input feature map I.

5.3.5 Long Short-Term Memory Network

LSTM is a type of recurrent neural network (RNN) architecture used in deep learning [207]. It has the ability to overcome the vanishing and exploding gradient problem in traditional RNNs. The output at each time step in conventional RNNs relies on the preceding time step. However, as time steps increase, the gradients can become very large or very small, making it difficult to train the network effectively. LSTM solves this problem by introducing a memory cell and

a set of gates: input, forget, update, or cell candidate and output gates. These gates control how the information enters and leaves a memory cell.

The memory cell maintains the long-term memory, while the input gate controls the extent to which incoming information should be incorporated into the memory cell. The forget gate determines the magnitude of the preceding memory that should be forgotten from the cell. Furthermore, the cell candidate supplements the cell state with additional information, and the output gate determines the proportion of the memory cell's contents to be emitted at the current time step.

The LSTM model consists of four main components, each with its own set of mathematical equations:

Input Gate

The input gate plays a pivotal role in determining what information will be memorized in the current hidden state. Input gate output vector i_t is calculated as:

$$i_t = \sigma\left(W_i\left[H_{t-1}, X_t\right] + b_i\right), \tag{5.4}$$

where σ represents the state activation function computed by using the hyperbolic tangent function $tanh$, the input vector is represented by X_t, the weight matrix as W_i and the bias vector as b_i.

Forget Gate

The forget gate determines which elements of the previous hidden state H_{t-1}, will be forgotten. Using H_{t-1} in conjunction with the current X_t, it produces a vector f_t with values between 0 and 1:

$$f_t = \sigma\left(W_f\left[H_{t-1}, X_t\right] + b_f\right), \tag{5.5}$$

where σ is the sigmoid function, weight matrix, and bias vector are represented by W_f and b_f, respectively.

Cell candidate

The cell candidate computes the new memory state C_t of the LSTM cell. Initially, it computes the potential values for the candidate hidden state denoted as g_t, a vector containing the new candidate values for the current memory cell:

$$g_t = \sigma\left(W_c\left[H_{t-1}, X_t\right] + b_c\right), \tag{5.6}$$

where W_c is the weight matrix, and b_c is the bias vector. Subsequently, the new state vector C_t is calculated through the summation of the preceding state vector C_{t-1} elementwise multiplied $\odot$ with the output vector of the forget gate f_t, and the elementwise multiplication of the output vector of the input gate i_t, and the corresponding vector g_t.

$$C_t = f_t \odot C_{t-1} + i_t \odot g_t, \tag{5.7}$$

Output gate

The output vector o_t is computed by the output gate by taking H_{t-1} and X_t:

$$o_t = \sigma\left(W_o\left[H_{t-1}, X_t\right] + b_o\right) \tag{5.8}$$

where W_o is the weight matrix, b_o is the bias vector. The hidden state output H_t is then calculated by elementwise multiplication of o_t with C_t in conjunction with σ:

$$H_t = o_t \odot \sigma\left(C_t\right). \tag{5.9}$$

The flow diagram of the cell and hidden states output is shown in Fig. 5.11

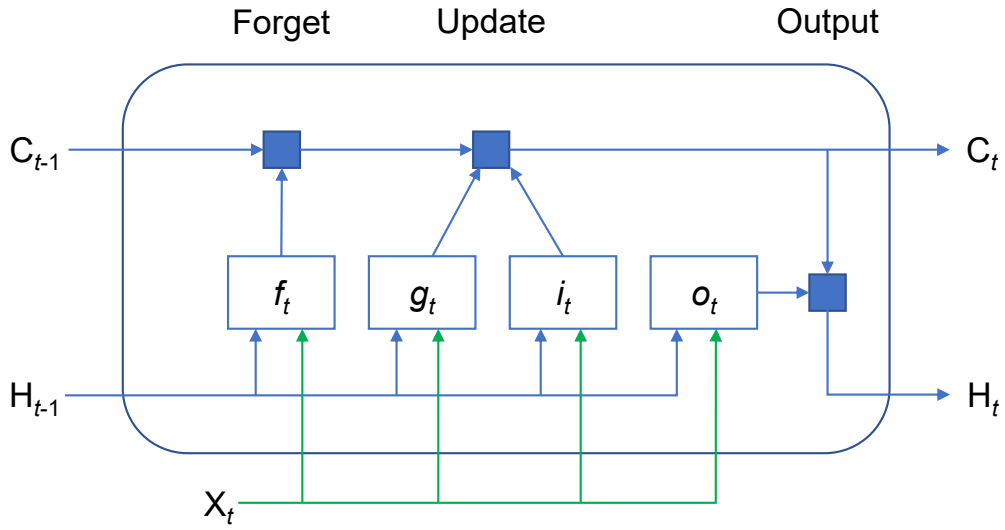

Figure 5.11: LSTM flow diagram

5.4 Proposed Hybrid Deep Learning Model

5.4.1 Layers of the Proposed Model

In the proposed approach, the CNN layer extracts local patterns and spatial features from the input sequence. Rectified Linear Unit (ReLU) activation function after the convolutional operation introduces non-linearity to the network and helps with better representation learning. Then, MaxPooling is used to downsample the feature maps, reducing the dimensionality while retaining important information. Finally, LSTM layers are employed to model the temporal dependencies and sequential patterns in the data, followed by Dropout layers to prevent overfitting.

Network Parameters

The input layer has a sequence length of 3. The convolutional layers have a kernel size of 3 and a number of filters used: 32, 64, and 128, respectively. The padding mode is set to *same*, which means that the output sequence has the same length as the input sequence. The ReLU activation function is used after each convolutional layer, while the max pooling layers have a stride of 1 and a pool size of 2. A filter (kernel) slides over the input data to extract features in a convolutional layer. The stride determines how much the filter moves horizontally and

vertically for each step. When the stride is set to 1, the filter shifts by a single unit at a time. This means that the filter covers adjacent regions of the input data, resulting in a relatively fine-grained analysis of the data. The pool size dictates the size of the pooling window. When the pool size is set to 2, the feature map is divided into non-overlapping regions of size 2×2.

The LSTM layers have a hidden state size of 64, while the dropout layers are used to regularize the network and prevent overfitting. The dropout rate is set to 0.2, which indicates that approximately 20% of the neurons in the LSTM layer will be randomly deactivated during each forward and backward pass in training. The remaining 80% of neurons will be used for computation. Introducing the dropout layers makes the model less likely to rely on specific neurons for making predictions, enhancing its ability to generalize and reducing the risk of overfitting. The dropout mechanism also encourages the network to develop a more robust representation of the input data by preventing the co-adaptation of neurons, ultimately improving the model's performance on unseen data.

The fully connected layer has 11 output neurons for ten faults and NF conditions. Lastly, the softmax activation function is used to normalize the output of the fully connected layer to represent a probability distribution over the 11 classes.

Hyper-Parameters

In addition to the parameters listed above, the network has numerous hyper-parameters. The learning rate is a hyperparameter that controls how much the network weights are updated during training. The initial learning rate is set to a relatively small value of 0.001, which helps to prevent the network from overfitting. The maximum number of epochs is set to 30, so the network is trained thirty times on the entire training dataset. A mini-batch size of 32 is employed to evenly partition the 320 training samples in each scenario. This mini-batch serves as a subset of the training dataset for assessing the gradient of the loss function and adjusting the weights.

The complete network is shown in Fig. 5.12.

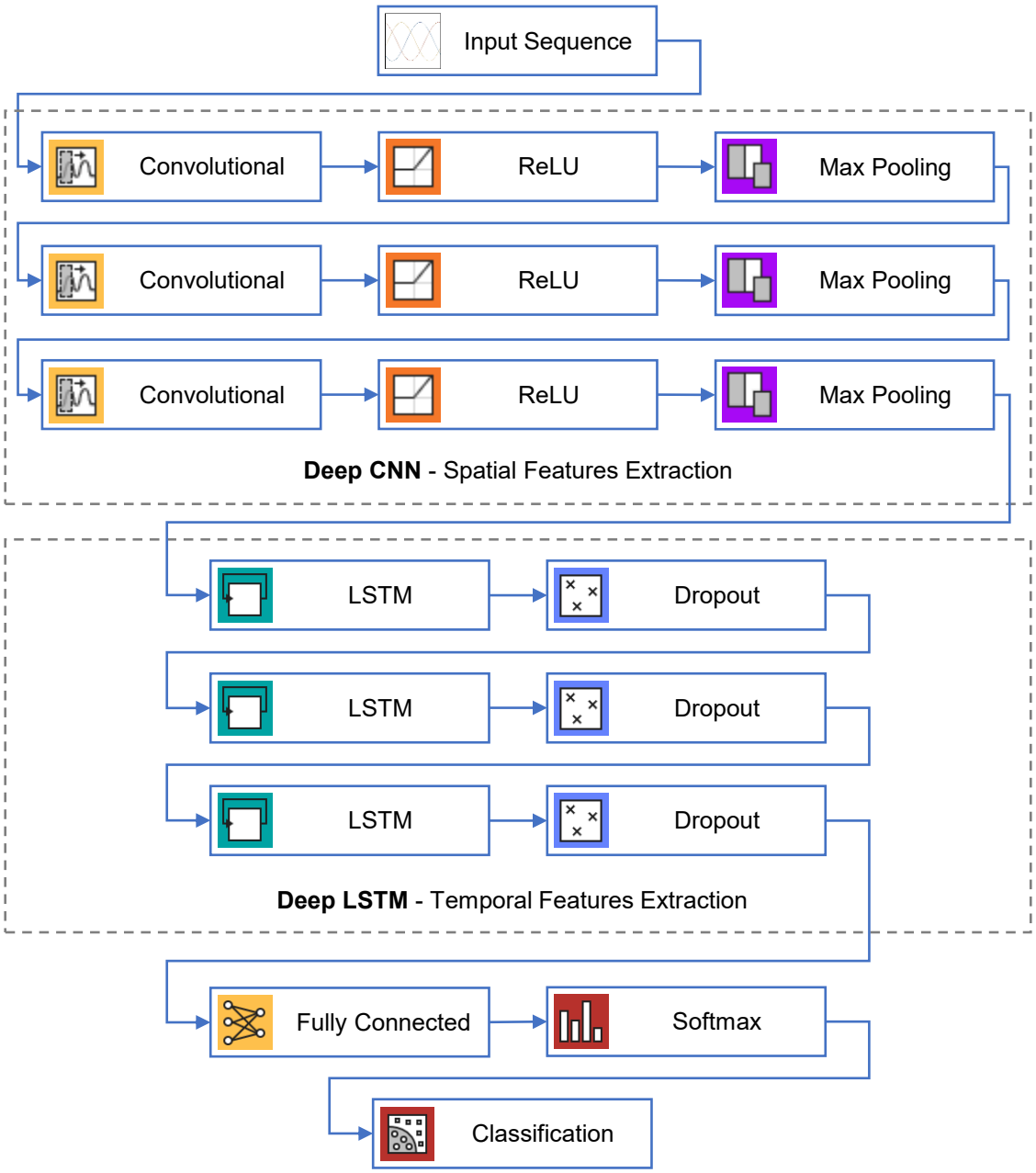

Figure 5.12: Architecture of the proposed model

5.4.2 Mathematical Expressions for Layer of the Proposed Model

For the parameters defined in Sections 5.3.4 and 5.3.5, the mathematical expressions of different layers of the proposed model are given as:

First Convolutional Layer

$$\mathbf{Z}_{conv_1} = Convolution\left(\mathbf{X}, \mathbf{W}_{conv_1}\right) + \mathbf{b}_{conv_1} \tag{5.10}$$

$$\mathbf{A}_{conv_1} = ReLU\left(\mathbf{Z}_{conv_1}\right) \tag{5.11}$$

where X is the input data, $\mathbf{W}_{conv_1}$ represents the weights and $\mathbf{b}_{conv_1}$ is the bias for the 1st layer. Whereas, $\mathbf{Z}_{conv_1}$ is the output of the convolution operation, $\mathbf{A}_{conv_1}$ is the output after applying the $ReLU$ activation.

$$\mathbf{X}_{maxpool_1} = MaxPooling\left(\mathbf{A}_{conv_1}, \text{pool-size}\right) \tag{5.12}$$

Second Convolutional Layer

$$\mathbf{Z}_{conv_2} = Convolution\left(\mathbf{X}_{maxpool_1}, \mathbf{W}_{conv_2}\right) + \mathbf{b}_{conv_2} \tag{5.13}$$

$$\mathbf{A}_{conv_2} = ReLU\left(\mathbf{Z}_{conv_2}\right) \tag{5.14}$$

$$\mathbf{X}_{maxpool_2} = MaxPooling\left(\mathbf{A}_{conv_2}, \text{pool-size}\right) \tag{5.15}$$

Third Convolutional Layer

$$\mathbf{Z}_{conv_3} = Convolution\left(\mathbf{X}_{maxpool_2}, \mathbf{W}_{conv_3}\right) + \mathbf{b}_{conv_3} \tag{5.16}$$

$$\mathbf{A}_{conv_3} = ReLU\left(\mathbf{Z}_{conv_3}\right) \tag{5.17}$$

$$\mathbf{X}_{maxpool_3} = MaxPooling\left(\mathbf{A}_{conv_3}, \text{pool-size}\right) \tag{5.18}$$

First LSTM Layer

Let $\mathbf{H}_{lstm_1}$ represent the hidden states, $\mathbf{C}_{lstm_1}$ represent the cell states, and $\mathbf{X}_{lstm_1}$ represent the input to first LSTM layer.

$$\mathbf{X}_{lstm_1} = Dropout\left(\mathbf{X}_{maxpool_3}, \text{Dropout Rate}_1\right) \tag{5.19}$$

$$\mathbf{H}_{lstm_1}, \mathbf{C}_{lstm_1} = LSTM\left(\mathbf{X}_{lstm_1}, \mathbf{W}_{lstm_1}, \mathbf{U}_{lstm_1}, \mathbf{b}_{lstm_1}\right) \tag{5.20}$$

where $\mathbf{W}_{lstm_1}$ is the weight matrix, connecting the input data to the LSTM layer, $\mathbf{U}_{lstm_1}$ is the weight matrix that connects the previous hidden state $\mathbf{H}_{(t-1)}$ to the LSTM layer, while the bias vector for the respective LSTM layer is represented by $\mathbf{b}_{lstm_1}$. $\mathbf{W}_{lstm_1}, \mathbf{U}_{lstm_1}, \mathbf{b}_{lstm_1}$ are the learnable parameters used in the LSTM layer to capture sequential patterns and dependencies in the input data.

Second LSTM Layer

$$\mathbf{X}_{lstm_2} = Dropout\left(\mathbf{X}_{lstm_1}, \text{Dropout Rate}_2\right) \tag{5.21}$$

$$\mathbf{H}_{lstm_2}, \mathbf{C}_{lstm_2} = LSTM\left(\mathbf{X}_{lstm_2}, \mathbf{W}_{lstm_2}, \mathbf{U}_{lstm_2}, \mathbf{b}_{lstm_2}\right) \tag{5.22}$$

Third LSTM Layer

$$\mathbf{X}_{lstm_3} = Dropout\left(\mathbf{X}_{lstm_2}, \text{Dropout Rate}_3\right) \tag{5.23}$$

$$\mathbf{H}_{lstm_3}, \mathbf{C}_{lstm_3} = LSTM\left(\mathbf{X}_{lstm_3}, \mathbf{W}_{lstm_3}, \mathbf{U}_{lstm_3}, \mathbf{b}_{lstm_3}\right) \tag{5.24}$$

Fully Connected Layer

Let $\mathbf{Z}_{\text{fc}}$ represent the output of the fully connected layer before applying the softmax activation.

$$\mathbf{Z}_{\text{fc}} = FullyConnected\left(\mathbf{H}_{lstm_3}, \mathbf{W}_{fc}\right) + \mathbf{b}_{fc} \tag{5.25}$$

The output of the network is given by $\mathbf{A}_{\text{fc}}$.

$$\mathbf{A}_{fc} = Softmax\left(\mathbf{Z}_{fc}\right) \tag{5.26}$$

The above represents the entire mathematical expression for the HDLBPS, proposed in this chapter.

5.5 Hybrid Deep Learning Network Analysis

A detailed analysis of all the layers in the deep learning network is presented in Table 5.4. It provides essential insights such as layer activation sizes, learnable parameter details, total learnable parameters, and recurrent layer state parameter sizes. This will help visualise and comprehend network architecture and validate correct architecture definition.

Table 5.4: Proposed Hybrid Deep Learning Network Analysis Results

	Name	Type	Activations	Learnable Properties	States
1	input Sequence input with length 3	Sequence Input	3(C) x 1(B) x 1(T)	-	-
2	conv 32 3 convolutions with stride 1 and padding 'same'	1-D Convolution	32(C) x 1(B) x 1(T)	Weights (3 x 3 x 32) Bias (1 x 32)	-
3	relu ReLU	ReLU	32(C) x 1(B) x 1(T)	-	-
4	maxpool Max pooling with pool size 2, stride 1, and padding 'same'	1-D Max Pooling	32(C) x 1(B) x 1(T)	-	-
5	conv_1 64 3 convolutions with stride 1 and padding 'same'	1-D Convolution	64(C) x 1(B) x 1(T)	Weights (3 x 32 x 64) Bias (1 x 64)	-
6	relu_1 ReLU	ReLU	64(C) x 1(B) x 1(T)	-	-
7	maxpool_1 Max pooling with pool size 2, stride 1, and padding 'same'	1-D Max Pooling	64(C) x 1(B) x 1(T)	-	-
8	conv_2 128 3 convolutions with stride 1 and padding 'same'	1-D Convolution	128(C) x 1(B) x 1(T)	Weights (3 x 64 x 128) Bias (1 x 128)	-
9	relu_2 ReLU	ReLU	128(C) x 1(B) x 1(T)	-	-
10	maxpool_2 Max pooling with pool size 2, stride 1, and padding 'same'	1-D Max Pooling	128(C) x 1(B) x 1(T)	-	-
11	lstm LSTM with 64 hidden units	LSTM	64(C) x 1(B) x 1(T)	InputWeights (256 x 64) RecurrentWeights (256 x 64) Bias (256 x 1)	HiddenState 64 x 1 CellState 64 x 1
12	dropout 20% dropout	Dropout	64(C) x 1(B) x 1(T)	-	-
13	lstm_1 LSTM with 64 hidden units	LSTM	64(C) x 1(B) x 1(T)	InputWeights (256 x 64) RecurrentWeights (256 x 64) Bias (256 x 1)	HiddenState 64 x 1 CellState 64 x 1
14	dropout_1 20% dropout	Dropout	64(C) x 1(B) x 1(T)	-	-
15	lstm_2 LSTM with 64 hidden units	LSTM	64(C) x 1(B)	InputWeights (256 x 64) RecurrentWeights (256 x 64) Bias (256 x 1)	HiddenState 64 x 1 CellState 64 x 1
16	dropout_2 20% dropout	Dropout	64(C) x 1(B)	-	-
17	fc 11 fully connected layer	Fully Connected	11(C) x 1(B)	Weights 11 x 64 Bias 11 x 1	-
18	softmax softmax	Softmax	11(C) x 1(B)	-	-
19	classification crossentropyex	Classification Output	11(C) x 1(B)	-	-

5.6 Results and Analysis

The proposed HDLBPS is thoroughly evaluated using the curated data set of AC microgrid faults. For the network architecture and training options mentioned earlier in this chapter, data for each of the five distribution lines (DL) are used for training. The DL1 fault and NF data training progress is shown in Fig. 5.13.

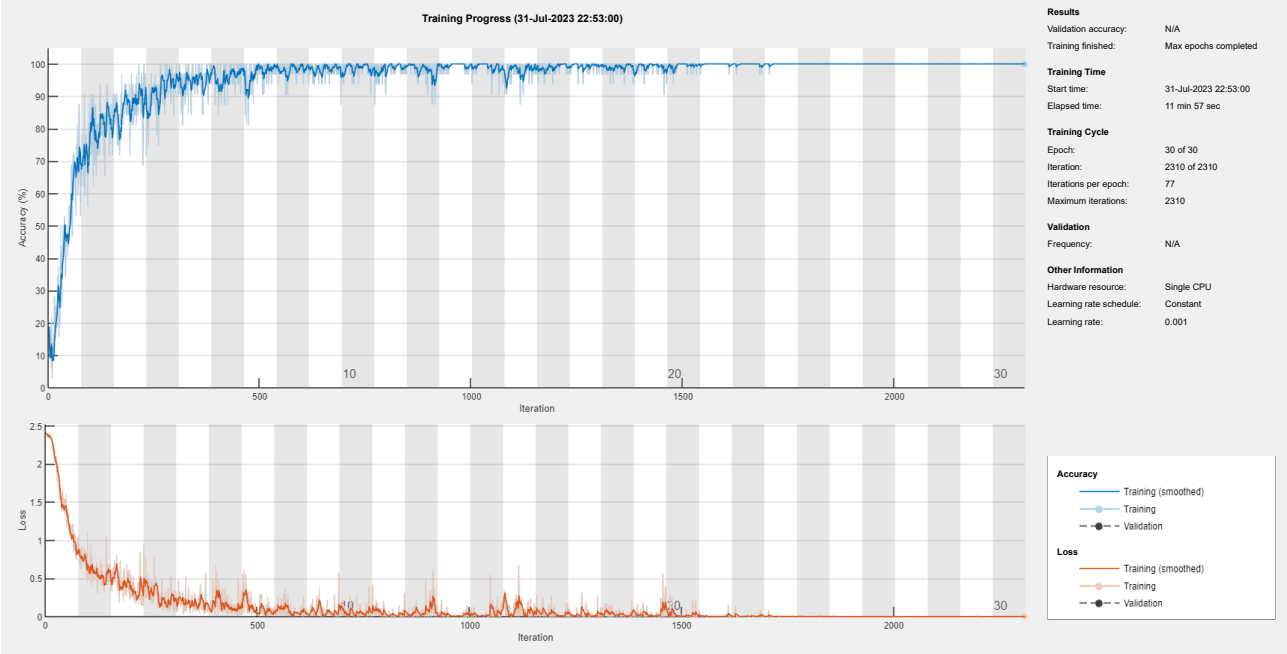

Figure 5.13: Training Progress

Fig. 5.14 and Fig. 5.15 show the Training and Test confusion matrix (CM) for DL1. Fig. 5.16 and Fig. 5.17 show the Training and Test CM for DL2. Similarly, Fig. 5.18 and Fig. 5.19 show the Training and Test CM for DL3, while Fig. 5.20 and Fig. 5.21 show the Training and Test CM for DL4 and lastly, Fig. 5.22 and Fig. 5.23 show the Training and Test CM for DL5.

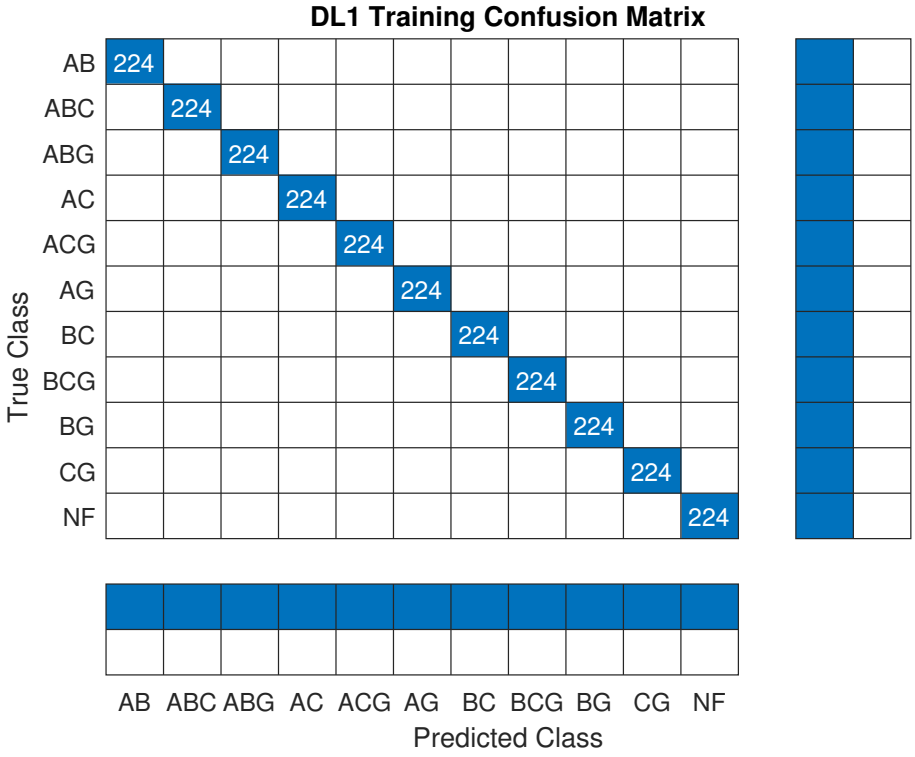

Figure 5.14: Training CM for DL1

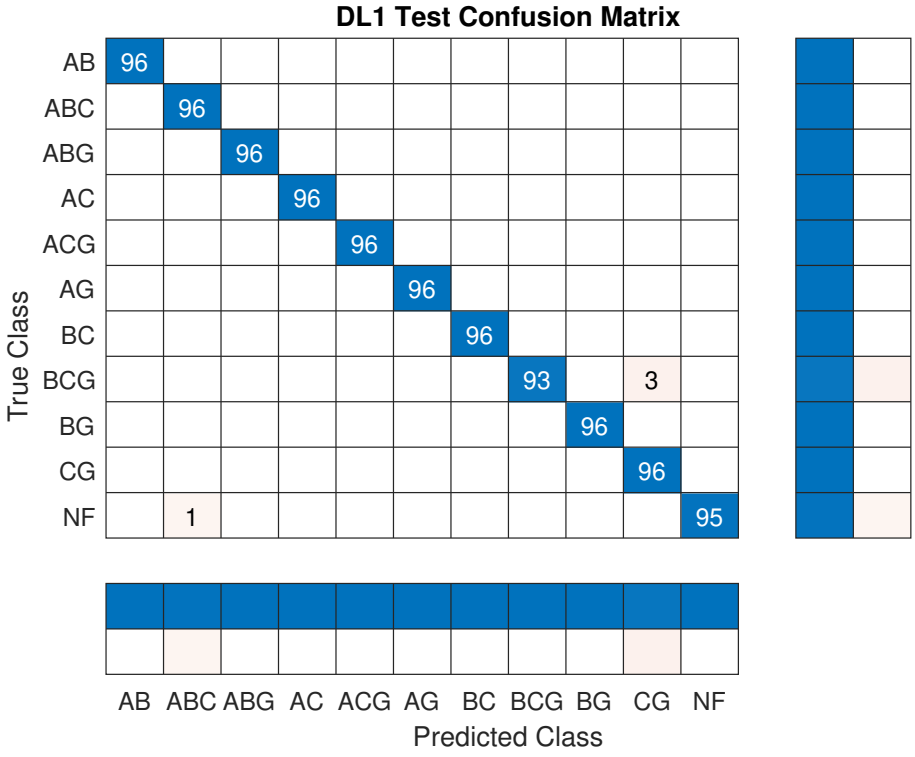

Figure 5.15: Test CM for DL1

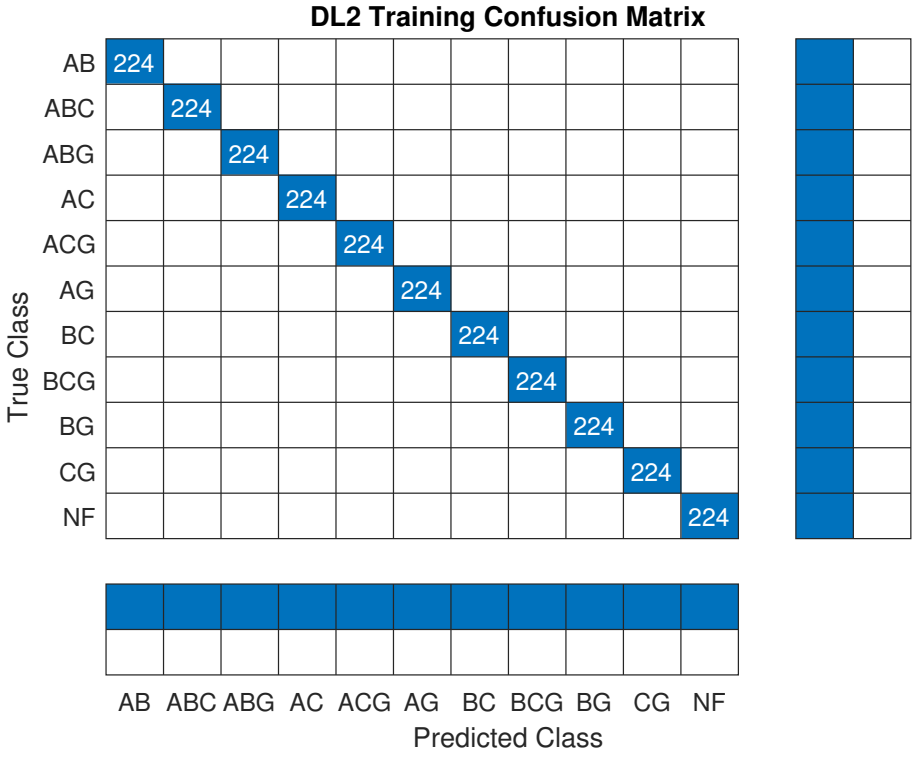

Figure 5.16: Training CM for DL2

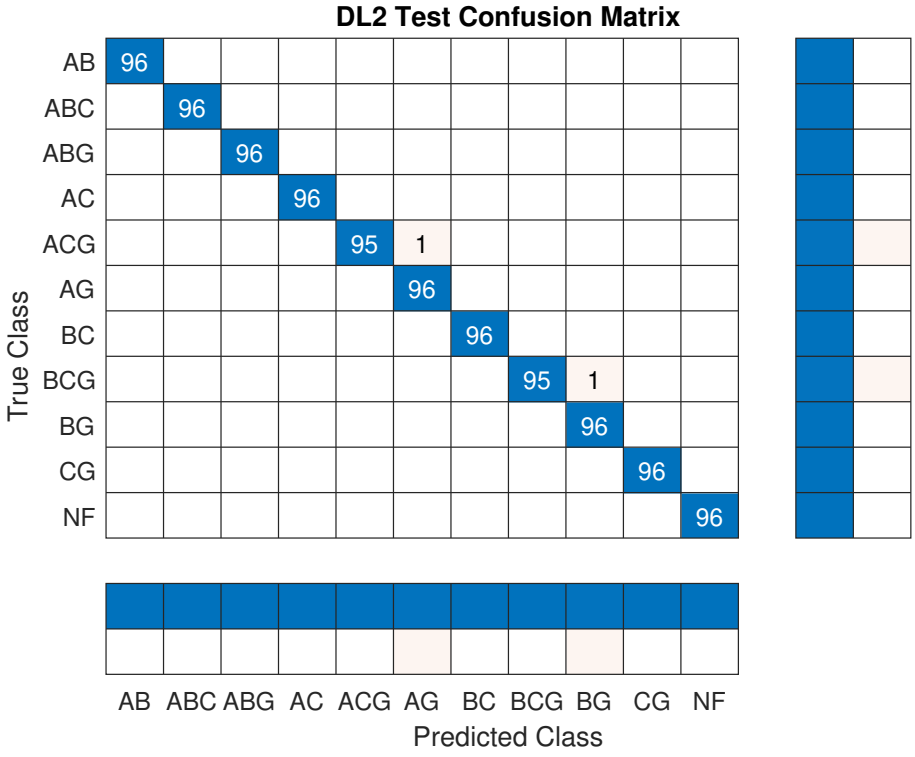

Figure 5.17: Test CM for DL2

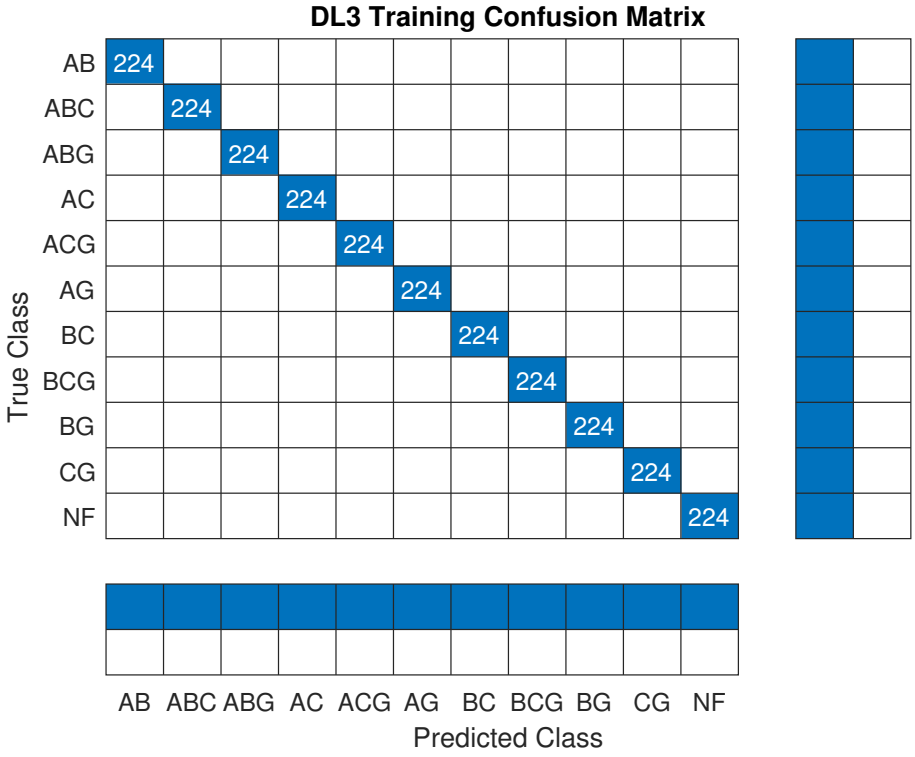

Figure 5.18: Training CM for DL3

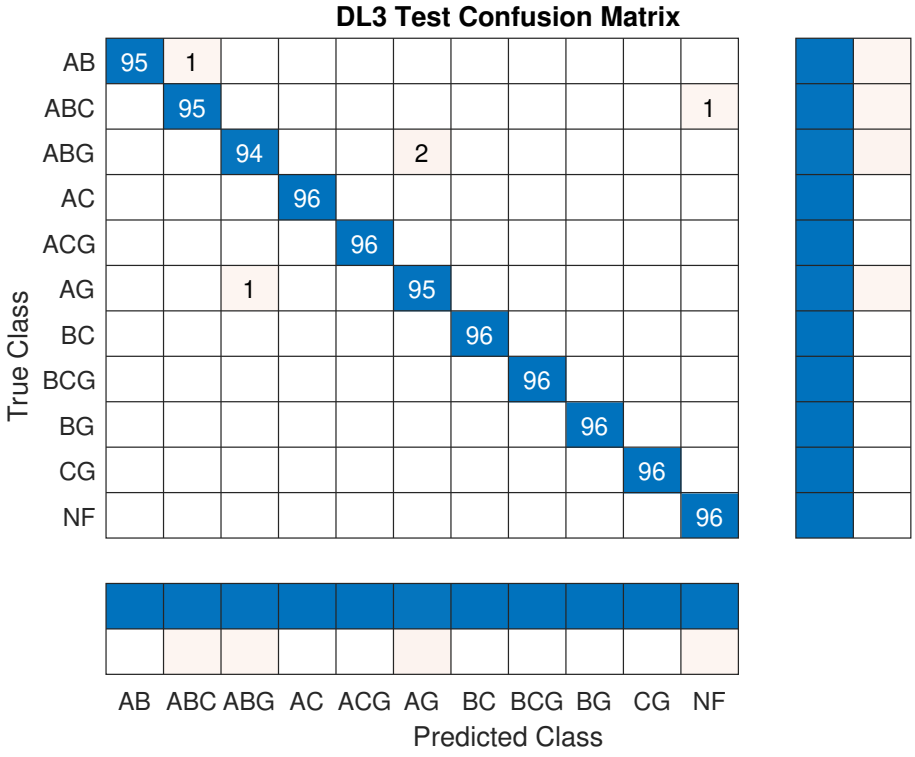

Figure 5.19: Test CM for DL3

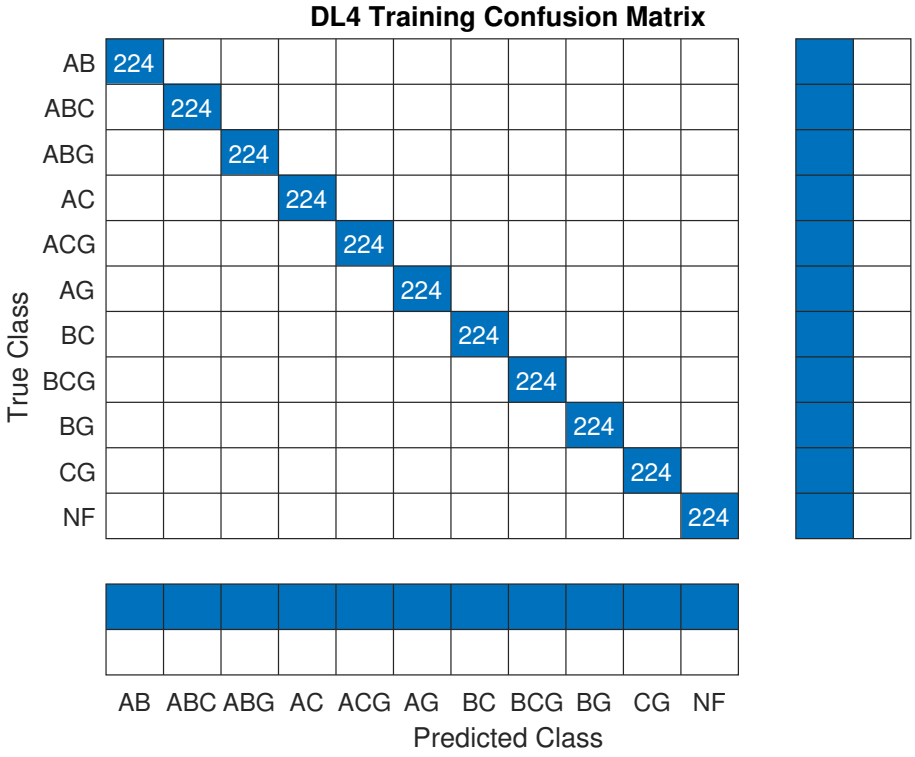

Figure 5.20: Training CM for DL4

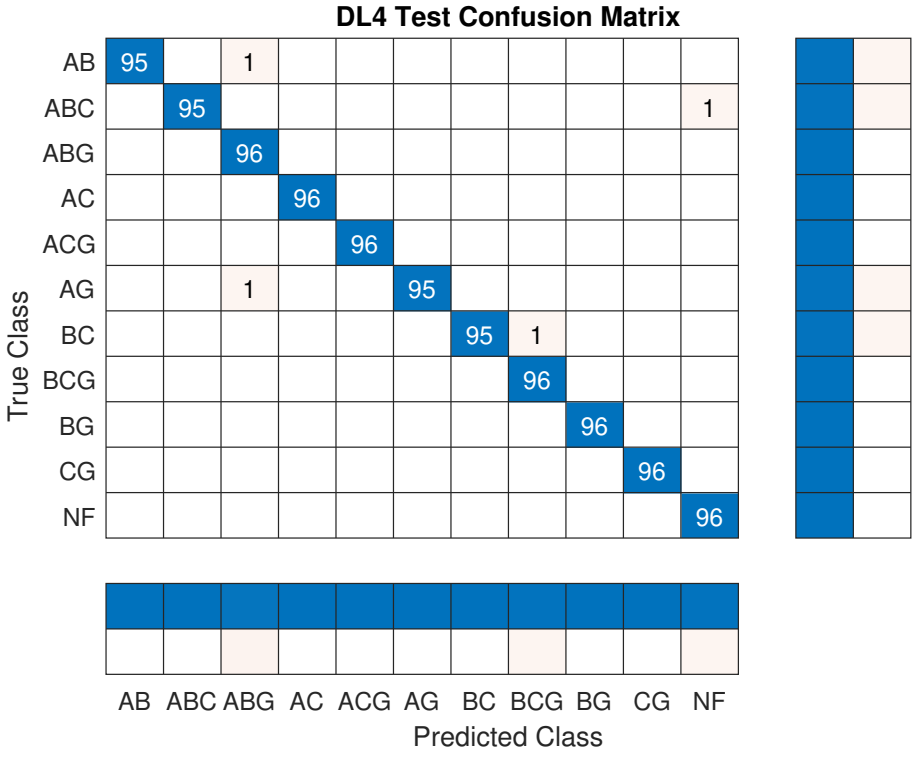

Figure 5.21: Test CM for DL4

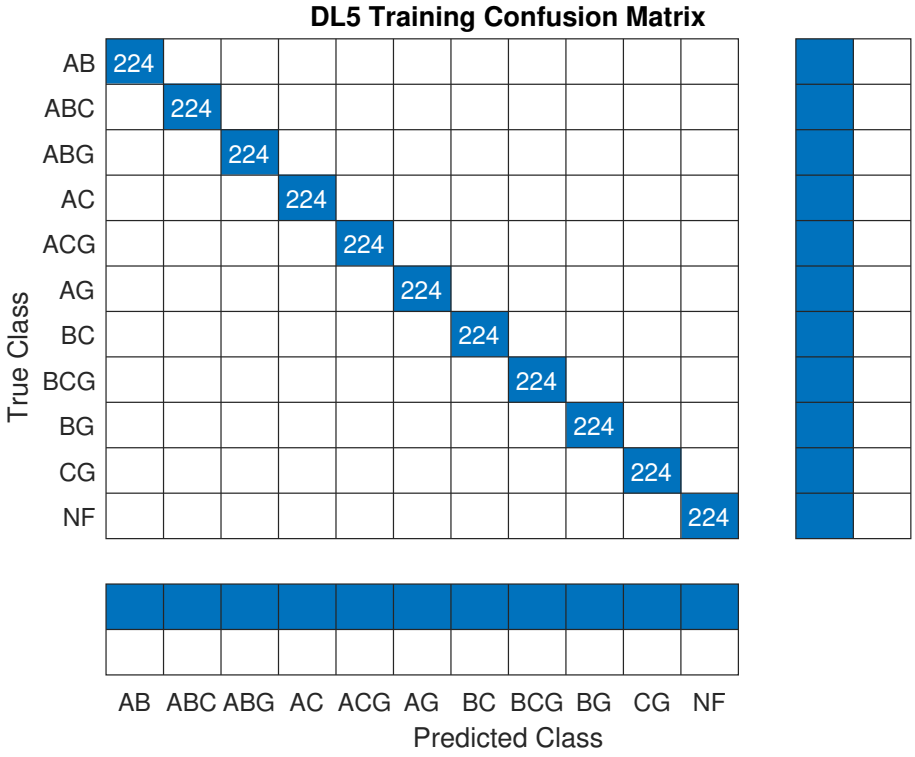

Figure 5.22: Training CM for DL5

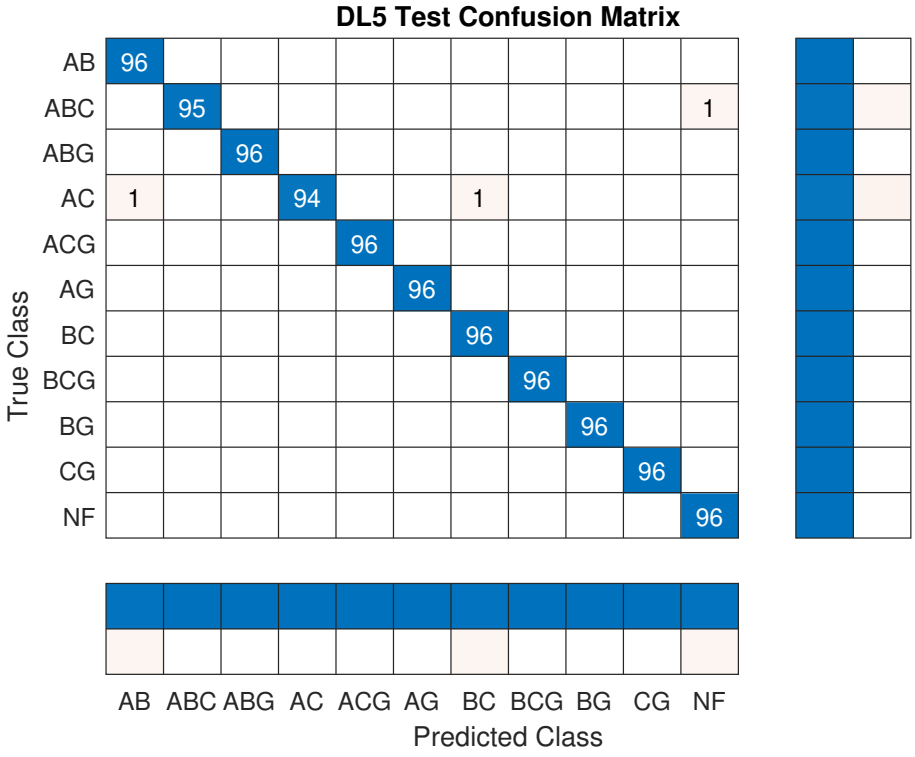

Figure 5.23: Test CM for DL5

The obtained results demonstrate a remarkable accuracy of 100% for training and close to 100% for testing using unseen data, indicating the model's proficiency in accurately identifying and classifying major faults within an AC microgrid for any mode of operation. The training and test accuracy for the five DLs is presented in Table 5.5.

Table 5.5: Training and Test Accuracy for Any Mode of Microgrid Operation

Line	**Training**	**Test**
DL-1	100%	99.62%
DL-2	100%	99.81%
DL-3	100%	99.53%
DL-4	100%	99.62%
DL-5	100%	99.72 %

We have used simulated fault and NF data; the accuracy might be slightly reduced for real-time data and implementation.

5.7 Discussion

Commonly, a multi-step process involving separate training for fault detection, fault type classification, and faulted phase identification is used. The proposed novel HDLBPS combines all these steps into a single unified process. The model demonstrates superior fault detection and classification capabilities by incorporating data from both grid-tied and autonomous modes for training and testing, regardless of the operating mode. Following are the advantages of the proposed unified approach and its potential implications for improving microgrid stability and reliability while reducing the cost:

5.7.1 Improved Robustness and Adaptability

The unified approach has the potential to be more flexible and adaptable than the commonly used multi-step process. This is because the single model is trained on a wider variety of data for a broader range of operating conditions. As a result, the model learns to detect and classify faults more effectively, demonstrating increased robustness and adaptability in real-world situations. Furthermore, the proposed model effortlessly adapts to different operating

modes, providing uninterrupted fault detection capabilities during mode transitions.

5.7.2 Enhanced Efficiency and Reduced Computational Cost

Combining the fault detection and classification processes into a single-step approach significantly reduces computation time and resource requirements and will bring the cost down, making it more feasible for real-time implementation. By leveraging the interconnected nature of these tasks, the model benefits from shared feature representations, leading to fast and accurate fault detection with faulted phase identification, increasing microgrid resilience.

5.8 Summary

This chapter presents a novel HDLBPS for fault detection and fault type classification in AC microgrids. The proposed method is a hybrid of DCNN and DLSTM. A standard IEC meshed microgrid model is developed, and a large dataset of 16000 cases for fault and 432 cases for no-fault conditions is obtained to train and test HDLBPS algorithms for fault detection and fault-type classification with faulted phase identification. Three-phase current signals are obtained for each fault and NF case. The combined dataset is partitioned into a Training dataset, comprising 70% of the data, and a Testing dataset, encompassing the remaining 30% of the data. The ability of HDLBPS to capture spatial and temporal features, coupled with its superior fault detection and fault type classification accuracy, holds significant promise for the development of robust protection systems for AC microgrids.

Chapter 6

Novel Protection Scheme for AC Microgrids Based On Multi-agent System Combined With Machine Learning

6.1 Fault Detection and Fault Type Classification

Applying domain knowledge and FS methods, the top 18 features are selected for FD, and 18 features are chosen for FTC with faulted phase identification. Numerous ML algorithms are trained and tested, as discussed in Chapter 4.

For FD and FTC, BT outperformed all other SML classifiers. The trained BT model is deployed to detect and classify faults. Fig. 6.1 presents a schematic diagram of the proposed methodology.

The process starts with measuring local signals, followed by FE. Simulink Classification Ensemble Predict block with trained BT model is used to validate the model predictions with trip signal issued by converting the data type of the label to the real-world numerical value when a fault is detected. For a set of 20 new observations, with alternating 5 NFs followed by 5 fault

This chapter is based on the work reported in M. Uzair, L. Li, J. G. Zhu, M. Eskandari, "A protection scheme for ac microgrids based on multi-agent system combined with machine learning", *Proc. IEEE 2019 Australasian Universities Power Engineering Conference (AUPEC)*, pp. 1–6, Nov 2019.

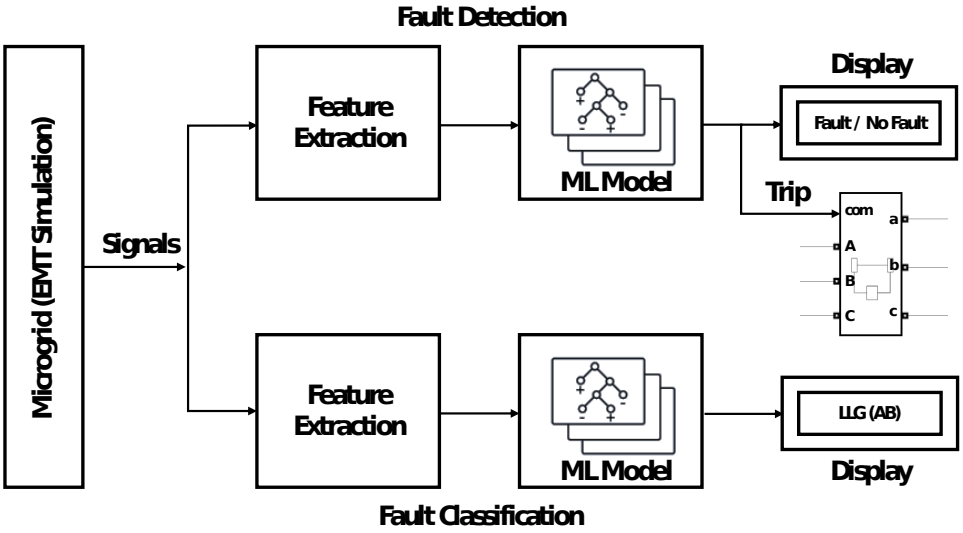

Figure 6.1: Proposed methodology

cases, the model only misclassified once, where it predicted a fault as an NF. Alternating trip signals for the 20 observations are shown in Fig. 6.2.

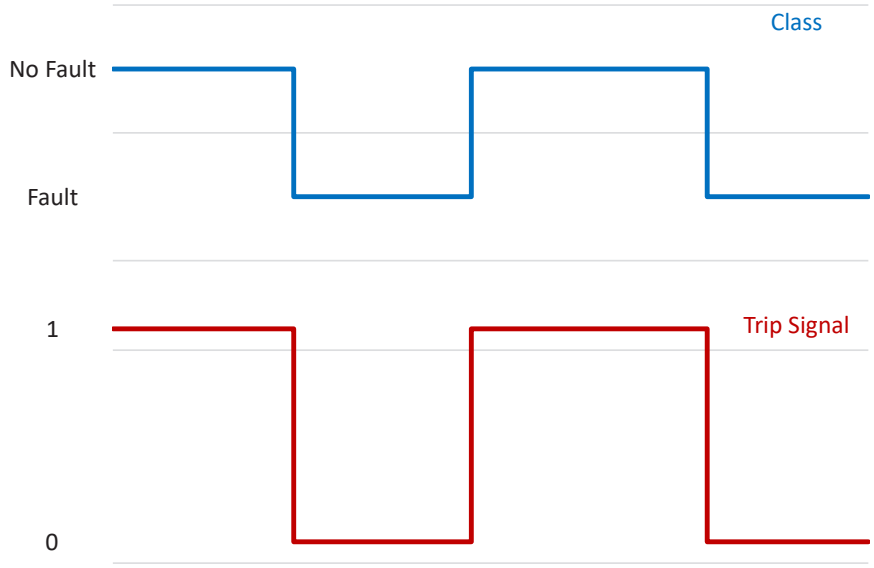

Figure 6.2: Fault as an NF detection and respective trip signal

Furthermore, FTC and FP are displayed, which can be used for accurate single- and double-pole tripping for future intelligent grids [32] to avoid tripping healthy phases in fault events. This will aid in increasing system resilience and economic benefits.

6.2 Agent and MAS

An agent in AI is a hardware or software with decision-making capabilities. It offers an interoperable interface to a diverse system. Multiple agents with similar or different goals, interacting with each other and the environment, form a MAS.

The inherent nature of agents is suitable for the development of a smart protection system for a smart power grid due to the following characteristics [134]:

- Independence: Agents can operate autonomously without human intervention, which can reduce fault detection and isolation time. This feature, in particular, will also enable intelligent protection schemes to be implemented.
- Social ability: Agents can interact with other agents. This feature is ideally suited for optimised protection coordination.
- Reactivity: Agents can detect and respond to environmental changes. This characteristic supports the plug-and-play function for DGs, loads and other devices within the microgrid and can enable the implementation of the adaptive protection scheme.
- Proactivity: Besides reacting to changes in the environment, an agent can take the initiative to attain assigned goals. This feature also supports the adaptive protection scheme.

Other features, such as distributed monitoring functions, enable MAS to monitor local parameters and can aid in implementing advanced protection functions. Similarly, distributed coordination capability can be used for fast service restoration, while the independent run-time capability of MAS can increase the speed of operation. Besides this, by recording the microgrid status continuously for a long duration, MAS can collect big data on fault types, locations, fault current levels and other vital features that can be used in self-learning algorithms.

The individual agent may have a limited view of the microgrid to achieve their own goal, but by interacting with each other, they can accomplish the overall goal of protecting the microgrid. Such a MAS will offer fast and accurate protection operation with the ability to adapt to varying conditions.

6.3 MAML Protection Architecture

Commonly, the MAS model and ML models are not mixed because the former is process-driven, while the latter is data-driven. A novel MAS-based solution combined with ML is developed to allow learning and decision-making abilities in microgrids.

FD and FTC technique based on novel features and SML is incorporated in a modified MAS structure, originally proposed in [135]. The proposed MAML-based method provides a complete PS with backup protection. A hybrid MAS-based protection architecture is proposed. It consists of three layers, as shown in Fig. 6.3. Some agents operate hierarchically, and some in parallel. Measurement agents (MA) are the only independent agents among various agents. The protection agent (PA) and local agent (LA) can be classified as learning or adaptive agents, while the verification agent (VA) uses logical reasoning. All other agents are dependent on other agents for data and messages to function hierarchically.

6.4 Layers and Role of Each Agent

The lowest layer of the proposed MAS structure is the equipment layer that comprises MA, PA, VA and backup agent (BA). MA monitors voltage, current, and other signals and acts as an input to PA. PA incorporates SML to detect faults within the microgrid based on the data received from MA and sends a trip signal to CB to segregate the faulty section. VA monitors the message exchange between agents to make sure that primary protection has responded to clear the fault, and in case a failure is detected, it communicates with LA to activate backup protection. Directional OC relay is used as BA, and its protection settings are dynamically updated for a particular microgrid's load and generation changes, based on the DL algorithm residing in LA. This will reduce the backup protection operating time compared to the traditionally used pre-defined waiting time.

The microgrid layer includes LA and can communicate with the system and equipment layer in the middle. Besides retaining information and messages shared between the agents in the equipment layer, it also contains a DL-based AP algorithm to calculate and update protection

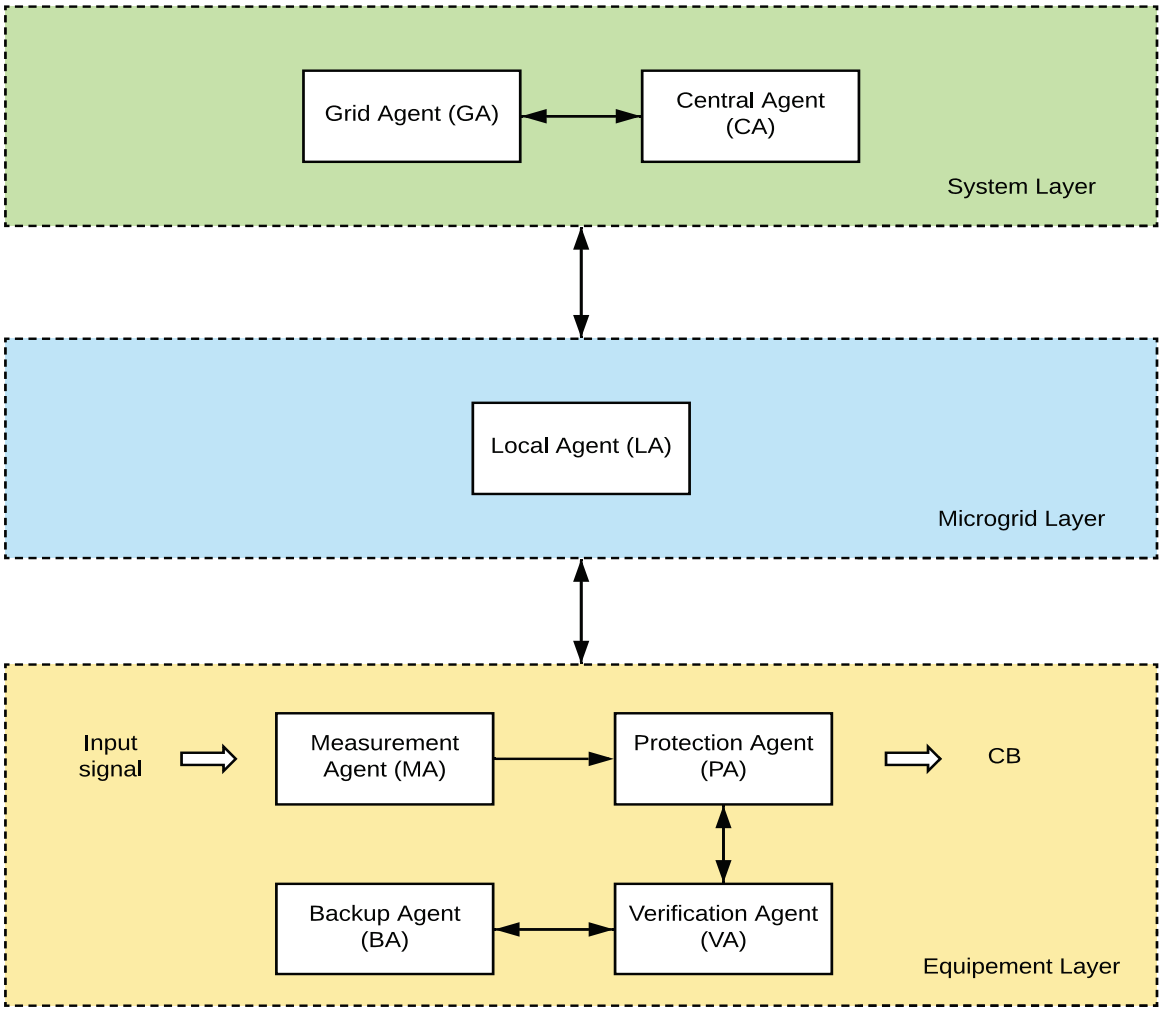

Figure 6.3: Layers of the proposed MAS structure

settings for BA. LA of each microgrid can communicate with other LAs and central agent (CA) to update the central database.

The highest is the system layer containing CA and grid agent (GA). Based on the information from all the LAs, CA has the complete information of the system. It also stores the islanded or grid-connected status of the microgrid. On the other hand, if there is an upstream fault, GA will command the CB at PCC for disconnection, operate in autonomous mode, and update the status to CA, which can also communicate with GA for intentional islanding. Both LA and CA can communicate directly with PA to shut off a section for maintenance, testing or intentional islanding. The entire process is shown in Fig. 6.4.

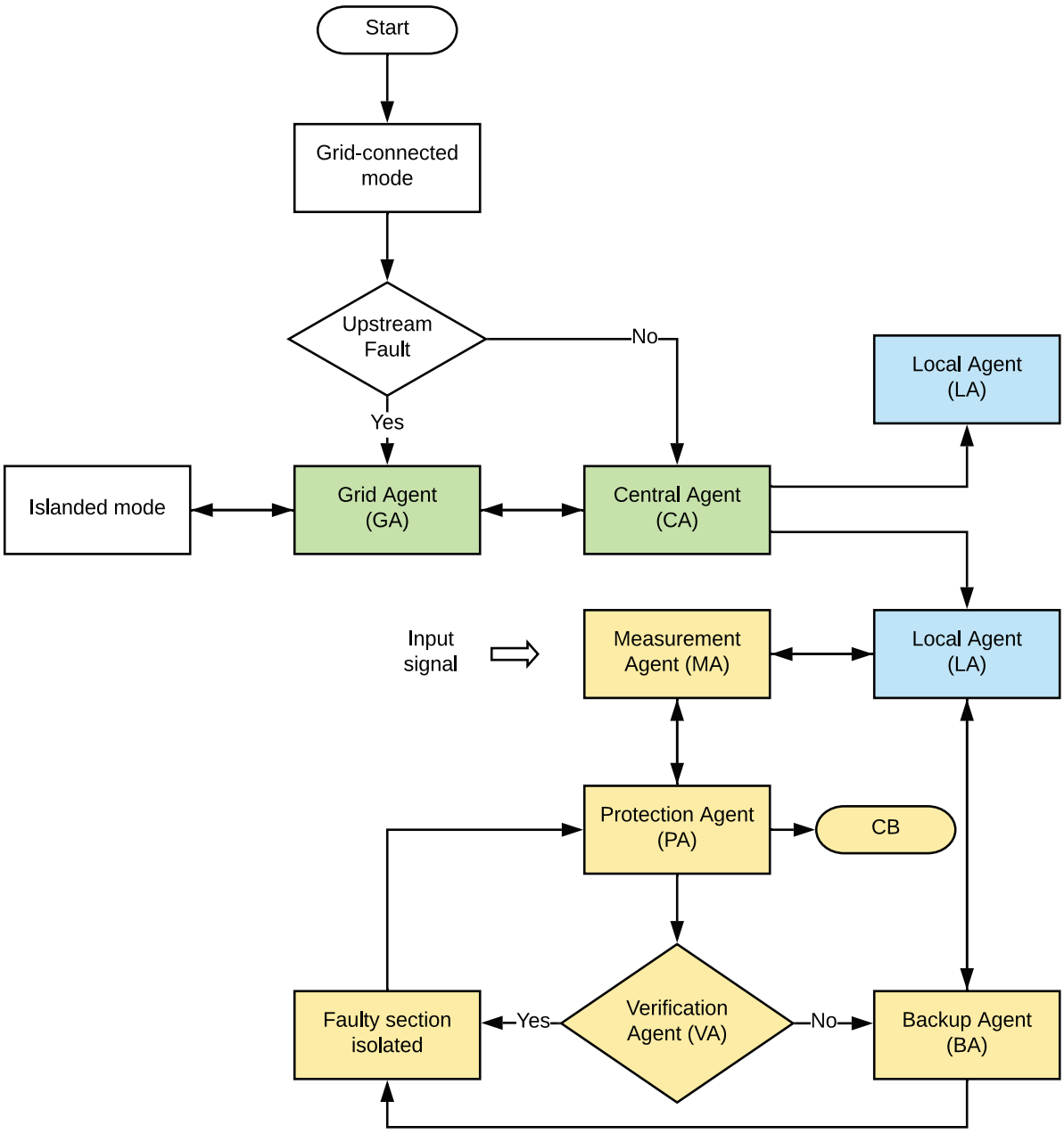

Figure 6.4: Proposed MAML protection algorithm

6.5 Analysis and Benefits of the Proposed Agent

6.5.1 Measurement Agent

The MA plays a crucial role in the equipment layer as it continuously monitors important parameters such as voltage, current, and other signals within the microgrid. Its primary function is to provide real-time data to other agents, particularly the PA. By ensuring accurate and up-to-date information, the MA enhances the overall effectiveness and responsiveness of the protection system. Additionally, its constant monitoring allows for early fault detection, which is essential for minimizing the impact of potential disturbances and ensuring grid stability.

Benefits of MA

a. Real-time Monitoring: The MA's ability to provide real-time data enables quick and precise fault detection, reducing the time required to identify and address potential issues.

b. Improved Protection: By supplying accurate measurements, the MA enhances the accuracy and reliability of the entire protection system, leading to better fault discrimination and improved system stability.

c. Enhanced Grid Resilience: Early fault detection and precise measurements contribute to the overall resilience of the microgrid, ensuring that faults are addressed promptly and minimizing the risk of cascading failures.

6.5.2 Protection Agent

The PA serves as a critical component of the equipment layer, responsible for detecting faults within the microgrid. Utilizing the Supervised ML algorithm, the PA can analyze the data received from the MA and determine if there are any abnormalities or faults in the system. Once a fault is identified, the PA sends a trip signal to the CB to isolate the faulty section, preventing further damage and protecting the rest of the microgrid.

Benefits of PA

a. Fault Detection Accuracy: The adoption of the ML algorithm enables the PA to achieve high levels of accuracy in fault detection. This minimizes false alarms and ensures that genuine faults are rapidly identified and handled appropriately.

b. Rapid Response: The PA's ability to promptly issue trip signals to disconnect faulty sections minimizes the duration of interruptions, leading to improved system reliability and continuity of service.

c. Adaptability: Using ML enables PA to adapt to changes in the microgrid's operational conditions over time.

6.5.3 Verification Agent

The VA is responsible for monitoring the message exchange between agents in the equipment layer, specifically focusing on the primary protection process. Its primary function is to confirm that the PA has adequately responded to clear the fault. In cases where a failure is detected, the VA communicates with the LA to activate the backup protection system, ensuring a reliable and redundant protection mechanism.

Benefits of VA

a. Redundancy and Reliability: The VA introduces an additional layer of protection verification, enhancing the overall reliability of the microgrid's protection system. If the primary protection process encounters issues, the VA can trigger the backup protection system, ensuring uninterrupted operation.

b. Enhanced Fault Management: By continuously monitoring the message exchange, the VA can detect and address any anomalies in the protection process swiftly, minimizing the risk of false tripping or delayed responses.

c. Improved Grid Resilience: The VA's ability to activate backup protection adds an extra layer of resilience to the microgrid, ensuring that faults are managed efficiently even in

adverse conditions.

6.5.4 Backup Agent

The BA is implemented using a Directional OC relay and resides in the equipment layer. Its primary function is to provide an alternative layer of protection in case the primary protection process fails to clear a fault. The protection settings of the BA are dynamically updated based on the DL algorithm residing in the LA, which takes into account the specific load and generation characteristics of the microgrid.

Benefits of BA

a. Redundant Protection: The BA serves as a reliable backup mechanism, ensuring that faults are addressed even if the primary protection process encounters issues. This redundancy minimizes the risk of prolonged interruptions and system failures.

b. Adaptive Protection: By utilizing the DL algorithm, the BA can adapt its protection settings in real time, optimizing its response based on the current operating conditions of the microgrid. This adaptability enhances protection efficiency and reduces unnecessary tripping.

c. Reduced Backup Operating Time: The dynamically updated protection settings in the BA lead to a faster response during fault situations compared to traditional pre-defined waiting times. This helps in minimizing the duration of interruptions and improving overall system performance.

6.5.5 Local Agent

The LA is a critical component of the microgrid and system layers. It serves as an intermediary between the equipment and microgrid layers, facilitating communication and information exchange. Additionally, the LA contains a DL-based AP algorithm that calculates and updates the protection settings for the BA, ensuring optimal and adaptive protection.

Benefits of LA

a. Communication Hub: The LA's ability to communicate with agents across different layers allows for efficient coordination and exchange of critical information, leading to improved system-wide responsiveness and fault management.

b. Adaptive Protection: The presence of the DL-based AP algorithm enables the LA to continuously adjust the protection settings of the BA based on the microgrid's changing conditions. This adaptability ensures that the protection system remains optimized and effective over time.

c. Enhanced Grid Intelligence: The LA's role in retaining information and messages shared between agents fosters a comprehensive understanding of the microgrid's behaviour, allowing for intelligent decision-making and improved system performance.

6.5.6 Central Agent

The CA is a pivotal component of the system layer, serving as the central repository of information for the entire microgrid system. It collects and consolidates data from all the LAs, providing a comprehensive and real-time overview of the system's status and performance.

Benefits of CA

a. System-Wide Visibility: The CA's ability to access data from all LAs ensures that it possesses a complete and up-to-date understanding of the entire microgrid system. This comprehensive visibility enables effective decision-making and system optimization.

b. Islanding Detection: The CA's awareness of the microgrid's status, including whether it is grid-connected or operating in islanded mode, allows for the timely detection of islanding events. This knowledge is crucial for ensuring a seamless transition between grid-connected and islanded operations.

c. Centralized Control: The CA serves as a central control point, facilitating communication and coordination between different agents within the microgrid. This centralized approach

streamlines the management of the system, leading to more efficient operations and better fault management.

6.5.7 Grid Agent

The GA operates within the system layer and is specifically responsible for handling upstream faults. In the event of an upstream fault, the GA commands the CB at PCC for disconnection, allowing the microgrid to operate autonomously if needed.

Benefits of GA

a. Upstream Fault Handling: The GA's ability to manage upstream faults ensures that the microgrid remains isolated from external disturbances, thereby enhancing its resilience and self-sufficiency.

b. Grid Connectivity Management: The GA's ability to communicate with the CA facilitates intentional islanding when required. This capability is essential for improving system stability during grid disturbances and optimizing microgrid performance.

c. Facilitating Autonomous Operation: In cases of grid disconnection due to upstream faults, the GA's ability to allow the microgrid to continue functioning independently minimizes the impact of external disruptions and ensures the continuity of critical services.

Each agent in the proposed system serves specific functions and contributes to the overall efficiency, reliability, and resilience of the microgrid's protection and management.

6.6 Agent Simulation Software Selection

Most researchers [141, 37] have demonstrated communication between agents using the Java Agent Development (JADE) platform. They have assumed that the digital relay acting as an RA after detecting fault will communicate with other RAs to update settings for protection coordination through message exchange (inform and request) or IEC 61850 GOOSE (Generic Object Oriented Substation Event) messaging between intelligent electronic devices to tackle

overcurrent protection issues in modern grids. Instead, we have used AnyLogic to validate the agent's behaviour and interactions because compared to JADE, AnyLogic requires basic Java coding, and its graphical interface, library objects and tools allow rapid modelling. It also allows agent-based simulation models to be combined with discrete events or system dynamics elements for comprehensive modelling. A detailed survey of all other agent simulation platforms is presented in [208].

6.7 MAML Based PS Simulation

The behaviour of individual agents and their interaction is validated in AnyLogic simulation software. MA, PA, BA, and LA are created as single agents, while the remaining agents are agent type only, not visible in the model but interacting in the background. A 3D View of the developed MAML model is shown in Fig. 6.5.

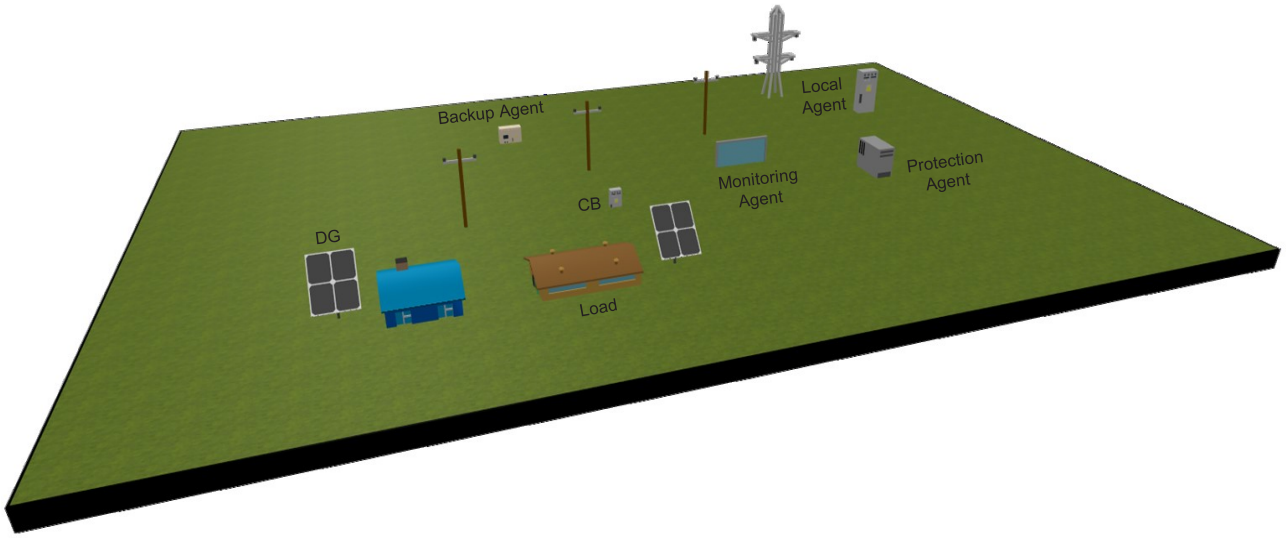

Figure 6.5: AnyLogic simulation model

A cyclic fault event is used to simulate the behaviour of PA and BA, as shown in Fig. 6.6, due to software limitation to add Simulink Classification Ensemble Predict block with trained BT model in MAS simulations.

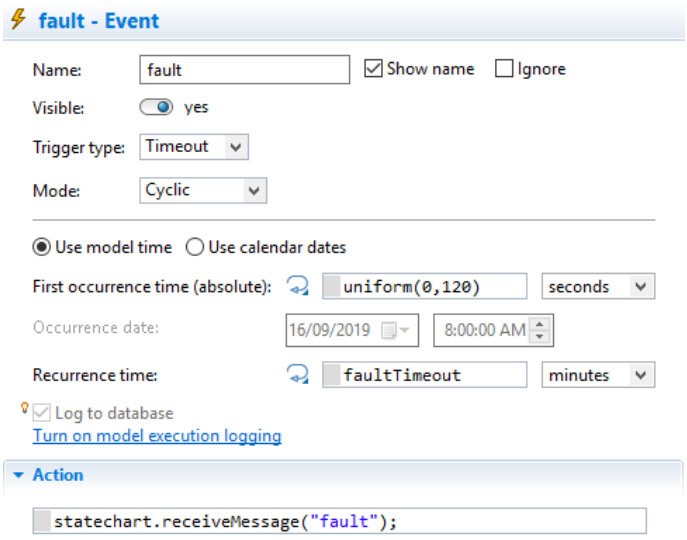

Figure 6.6: Fault event

State transition of these agents is triggered upon receiving the message "fault", shown in Fig. 6.7.

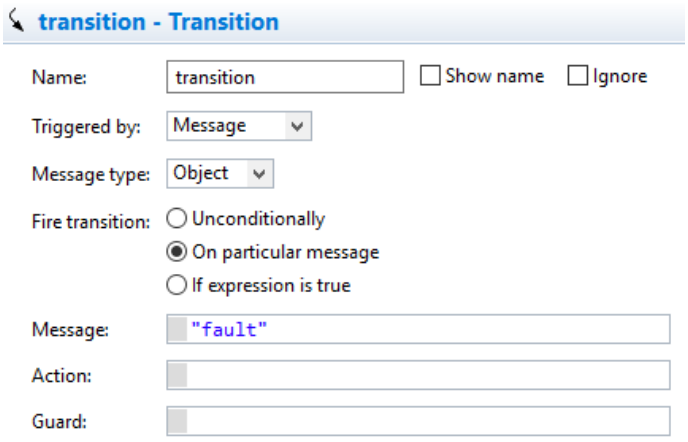

Figure 6.7: State transition

The simulation results confirmed that the proposed novel MAS algorithm provides both primary and backup protection and shows excellent performance compared to previous methods. Besides achieving very high accuracy for FD and FTC with FP, very high protection sensitivity is also attained for both modes of microgrid operation for various fault types and cases. Successful coordination is achieved by MAS.

6.8 Summary

In this chapter, an intelligent protection scheme for LV AC microgrids based on novel FE techniques, MAS with ML is presented. A comprehensive MAS framework with various layers and roles of each agent is developed. Moreover, the idea of incorporating data-driven ML models with a process-driven MAS structure is put forward to achieve reliable coordination, fast segregation, and adaptive backup protection. The simulation results confirm that the proposed protection scheme shows excellent performance compared to previous methods. Besides achieving very high accuracy for FD and FTC with FP identification, very high protection sensitivity is also attained for both modes of microgrid operation for various fault types and cases.

Chapter 7

Conclusion, Research contribution and Future work

After the introduction, a comprehensive literature review is presented to identify the research gap. The focus is on recently proposed methods using modern techniques, besides critically reviewing other proposed methods. Based on the literature review, it is found that primary and backup protection based on hybrid protection, autonomous systems like multi-agents using computational intelligence with real-time data analysis, and application of ML and DL for adaptability can offer promising microgrid protection solutions. Adaptive protection schemes using MAS incorporating ML and DL will increase the sensitivity of detecting the faults, segregating speed, and coordination reliability. Moreover, there is a need for faulted phase identification, besides fault detection and classification, for accurate single- and double-pole tripping, which will increase system resilience and economic benefits. This research work has tried to address all the above-mentioned findings.

The main focus of Chapter 3 is the classification of bolted, low- and high-impedance LG faults in AC microgrids using Supervised Machine Learning. Three classifiers, SVM, KNN, and BT, were trained and tested. KNN demonstrated the highest overall accuracy to identify the correct faulted phase for different LG faults. In Chapter 4, data sets of various fault signals are built and presented. Supervised machine learning is used to detect and classify faults in a radial AC microgrid. New feature extraction techniques, Peaks Metric, and Max Factor are formulated and applied. Additionally, various feature selection methods are used to reduce the number of

predictors. These reduced features are input to training and testing 35 classification learners for FD and FTC with FP identification. 10-fold cross-validation is applied to the training dataset to protect against overfitting. Hyperparameter tuning of all models was performed to improve accuracy. Trained ML models are tested on an unseen dataset to check the accuracy of predictions. The Bagged Trees ensemble classifier outperformed all other ML classifiers for FD and FTC.

The next chapter presents a novel hybrid deep learning approach using deep CNN and deep LSTM for FD and FTC in radial and meshed AC microgrids for various operating conditions. A standard IEC meshed microgrid model is developed. A large dataset of 16000 cases for fault and 432 cases for no-fault conditions is obtained to train and test hybrid DL algorithms for fault detection and fault-type classification with faulted phase identification. Results show superior performance of the proposed method compared to other methods. Lastly, in Chapter 6, an intelligent protection scheme for AC microgrids based on MAS and ML for detecting and classifying symmetrical and unsymmetrical faults, developed in earlier chapters, is presented. A comprehensive MAS framework with various layers and roles of each agent is developed. The communication between agents is verified by simulation.

In conclusion, this research contributes valuable insights into microgrid protection, particularly in the FD, FTC, and FP identification context. The research delves into the application of various intelligent systems, including hybrid protection schemes, MAS incorporating ML and DL techniques, and integrating computational intelligence for real-time data analysis. These findings highlight the potential of such innovative approaches to enhance the sensitivity, reliability, and adaptability of microgrid protection solutions.

7.1 Research Contribution

a. Different radial and meshed AC microgrid models are developed to collect fault and no-fault data and evaluate the performance.

b. Three data sets for fault and no-fault data are prepared for ML and DL algorithms. The

first one classifies bolted, low, and high resistance line-to-ground faults for 9 signals, each with 1000 samples for 60 different cases. Second, for varying fault conditions and no-fault cases in a radial microgrid. There are 400 scenarios, each with 500 samples for 10 signals. Lastly, a standard IEC meshed microgrid model is developed, and a large data set of 16000 cases for fault and 432 cases for no-fault conditions is obtained to train and test the hybrid DL algorithm.

c. Two new FE techniques, Peaks Metric and Max Factor, are formulated and applied. Eight other FE methods, most of which have not been used for microgrid fault detection and classification, are investigated for suitability.

d. Various feature ranking techniques have been used to reduce the number of predictors, and 35 ML algorithms have been used to find the most accurate model.

e. A novel hybrid Deep CNN and Deep LSTM-based protection method for fault detection and classification is developed and presented.

f. Validation of the trained models is carried out using unseen data.

g. A comprehensive MAS framework with various layers and roles of each agent is developed and presented.

h. The idea of incorporating data-driven ML and DL models with a process-driven MAS structure is put forward to achieve reliable coordination, fast segregation, and adaptive backup protection.

i. An intelligent protection scheme based on unique features, MAS with ML and DL, is developed to detect symmetrical and unsymmetrical faults, classify fault types, and identify the faulted phase in radial and meshed AC microgrids. The comprehensive protection scheme provides primary and backup protection and coordination, besides displaying fault type and faulted phase. This can be used for accurate single- and double-pole tripping, which is needed for future intelligent grids to avoid tripping healthy phases in fault events. This will also aid in increasing system resilience and economic benefits.

7.2 Novelty and Significant Contribution

The primary novelty of this research lies in integrating a MAS with ML to develop an intelligent PS for microgrids. Typically, MAS models and ML models are not combined due to their differing foundations: MAS is process-driven, focusing on interactions and processes, while ML is data-driven, relying on data analysis for learning and decision-making. This research bridges this gap by proposing a novel MAS-based solution incorporating ML, allowing for enhanced learning and decision-making capabilities in microgrids. Unlike traditional protection schemes that separately address fault detection and protection coordination, the proposed method integrates these functions into a unified framework. In summary, integrating MAS and ML in this research offers a novel and comprehensive solution to microgrid protection challenges. The hybrid architecture, innovative feature extraction techniques, and robust validation differentiate this work from existing studies, significantly advancing microgrid protection.

7.3 Future Research Directions in AC Microgrid Protection: Addressing Industry Needs

By addressing the following future research directions and incorporating industry insights, the development of robust, secure, and intelligent protection schemes for future smart microgrids will be significantly advanced.

7.3.1 Deepen Exploration of ML and DL Techniques

- Customizing and developing novel architectures tailored to AC microgrid protection challenges could significantly advance the field. Future work can investigate techniques like Generative Adversarial Networks for synthetic fault data generation and Graph Neural Networks to model complex network topologies of microgrids.

- Integrating Explainable AI methods can clarify the decision-making processes of ML/DL models, which is crucial for building trust within the industry and regulatory bodies.

- Applying emerging deep learning architectures and unsupervised learning methods for anomaly detection and improving fault classification and localization, effectively handling complex, non-linear microgrid dynamics.

7.3.2 Integration with Emerging Technologies

- Investigating protection strategies for integrating electric vehicles (EVs) with bi-directional charging capabilities into microgrids is essential. This includes developing fault detection methods that account for the unique transient behaviour of EVs during charging and discharging cycles.
- Researching protection schemes for incorporating battery energy storage systems (BESS) with diverse functionalities, such as frequency regulation and peak shaving, is vital. The protection strategy needs to consider the dynamic response characteristics of BESS during fault events.

7.3.3 Seamless Islanding with Advanced Fault Detection and Reconnection

- Exploring machine learning algorithms like anomaly detection for faster and more accurate islanding detection during abnormal system behaviour.
- Collaborating with industry stakeholders to develop standards for seamless reconnection, considering factors like power quality and synchronization, is essential.

7.3.4 Co-simulation and Protection System Optimization

- Leveraging the advantages of co-simulation. Collect diverse fault data using PowerFactory. Train ML and DL models in MATLAB to accurately predict fault type, FP, and location. Validate the coordination between IEDs and agents in Anylogic.
- Explore co-simulation with other relevant tools to optimize protection relay settings and communication delays for improved system-wide response.

7.3.5 Standardization and Interoperability

- Ensuring the proposed protection scheme adheres to existing and upcoming standards like IEEE Std 1547 series and IEC 61850 is essential for promoting interoperability with different protection relays and microgrid controllers.
- Analyzing industry reports, and relevant standards to identify industry needs and ensure the proposed research aligns with practical implementation considerations is crucial.

7.3.6 Cybersecurity and Secure Communication Protocols

- Integrating recent industry reports from IEEE and CIGRE on microgrid cybersecurity threats and mitigation strategies into the protection scheme design is necessary.
- Exploring communication protocols like the IEC 62351 series, which provides comprehensive security measures for both physical locations and communication networks, is recommended.

7.3.7 Real-Time Digital Simulator (RTDS), Hardware-in-the-Loop (HIL), and Real-World Validation

- Investigating using RTDS for high-fidelity microgrid emulation is crucial. RTDS can simulate complex system behaviour with faster-than-real-time execution, enabling comprehensive testing of protection strategies.
- Moving beyond real-time simulation to incorporate HIL testing for proposed protection schemes allows evaluation with actual protection relays and power electronic converters, providing a more realistic performance assessment.
- Partnering with utilities and research institutions to conduct field tests and validate the protection scheme's performance in real-world microgrid deployments is essential.

References

[1] A. Kavousi-Fard, S. Nikkhah, M. Pourbehzadi, M. Dabbaghjamanesh, and A. Farughian, "Iot-based data-driven fault allocation in microgrids using advanced μPMUs," *Ad Hoc Networks*, vol. 119, p. 102520, 2021.

[2] Powerside, "micropmu & lv," 2021. [Online]. Available: https://powerside.com/wp-content/uploads/2021/05/MicroPMU-LV-Data-Sheet.V2_En.pdf

[3] B. Ram Vara Prasad, B. Sesha Sai, J. Vijaychandra, and R. Babu, "A review on the micro-phasor measurement unit in distribution networks," in *Recent Advances in Power Systems*. Springer, 2022, pp. 93–104.

[4] "Clean energy council report 2023," accessed: 10 Aug 2023. [Online]. Available: https://assets.cleanenergycouncil.org.au/documents/Clean-Energy-Australia-Report-2023.pdf

[5] "Net zero: Australia's path to a clean energy future," accessed: 10 Aug 2023. [Online]. Available: https://www.globalaustralia.gov.au/industries/net-zero

[6] A. C. Adewole, R. Tzoneva, and A. Apostolov, "Protection of distribution systems integrated with distributed generation," in *Handbook of Distributed Generation*. Springer, 2017, pp. 583–627.

[7] T. Gallery, L. Martinez, and D. Klopotan, "Impact of distributed generation on distribution network protection," *ESBI Engineering & Facility Management, Ireland*, 2005.

[8] J. Kennedy, P. Ciufo, and A. Agalgaonkar, "A review of protection systems for distribution networks embedded with renewable generation," *Renewable and Sustainable Energy Reviews*, vol. 58, pp. 1308–1317, 2016.

[9] J. M. Gers and E. J. Holmes, *Protection of electricity distribution networks*, ser. Energy Engineering. Institution of Engineering and Technology, 2011.

[10] A. Girgis and S. Brahma, "Effect of distributed generation on protective device coordination in distribution system," in *Large Engineering Systems Conference on Power Engineering. Conference Proceedings.* IEEE, 2001, pp. 115–119.

[11] D. M. Laverty, R. J. Best, and D. J. Morrow, "Loss-of-mains protection system by application of phasor measurement unit technology with experimentally assessed threshold settings," *IET Generation, Transmission & Distribution*, vol. 9, no. 2, pp. 146–153, 2015.

[12] A. Standards, "AS/NZS 4777.1:2016 grid connection of energy systems via inverters: Installation requirements," Standards Australia, Tech. Rep., 2016.

[13] Nov 2012. [Online]. Available: https://www.aemc.gov.au/sites/default/files/content//Distributed-generation.pdf

[14] D. Zheng, W. Zhang, S. Netsanet, P. Wang, G. T. Bitew, D. Wei, and J. Yue, *Microgrid Protection and Control.* Academic Press, 2021.

[15] F. Katiraei, M. R. Iravani, and P. W. Lehn, "Micro-grid autonomous operation during and subsequent to islanding process," *IEEE Transactions on power delivery*, vol. 20, no. 1, pp. 248–257, 2005.

[16] P. Piagi and R. H. Lasseter, "Autonomous control of microgrids," in *2006 IEEE Power Engineering Society General Meeting.* IEEE, 2006, pp. 8–pp.

[17] N. Pogaku, M. Prodanovic, and T. C. Green, "Modeling, analysis and testing of autonomous operation of an inverter-based microgrid," *IEEE Transactions on power electronics*, vol. 22, no. 2, pp. 613–625, 2007.

[18] D. T. Ton and M. A. Smith, "The us department of energy's microgrid initiative," *The Electricity Journal*, vol. 25, no. 8, pp. 84–94, 2012.

[19] A. Dagar, P. Gupta, and V. Niranjan, "Microgrid protection: A comprehensive review," *Renewable and Sustainable Energy Reviews*, vol. 149, p. 111401, 2021.

[20] E. Planas, J. Andreu, J. I. Gárate, I. M. De Alegría, and E. Ibarra, "Ac and dc technology in microgrids: A review," *Renewable and Sustainable Energy Reviews*, vol. 43, pp. 726–749, 2015.

[21] S. Ullah, A. Haidar, and H. Zen, "Assessment of technical and financial benefits of ac and dc microgrids based on solar photovoltaic." *Electrical Engineering*, vol. 102, no. 3, 2020.

[22] T. Logenthiran, D. Srinivasan, A. M. Khambadkone, and H. N. Aung, "Multiagent system for real-time operation of a microgrid in real-time digital simulator," *IEEE Transactions on smart grid*, vol. 3, no. 2, pp. 925–933, 2012.

[23] B. Liang, L. Kang, J. He, F. Zheng, Y. Xia, Z. Zhang, Z. Zhang, G. Liu, and Y. Zhao, "Coordination control of hybrid ac/dc microgrid," *The Journal of Engineering*, vol. 2019, no. 16, pp. 3264–3269, 2019.

[24] O. Malik, "Microgrids: Concept and challenges in practical implementation," *IEEE Can. Rev.*, pp. 33–35, 2015.

[25] A. Mohamed, S. Vanteddu, and O. Mohammed, "Protection of bi-directional ac-dc/dc-ac converter in hybrid ac/dc microgrids," in *2012 Proceedings of IEEE Southeastcon.* IEEE, 2012, pp. 1–6.

[26] A. Recioui, B. Benseghier, and H. Khalfallah, "Power system fault detection, classification and location using the k-nearest neighbors," in *2015 4th International Conference on Electrical Engineering (ICEE).* IEEE, 2015, pp. 1–6.

[27] M. F. McGranaghan, D. R. Mueller, and M. J. Samotyj, "Voltage sags in industrial systems," *IEEE Transactions on industry applications*, vol. 29, no. 2, pp. 397–403, 1993.

[28] L. Hewitson, M. Brown, and R. Balakrishnan, *Practical power system protection.* Elsevier, 2004.

[29] J. L. Blackburn and T. J. Domin, *Protective relaying: principles and applications.* CRC press, 2014.

[30] P. Pabst, "Challenges of microgrid deployment," Feb 2017. [Online]. Available: https://resourcecenter.smartgrid.ieee.org/publications/newsletters/SGNL0239.html

[31] M. R. Islam and H. A. Gabbar, "Analysis of microgrid protection strategies," in *2012 International Conference on Smart Grid (SGE)*. IEEE, 2012, pp. 1–6.

[32] O. A. Youssef, "New algorithm to phase selection based on wavelet transforms," *IEEE transactions on Power Delivery*, vol. 17, no. 4, pp. 908–914, 2002.

[33] T. A. Short, *Electric power distribution handbook*. CRC press, 2018.

[34] F. Li, R. Li, and F. Zhou, *Microgrid technology and engineering application*. Elsevier, 2015.

[35] N. Hatziargyriou, *Microgrids: architectures and control*. John Wiley & Sons, 2014.

[36] A. Hooshyar and R. Iravani, "Microgrid protection," *Proceedings of the IEEE*, vol. 105, no. 7, pp. 1332–1353, 2017.

[37] M. H. Cintuglu, T. Ma, and O. A. Mohammed, "Protection of autonomous microgrids using agent-based distributed communication," *IEEE Transactions on Power Delivery*, vol. 32, no. 1, pp. 351–360, 2016.

[38] L. Che, M. E. Khodayar, and M. Shahidehpour, "Adaptive protection system for microgrids: Protection practices of a functional microgrid system." *IEEE Electrification magazine*, vol. 2, no. 1, pp. 66–80, 2014.

[39] D. Turcotte and F. Katiraei, "Fault contribution of grid-connected inverters," in *2009 IEEE Electrical Power & Energy Conference (EPEC)*. IEEE, 2009, pp. 1–5.

[40] X. Kang, C. E. Nuworklo, B. S. Tekpeti, and M. Kheshti, "Protection of micro-grid systems: a comprehensive survey," *The Journal of Engineering*, vol. 2017, no. 13, pp. 1515–1518, 2017.

[41] S. Boljevic and M. F. Conlon, "Fault current level issues for urban distribution network with high penetration of distributed generation," in *2009 6th International Conference on the European Energy Market*. IEEE, 2009, pp. 1–6.

[42] R. Nelson, H. Ma, and N. Goldenbaum, "Fault ride-through capabilities of siemens full-converter wind turbines," in *2011 IEEE Power and Energy Society General Meeting*. IEEE, 2011, pp. 1–5.

[43] G. Lammert, T. Heß, M. Schmidt, P. Schegner, and M. Braun, "Dynamic grid support in low voltage grids fault ride-through and reactive power/voltage support during grid disturbances," in *2014 Power Systems Computation Conference*. IEEE, 2014, pp. 1–7.

[44] J. H. Eto, R. Lasseter, D. Klapp, A. Khalsa, B. Schenkman, M. Illindala, and S. Baktiono, "The certs microgrid concept, as demonstrated at the certs/aep microgrid test bed," *US Department of Energy, Berkeley*, vol. 53, 2018.

[45] N. Ullah, A. Ali, H. Ali, and K. Mahmood, "Frequency stability and synthetic inertia," in *Variability, Scalability and Stability of Microgrids*. Institution of Engineering and Technology, 2019, pp. 377–394.

[46] Q. Hong, S. M. Blair, V. M. Catterson, A. Dyśko, C. D. Booth, and T. Rahman, "Standardization of power system protection settings using iec 61850 for improved interoperability," in *2013 IEEE Power & Energy Society General Meeting*. IEEE, 2013, pp. 1–5.

[47] P. Zhang, L. Portillo, and M. Kezunovic, "Compatibility and interoperability evaluation for all-digital protection system through automatic application test," in *2006 IEEE Power Engineering Society General Meeting*. IEEE, 2006, pp. 7–pp.

[48] T. S. Ustun, "Interoperability and interchangeability for microgrid protection systems using iec 61850 standard," in *2016 IEEE International Conference on Power and Energy (PECon)*. IEEE, 2016, pp. 7–12.

[49] S. De Dutta and R. Prasad, "Security for smart grid in 5g and beyond networks," *Wireless Personal Communications*, vol. 106, no. 1, pp. 261–273, 2019.

[50] M. M. Rana, L. Li, and S. W. Su, "Microgrid protection and control through reliable smart grid communication systems," in *2016 14th International Conference on Control, Automation, Robotics and Vision (ICARCV)*. IEEE, 2016, pp. 1–6.

[51] V. C. Nikolaidis, E. Papanikolaou, and A. S. Safigianni, "A communication-assisted overcurrent protection scheme for radial distribution systems with distributed generation," *IEEE transactions on smart grid*, vol. 7, no. 1, pp. 114–123, 2015.

[52] P. Dehghanian, B. Wang, and M. Tasdighi, "New protection schemes in smarter power grids with higher penetration of renewable energy systems," in *Pathways to a Smarter Power System*. Academic Press, 2019, pp. 317–342.

[53] Q.-C. Zhong, *Power electronics-enabled autonomous power systems: next generation smart grids*. John Wiley & Sons, 2020.

[54] A. Hooshyar and R. Iravani, "A new directional element for microgrid protection," *IEEE Transactions on Smart Grid*, vol. 9, no. 6, pp. 6862–6876, 2017.

[55] H. Laaksonen, D. Ishchenko, and A. Oudalov, "Adaptive protection and microgrid control design for hailuoto island," *IEEE Transactions on Smart Grid*, vol. 5, no. 3, pp. 1486–1493, 2014.

[56] M. Khederzadeh, "Adaptive setting of protective relays in microgrids in grid-connected and autonomous operation," in *11th IET International Conference on Developments in Power Systems Protection*, 2012, pp. 1–4.

[57] J.-C. Gu, H.-Y. Chun, Y. Yen, and M.-T. Yang, "Apply setting group function of ied in protection management systems for microgrid reconfiguration," in *2019 International Youth Conference on Radio Electronics, Electrical and Power Engineering (REEPE)*. IEEE, 2019, pp. 1–6.

[58] Y. Ates, A. Boynuegri, M. Uzunoglu, A. Nadar, R. Yumurtacı, O. Erdinc, N. Paterakis, and J. Catalão, "Adaptive protection scheme for a distribution system considering grid-connected and islanded modes of operation," *Energies*, vol. 9, no. 5, p. 378, 2016.

[59] M. Singh and P. Basak, "Adaptive protection methodology in microgrid for fault location and nature detection using q0 components of fault current," *IET Generation, Transmission & Distribution*, vol. 13, no. 6, pp. 760–769, 2019.

[60] R. Jain, D. L. Lubkeman, and S. M. Lukic, "Dynamic adaptive protection for distribution systems in grid-connected and islanded modes," *IEEE Transactions on Power Delivery*, vol. 34, no. 1, pp. 281–289, 2018.

[61] S. Conti, L. Raffa, and U. Vagliasindi, "Innovative solutions for protection schemes in autonomous mv micro-grids," in *2009 International Conference on Clean Electrical Power*. IEEE, 2009, pp. 647–654.

[62] B. Patnaik, M. Mishra, R. C. Bansal, and R. K. Jena, "Ac microgrid protection–a review: Current and future prospective," *Applied Energy*, vol. 271, p. 115210, 2020.

[63] K. Dubey and P. Jena, "Impedance angle-based differential protection scheme for microgrid feeders," *IEEE Systems Journal*, 2020.

[64] S. Ansari and O. H. Gupta, "Differential positive sequence power angle-based microgrid feeder protection," *International Journal of Emerging Electric Power Systems*, 2021.

[65] W. Xingguo, Z. Zexin, and D. Dingxiang, "A phase selection element for zero sequence current differential protection," in *2014 International Conference on Power System Technology*. IEEE, 2014, pp. 362–367.

[66] T. Nengling and J. Stenzel, "Differential protection based on zero-sequence voltages for generator stator ground fault," *IEEE transactions on power delivery*, vol. 22, no. 1, pp. 116–121, 2006.

[67] E. Sortomme, S. Venkata, and J. Mitra, "Microgrid protection using communication-assisted digital relays," *IEEE Transactions on Power Delivery*, vol. 25, no. 4, pp. 2789–2796, 2009.

[68] T. S. Ustun and R. H. Khan, "Multiterminal hybrid protection of microgrids over wireless communications network," *IEEE Transactions on Smart Grid*, vol. 6, no. 5, pp. 2493–2500, 2015.

[69] A. Pathirana, A. Rajapakse, and N. Perera, "Development of a hybrid protection scheme for active distribution systems using polarities of current transients," *Electric Power*

Systems Research, vol. 152, pp. 377–389, 2017.

[70] S. Chakraborty and S. Das, "Communication-less protection scheme for ac microgrids using hybrid tripping characteristic," *Electric Power Systems Research*, vol. 187, p. 106453, 2020.

[71] G. Benmouyal, M. Meisinger, J. Burnworth, W. Elmore, K. Freirich, P. Kotos, P. Leblanc, P. Lerley, J. McConnell, J. Mizener *et al.*, "Ieee standard inverse-time characteristic equations for overcurrent relays," *IEEE Transactions on Power Delivery*, vol. 14, no. 3, pp. 868–872, 1999.

[72] S. IEC, "Measuring relays and protection equipment-part 127: Functional requirements for over/under voltage protection," *IEC 60255-127*, 2010.

[73] P. Hindle and J. Sanderson, "Overcurrent protection co-ordination: a modern approach for modern devices," in *Sixth International Conference on Developments in Power System Protection (Conf. Publ. No. 434)*. IET, 1997, pp. 62–65.

[74] G. S. Babu, S. Venugopal, and T. M. Krishna, "Inverse definite minimum time relay coordination in radial traction system," *International Journal of Electrical Engineering and Technology*, vol. 11, no. 4, 2020.

[75] M. E. Hamidi and R. M. Chabanloo, "Optimal allocation of distributed generation with optimal sizing of fault current limiter to reduce the impact on distribution networks using nsga-ii," *IEEE Systems Journal*, vol. 13, no. 2, pp. 1714–1724, 2018.

[76] J. Ma, X. Wang, Y. Zhang, Q. Yang, and A. Phadke, "A novel adaptive current protection scheme for distribution systems with distributed generation," *International Journal of Electrical Power & Energy Systems*, vol. 43, no. 1, pp. 1460–1466, 2012.

[77] T. Ghanbari and E. Farjah, "Unidirectional fault current limiter: An efficient interface between the microgrid and main network," *IEEE Transactions on Power Systems*, vol. 28, no. 2, pp. 1591–1598, 2012.

[78] A. Heidary, H. Radmanesh, K. Rouzbehi, A. Mehrizi-Sani, and G. B. Gharehpetian, "Inductive fault current limiters: A review," *Electric Power Systems Research*, vol. 187, p. 106499, 2020.

[79] A. E. Dahej, S. Esmaeili, and H. Hojabri, "Co-optimization of protection coordination and power quality in microgrids using unidirectional fault current limiters," *IEEE Transactions on Smart Grid*, vol. 9, no. 5, pp. 5080–5091, 2017.

[80] M. Firouzi, "Low-voltage ride-through (lvrt) capability enhancement of dfig-based wind farm by using bridge-type superconducting fault current limiter (btsfcl)," *Journal of Power Technologies*, vol. 99, no. 4, pp. 245–253, 2020.

[81] P. Zolfi, F. Barmoudeh, and N. Taghizadegan Kalantari, "Bidirectional non-superconducting fault current limiter (bnsfcl) for smart grid applications," *Journal of Energy Management and Technology*, vol. 3, no. 3, pp. 60–66, 2019.

[82] M. Farzinfar and M. Jazaeri, "A novel methodology in optimal setting of directional fault current limiter and protection of the mg," *International Journal of Electrical Power & Energy Systems*, vol. 116, p. 105564, 2020.

[83] Ł. Huchel and H. H. Zeineldin, "Planning the coordination of directional overcurrent relays for distribution systems considering dg," *IEEE Transactions on Smart Grid*, vol. 7, no. 3, pp. 1642–1649, 2015.

[84] N. Rezaei and M. Uddin, "An analytical review on state-of-the-art microgrid protective relaying and coordination techniques," *IEEE Transactions on Industry Applications*, 2021.

[85] E. Dehghanpour, H. K. Karegar, R. Kheirollahi, and T. Soleymani, "Optimal coordination of directional overcurrent relays in microgrids by using cuckoo-linear optimization algorithm and fault current limiter," *IEEE Transactions on Smart Grid*, vol. 9, no. 2, pp. 1365–1375, 2016.

[86] H. Al-Nasseri, M. Redfern, and F. Li, "A voltage based protection for micro-grids containing power electronic converters," in *2006 IEEE Power Engineering Society General*

Meeting. IEEE, 2006, pp. 7–pp.

[87] P. T. Manditereza and R. C. Bansal, "Protection of microgrids using voltage-based power differential and sensitivity analysis," *International Journal of Electrical Power & Energy Systems*, vol. 118, p. 105756, 2020.

[88] E. O. Schweitzer, A. Guzmán, M. V. Mynam, V. Skendzic, B. Kasztenny, and S. Marx, "Locating faults by the traveling waves they launch," in *2014 67th annual conference for protective relay engineers*. IEEE, 2014, pp. 95–110.

[89] M. A. Aftab, S. S. Hussain, I. Ali, and T. S. Ustun, "Dynamic protection of power systems with high penetration of renewables: A review of the traveling wave based fault location techniques," *International Journal of Electrical Power & Energy Systems*, vol. 114, p. 105410, 2020.

[90] S. Sawai and A. K. Pradhan, "Travelling-wave-based protection of transmission line using single-end data," *IET Generation, Transmission & Distribution*, vol. 13, no. 20, pp. 4659–4666, 2019.

[91] X. Li, A. Dyśko, and G. Burt, "Enhanced protection for inverter dominated microgrid using transient fault information," in *11th IET International Conference on Developments in Power Systems Protection (DPSP 2012)*. IET, 2012, pp. 1–5.

[92] S. Robson, A. Haddad, and H. Griffiths, "Fault location on branched networks using a multiended approach," *IEEE transactions on power delivery*, vol. 29, no. 4, pp. 1955–1963, 2014.

[93] S. Lin, Z. He, X. Li, and Q. Qian, "Travelling wave time–frequency characteristic-based fault location method for transmission lines," *IET generation, transmission & distribution*, vol. 6, no. 8, pp. 764–772, 2012.

[94] V. Gonzalez-Sanchez, V. Torres-García, and D. Guillen, "Fault location on transmission lines based on travelling waves using correlation and modwt," *Electric Power Systems Research*, vol. 197, p. 107308, 2021.

[95] X. Li, A. Dyśko, and G. M. Burt, "Traveling wave-based protection scheme for inverter-dominated microgrid using mathematical morphology," *IEEE Transactions on Smart Grid*, vol. 5, no. 5, pp. 2211–2218, 2014.

[96] F. B. Costa, B. A. Souza, and N. S. D. Brito, "Real-time detection of fault-induced transients in transmission lines," *Electronics letters*, vol. 46, no. 11, pp. 753–755, 2010.

[97] A. Chandra, G. Singh, and V. Pant, "Protection of ac microgrid integrated with renewable energy sources–a research review and future trends," *Electric Power Systems Research*, vol. 193, p. 107036, 2021.

[98] J. Qiao, X. Yin, Y. Wang, W. Xu, and L. Tan, "A multi-terminal traveling wave fault location method for active distribution network based on residual clustering," *International Journal of Electrical Power & Energy Systems*, vol. 131, p. 107070, 2021.

[99] K. Saleh, A. Hooshyar, and E. F. El-Saadany, "Fault detection and location in medium-voltage dc microgrids using travelling-wave reflections," *IET Renewable Power Generation*, vol. 14, no. 4, pp. 571–579, 2020.

[100] E. C. Maritz, J. M. Maritz, and M. Salehi, "A travelling wave-based fault location strategy using the concepts of metric dimension and vertex covers in a graph," *IEEE Access*, vol. 9, pp. 155 815–155 825, 2021.

[101] S. Shi, A. Lei, X. He, S. Mirsaeidi, and X. Dong, "Travelling waves-based fault location scheme for feeders in power distribution network," *The Journal of Engineering*, vol. 2018, no. 15, pp. 1326–1329, 2018.

[102] S. Gupta and S. Gangolu, "Microgrid islanding detection using travelling wave based hybrid protection scheme," in *International Conference on Electrical and Electronics Engineering*. Springer, 2022, pp. 92–105.

[103] C. H. Kim and R. Aggarwal, "Wavelet transforms in power systems. part 1: General introduction to the wavelet transforms," *Power Engineering Journal*, vol. 14, no. 2, pp. 81–87, 2000.

[104] J. Liang, S. Elangovan, and J. Devotta, "Application of wavelet transform in travelling wave protection," *International journal of electrical power & energy systems*, vol. 22, no. 8, pp. 537–542, 2000.

[105] W. K. Ngui, M. S. Leong, L. M. Hee, and A. M. Abdelrhman, "Wavelet analysis: mother wavelet selection methods," in *Applied mechanics and materials*, vol. 393. Trans Tech Publ, 2013, pp. 953–958.

[106] J. De La Ree, V. Centeno, J. S. Thorp, and A. G. Phadke, "Synchronized phasor measurement applications in power systems," *IEEE Transactions on smart grid*, vol. 1, no. 1, pp. 20–27, 2010.

[107] N. K. Sharma and S. R. Samantaray, "Assessment of pmu-based wide-area angle criterion for fault detection in microgrid," *IET Generation, Transmission & Distribution*, vol. 13, no. 19, pp. 4301–4310, 2019.

[108] ——, "Pmu assisted integrated impedance angle-based microgrid protection scheme," *IEEE Transactions on Power Delivery*, vol. 35, no. 1, pp. 183–193, 2019.

[109] Y. Liu, L. Wu, and J. Li, "D-pmu based applications for emerging active distribution systems: A review," *Electric Power Systems Research*, vol. 179, p. 106063, 2020.

[110] A. Von Meier, D. Culler, A. McEachern, and R. Arghandeh, "Micro-synchrophasors for distribution systems," in *ISGT 2014*. IEEE, 2014, pp. 1–5.

[111] L.-A. Lee and V. Centeno, "Comparison of μpmu and pmu," in *2018 Clemson University Power Systems Conference (PSC)*. IEEE, 2018, pp. 1–6.

[112] M. G. M. Zanjani, K. Mazlumi, and I. Kamwa, "Application of μpmus for adaptive protection of overcurrent relays in microgrids," *IET Generation, Transmission & Distribution*, vol. 12, no. 18, pp. 4061–4068, 2018.

[113] K. Al-Maitah and A. Al-Odienat, "Wide area protection scheme for active distribution network aided μPMU," in *2020 IEEE PES/IAS PowerAfrica*. IEEE, 2020, pp. 1–5.

[114] M. Gholami, A. Abbaspour, M. Moeini-Aghtaie, M. Fotuhi-Firuzabad, and M. Lehtonen, "Detecting the location of short-circuit faults in active distribution network using pmu-based state estimation," *IEEE Transactions on Smart Grid*, vol. 11, no. 2, pp. 1396–1406, 2019.

[115] M. S. Elbana, N. Abbasy, A. Meghed, and N. Shaker, "μpmu-based smart adaptive protection scheme for microgrids," *Journal of Modern Power Systems and Clean Energy*, vol. 7, no. 4, pp. 887–898, 2019.

[116] S. Som, R. Dutta, A. Gholami, A. K. Srivastava, S. Chakrabarti, and S. R. Sahoo, "Dpmu-based multiple event detection in a microgrid considering measurement anomalies," *Applied Energy*, vol. 308, p. 118269, 2022.

[117] R. Xinyu, H. Jinhan, W. Xiaojun, and W. Zhenji, "Analysis of μpmu noise characteristics and its influence on distribution network fault location," in *2018 IEEE 2nd International Electrical and Energy Conference (CIEEC)*. IEEE, 2018, pp. 190–195.

[118] M. H. Cintuglu, A. T. Elsayed, and O. A. Mohammed, "Microgrid automation assisted by synchrophasors," in *2015 IEEE Power & Energy Society Innovative Smart Grid Technologies Conference (ISGT)*. IEEE, 2015, pp. 1–5.

[119] H. Al-Nasseri and M. Redfern, "Harmonics content based protection scheme for microgrids dominated by solid state converters," in *2008 12th International Middle-East Power System Conference*. IEEE, 2008, pp. 50–56.

[120] Z. Chen, X. Pei, M. Yang, L. Peng, and P. Shi, "A novel protection scheme for inverter-interfaced microgrid (iim) operated in islanded mode," *IEEE Transactions on Power Electronics*, vol. 33, no. 9, pp. 7684–7697, 2017.

[121] D. Jeerings and J. Linders, "Unique aspects of distribution system harmonics due to high impedance ground faults," *IEEE Transactions on Power delivery*, vol. 5, no. 2, pp. 1086–1094, 1990.

[122] S. Mirsaeidi, D. M. Said, M. W. Mustafa, and M. H. Habibuddin, "A protection strategy for micro-grids based on positive-sequence component," *IET Renewable Power Genera-*

tion, vol. 9, no. 6, pp. 600–609, 2015.

[123] K. Dang, X. He, D. Bi, and C. Feng, "An adaptive protection method for the inverter dominated microgrid," in *2011 International Conference on Electrical Machines and Systems*. IEEE, 2011, pp. 1–5.

[124] H. Nikkhajoei and R. H. Lasseter, "Microgrid protection," in *2007 IEEE Power Engineering Society General Meeting*. IEEE, 2007, pp. 1–6.

[125] P. S. Addison, *The illustrated wavelet transform handbook: introductory theory and applications in science, engineering, medicine and finance*. London: CRC press, 2017.

[126] R. X. Gao and R. Yan, *Wavelets: Theory and applications for manufacturing*. New York: Springer Science & Business Media, 2010.

[127] B. K. Panigrahi, P. K. Ray, P. K. Rout, and S. K. Sahu, "Detection and location of fault in a micro grid using wavelet transform," in *2017 International Conference on Circuit, Power and Computing Technologies (ICCPCT)*. IEEE, 2017, pp. 1–5.

[128] G. Swain, P. Sinha, and M. Maharana, "Detection of islanding and power quality disturbance in micro grid connected distributed generation," in *2017 International Conference on Innovative Mechanisms for Industry Applications (ICIMIA)*. IEEE, 2017, pp. 388–393.

[129] R. Escudero, J. Noel, J. Elizondo, and J. Kirtley, "Microgrid fault detection based on wavelet transformation and park's vector approach," *Electric Power Systems Research*, vol. 152, pp. 401–410, 2017.

[130] A. Megahed, A. M. Moussa, H. Elrefaie, and Y. Marghany, "Selection of a suitable mother wavelet for analyzing power system fault transients," in *2008 IEEE Power and Energy Society General Meeting-Conversion and Delivery of Electrical Energy in the 21st Century*. IEEE, 2008, pp. 1–7.

[131] W. A. Wilkinson and M. Cox, "Discrete wavelet analysis of power system transients," *IEEE Transactions on Power systems*, vol. 11, no. 4, pp. 2038–2044, 1996.

[132] C. Macal and M. North, "Introductory tutorial: Agent-based modeling and simulation," in *Proceedings of the Winter Simulation Conference 2014*. IEEE, 2014, pp. 6–20.

[133] F. L. Bellifemine, G. Caire, and D. Greenwood, *Developing multi-agent systems with JADE*. John Wiley & Sons, 2007, vol. 7.

[134] M. Wooldridge and N. R. Jennings, "Intelligent agents: Theory and practice," *The knowledge engineering review*, vol. 10, no. 2, pp. 115–152, 1995.

[135] M.-y. Yang and Y.-l. Zhu, "A cooperative protection system with multi-agent system," in *2005 IEEE/PES Transmission & Distribution Conference & Exposition: Asia and Pacific*. IEEE, 2005, pp. 1–4.

[136] M. Uzair, L. Li, J. G. Zhu, and M. Eskandari, "A protection scheme for ac microgrids based on multi-agent system combined with machine learning," in *2019 Australasian Universities Power Engineering Conference (AUPEC)*. IEEE, 2019, pp. 1–6.

[137] H. F. Habib, T. Youssef, M. H. Cintuglu, and O. A. Mohammed, "Multi-agent-based technique for fault location, isolation, and service restoration," *IEEE Transactions on Industry Applications*, vol. 53, no. 3, pp. 1841–1851, 2017.

[138] M. J. Daryani and A. E. Karkevandi, "Decentralized cooperative protection strategy for smart distribution grid using multi-agent system," in *2018 6th International Istanbul Smart Grids and Cities Congress and Fair (ICSG)*. IEEE, 2018, pp. 134–138.

[139] E. Kremers, J. G. de Durana, and O. Barambones, "Multi-agent modeling for the simulation of a simple smart microgrid," *Energy Conversion and Management*, vol. 75, pp. 643–650, 2013.

[140] H. Karimi, B. Fani, and G. Shahgholian, "Multi agent-based strategy protecting the loop-based micro-grid via intelligent electronic device-assisted relays," *IET Renewable Power Generation*, vol. 14, no. 19, pp. 4132–4141, 2020.

[141] H. Wan, K. Wong, and C. Chung, "Multi-agent application in protection coordination of power system with distributed generations," in *2008 IEEE Power and Energy Soci-*

ety General Meeting-Conversion and Delivery of Electrical Energy in the 21st Century. IEEE, 2008, pp. 1–6.

[142] J. Ocampo-Wilches, A. Ustariz-Farfan, and E. Cano-Plata, "Modeling of a centralized microgrid protection scheme," in *2017 IEEE Workshop on Power Electronics and Power Quality Applications (PEPQA).* IEEE, 2017, pp. 1–6.

[143] F. B. dos Reis, J. O. C. Pinto, F. S. dos Reis, D. Issicaba, and J. G. Rolim, "Multi-agent dual strategy based adaptive protection for microgrids," *Sustainable Energy, Grids and Networks*, p. 100501, 2021.

[144] L. L. do Nascimento and J. G. Rolim, "Multi-agent system for adaptive protection in microgrids," in *2013 IEEE PES Conference on Innovative Smart Grid Technologies (ISGT Latin America).* IEEE, 2013, pp. 1–8.

[145] A. Hussain, M. Aslam, and S. M. Arif, "N-version programming-based protection scheme for microgrids: A multi-agent system based approach," *Sustainable Energy, Grids and Networks*, vol. 6, pp. 35–45, 2016.

[146] T. S. Aghdam, H. K. Karegar, and H. H. Zeineldin, "Variable tripping time differential protection for microgrids considering dg stability," *IEEE Transactions on Smart Grid*, vol. 10, no. 3, pp. 2407–2415, 2018.

[147] Y. Zhu, S. Song, and D. Wang, "Multiagents-based wide area protection with best-effort adaptive strategy," *International Journal of Electrical Power & Energy Systems*, vol. 31, no. 2, pp. 94–99, 2009.

[148] S. Kar, S. Samantaray, and M. D. Zadeh, "Data-mining model based intelligent differential microgrid protection scheme," *IEEE Systems Journal*, vol. 11, no. 2, pp. 1161–1169, 2015.

[149] D. P. Mishra, S. R. Samantaray, and G. Joos, "A combined wavelet and data-mining based intelligent protection scheme for microgrid," *IEEE Transactions on Smart Grid*, vol. 7, no. 5, pp. 2295–2304, 2015.

[150] S. Ranjbar, A. R. Farsa, and S. Jamali, "Voltage-based protection of microgrids using decision tree algorithms," *International Transactions on Electrical Energy Systems*, vol. 30, no. 4, p. e12274, 2020.

[151] T. K. Ho, "Random decision forests," in *Proceedings of 3rd international conference on document analysis and recognition*, vol. 1. IEEE, 1995, pp. 278–282.

[152] M. Esteve, J. Aparicio, A. Rabasa, and J. J. Rodriguez-Sala, "Efficiency analysis trees: A new methodology for estimating production frontiers through decision trees," *Expert Systems with Applications*, vol. 162, p. 113783, 2020.

[153] L. Breiman, "Random forests," *Machine learning*, vol. 45, no. 1, pp. 5–32, 2001.

[154] T. Hastie, R. Tibshirani, and J. Friedman, "Random forests," in *The elements of statistical learning*. Springer, 2009, pp. 587–604.

[155] A. J. Sage, U. Genschel, and D. Nettleton, "Tree aggregation for random forest class probability estimation," *Statistical Analysis and Data Mining: The ASA Data Science Journal*, vol. 13, no. 2, pp. 134–150, 2020.

[156] M. Al Karim, J. Currie, and T.-T. Lie, "Dynamic event detection using a distributed feature selection based machine learning approach in a self-healing microgrid," *IEEE Transactions on Power Systems*, vol. 33, no. 5, pp. 4706–4718, 2018.

[157] M. Uzair, M. Eskandari, L. Li, and J. Zhu, "Machine learning based protection scheme for low voltage ac microgrids," *Energies*, vol. 15, no. 24, p. 9397, 2022.

[158] S. Baloch, S. S. Samsani, and M. S. Muhammad, "Fault protection in microgrid using wavelet multiresolution analysis and data mining," *IEEE Access*, vol. 9, pp. 86 382–86 391, 2021.

[159] S. Baloch, S. Z. Jamali, and S. A. R. Shah, "A protection technique for microgrid using wavelet packet transform and data mining classifier," *Engineering Proceedings*, vol. 20, no. 1, p. 33, 2022.

[160] S. Netsanet, J. Zhang, and D. Zheng, "Bagged decision trees based scheme of microgrid protection using windowed fast fourier and wavelet transforms," *Electronics*, vol. 7, no. 5, p. 61, 2018.

[161] Q. Cui and Y. Weng, "Enhance high impedance fault detection and location accuracy via μPMU," *IEEE Transactions on Smart Grid*, vol. 11, no. 1, pp. 797–809, 2019.

[162] G. Niu, B. Dai, M. Yamada, and M. Sugiyama, "Information-theoretic semi-supervised metric learning via entropy regularization," *Neural computation*, vol. 26, no. 8, pp. 1717–1762, 2014.

[163] S. Kolla and P. Onwonga, "Identification of faults in microgrid using artificial neural networks," in *2020 IEEE Green Technologies Conference (GreenTech)*. IEEE, 2020, pp. 115–120.

[164] P. J. Haley and D. Soloway, "Extrapolation limitations of multilayer feedforward neural networks," in *[Proceedings 1992] IJCNN International Joint Conference on Neural Networks*, vol. 4. IEEE, 1992, pp. 25–30.

[165] R. Ransing, M. Ransing, and R. Lewis, "On the limitations of neural network techniques for analysing cause and effect relationships in manufacturing processes–a case study," *WIT Transactions on Information and Communication Technologies*, vol. 29, 2003.

[166] M. Manohar, E. Koley, and S. Ghosh, "Microgrid protection under wind speed intermittency using extreme learning machine," *Computers & Electrical Engineering*, vol. 72, pp. 369–382, 2018.

[167] G.-B. Huang, Q.-Y. Zhu, and C.-K. Siew, "Extreme learning machine: theory and applications," *Neurocomputing*, vol. 70, no. 1-3, pp. 489–501, 2006.

[168] X. Liu, S. Lin, J. Fang, and Z. Xu, "Is extreme learning machine feasible? a theoretical assessment (part i)," *IEEE Transactions on Neural Networks and Learning Systems*, vol. 26, no. 1, pp. 7–20, 2014.

[169] I. Goodfellow, Y. Bengio, and A. Courville, *Deep learning*. MIT press, 2016.

[170] E. Casagrande, W. L. Woon, H. H. Zeineldin, and N. H. Kan'an, "Data mining approach to fault detection for isolated inverter-based microgrids," *IET Generation, Transmission & Distribution*, vol. 7, no. 7, pp. 745–754, 2013.

[171] M. Uzair, L. Li, and J. G. Zhu, "Identifying line-to-ground faulted phase in low and medium voltage ac microgrid using principal component analysis and supervised machine-learning," in *2018 Australasian Universities Power Engineering Conference (AUPEC)*. IEEE, 2018, pp. 1–6.

[172] T. S. Abdelgayed, W. G. Morsi, and T. S. Sidhu, "A new approach for fault classification in microgrids using optimal wavelet functions matching pursuit," *IEEE Transactions on Smart Grid*, vol. 9, no. 5, pp. 4838–4846, 2017.

[173] M. Mishra and P. K. Rout, "Detection and classification of micro-grid faults based on hht and machine learning techniques," *IET Generation, Transmission & Distribution*, vol. 12, no. 2, pp. 388–397, 2017.

[174] T. S. Abdelgayed, W. G. Morsi, and T. S. Sidhu, "Fault detection and classification based on co-training of semisupervised machine learning," *IEEE Transactions on Industrial Electronics*, vol. 65, no. 2, pp. 1595–1605, 2017.

[175] H. Lin, K. Sun, Z.-H. Tan, C. Liu, J. M. Guerrero, and J. C. Vasquez, "Adaptive protection combined with machine learning for microgrids," *IET Generation, Transmission & Distribution*, vol. 13, no. 6, pp. 770–779, 2019.

[176] J. James, Y. Hou, A. Y. Lam, and V. O. Li, "Intelligent fault detection scheme for microgrids with wavelet-based deep neural networks," *IEEE Transactions on Smart Grid*, vol. 10, no. 2, pp. 1694–1703, 2019.

[177] K. Cho, B. Van Merriënboer, C. Gulcehre, D. Bahdanau, F. Bougares, H. Schwenk, and Y. Bengio, "Learning phrase representations using rnn encoder-decoder for statistical machine translation," *arXiv preprint arXiv:1406.1078*, 2014.

[178] S. Samal, S. Samantaray, and M. Manikandan, "A dnn based intelligent protective relaying scheme for microgrids," in *2019 8th International Conference on Power Systems*

(ICPS). IEEE, 2019, pp. 1–6.

[179] G. Panchal, A. Ganatra, Y. Kosta, and D. Panchal, "Behaviour analysis of multilayer perceptrons with multiple hidden neurons and hidden layers," *International Journal of Computer Theory and Engineering*, vol. 3, no. 2, pp. 332–337, 2011.

[180] A. Malik, A. Haque, and K. S. Bharath, "Deep learning based fault diagnostic technique for grid connected inverter," in *2021 IEEE 12th Energy Conversion Congress & Exposition-Asia (ECCE-Asia)*. IEEE, 2021, pp. 1390–1395.

[181] H. Abdi and L. J. Williams, "Principal component analysis," *Wiley interdisciplinary reviews: computational statistics*, vol. 2, no. 4, pp. 433–459, 2010.

[182] I. Guyon, S. Gunn, M. Nikravesh, and L. A. Zadeh, *Feature extraction: foundations and applications*. Springer, 2008, vol. 207.

[183] J. B. Ali, L. Saidi, S. Harrath, E. Bechhoefer, and M. Benbouzid, "Online automatic diagnosis of wind turbine bearings progressive degradations under real experimental conditions based on unsupervised machine learning," *Applied Acoustics*, vol. 132, pp. 167–181, 2018.

[184] B. Van Hecke, Y. Qu, and D. He, "Bearing fault diagnosis based on a new acoustic emission sensor technique," *Proceedings of the Institution of Mechanical Engineers, Part O: Journal of Risk and Reliability*, vol. 229, no. 2, pp. 105–118, 2015.

[185] S. Wold, K. Esbensen, and P. Geladi, "Principal component analysis," *Chemometrics and intelligent laboratory systems*, vol. 2, no. 1-3, pp. 37–52, 1987.

[186] A. Inselberg, "The plane with parallel coordinates," *The visual computer*, vol. 1, pp. 69–91, 1985.

[187] A. Inselberg and B. Dimsdale, "Parallel coordinates: A tool for visualizing multivariate relations," in *Human-Machine Interactive Systems*. Springer, 1991, pp. 199–233.

[188] T. W. MacFarland and J. M. Yates, "Kruskal–wallis h-test for oneway analysis of variance (anova) by ranks," in *Introduction to nonparametric statistics for the biological sciences*

using R. Springer, 2016, pp. 177–211.

[189] L. Breiman, "Bagging predictors," *Machine learning*, vol. 24, no. 2, pp. 123–140, 1996.

[190] R.-C. Chen, C. Dewi, S.-W. Huang, and R. E. Caraka, "Selecting critical features for data classification based on machine learning methods," *Journal of Big Data*, vol. 7, pp. 1–26, 2020.

[191] V. Timčenko and S. Gajin, "Ensemble classifiers for supervised anomaly based network intrusion detection," in *2017 13th IEEE international conference on intelligent computer communication and processing (ICCP)*. IEEE, 2017, pp. 13–19.

[192] Y. Wang, M. Liu, and Z. Bao, "Deep learning neural network for power system fault diagnosis," in *2016 35th Chinese control conference (CCC)*. IEEE, 2016, pp. 6678–6683.

[193] P. Xi, P. Feilai, L. Yongchao, L. Zhiping, and L. Long, "Fault detection algorithm for power distribution network based on sparse self-encoding neural network," in *2017 International Conference on Smart Grid and Electrical Automation (ICSGEA)*. IEEE, 2017, pp. 9–12.

[194] S. Zhang, Y. Wang, M. Liu, and Z. Bao, "Data-based line trip fault prediction in power systems using lstm networks and svm," *Ieee Access*, vol. 6, pp. 7675–7686, 2017.

[195] S.-R. Han and Y.-S. Kim, "A fault identification method using lstm for a closed-loop distribution system protective relay," *International Journal of Electrical Power & Energy Systems*, vol. 148, p. 108925, 2023.

[196] S. B. A. Bukhari, C.-H. Kim, K. K. Mehmood, R. Haider, and M. Saeed Uz Zaman, "Convolutional neural network-based intelligent protection strategy for microgrids," *IET Generation, Transmission & Distribution*, vol. 14, no. 7, pp. 1177–1185, 2020.

[197] O. Gashteroodkhani, M. Majidi, and M. Etezadi-Amoli, "A combined deep belief network and time-time transform based intelligent protection scheme for microgrids," *Electric Power Systems Research*, vol. 182, p. 106239, 2020.

[198] M. Manohar, E. Koley, and S. Ghosh, "Enhancing the reliability of protection scheme for pv integrated microgrid by discriminating between array faults and symmetrical line faults using sparse auto encoder," *IET Renewable Power Generation*, vol. 13, no. 2, pp. 308–317, 2019.

[199] G. Luo, Y. Tan, M. Li, M. Cheng, Y. Liu, and J. He, "Stacked auto-encoder-based fault location in distribution network," *IEEE Access*, vol. 8, pp. 28 043–28 053, 2020.

[200] J. Liang, T. Jing, H. Niu, and J. Wang, "Two-terminal fault location method of distribution network based on adaptive convolution neural network," *IEEE Access*, vol. 8, pp. 54 035–54 043, 2020.

[201] S. Karan and H.-G. Yeh, "Fault classification in microgrids using deep learning," in *2020 IEEE Green Energy and Smart Systems Conference (IGESSC)*. IEEE, 2020, pp. 1–7.

[202] A. K. Özcanlı and M. Baysal, "A novel multi-lstm based deep learning method for islanding detection in the microgrid," *Electric Power Systems Research*, vol. 202, p. 107574, 2022.

[203] M. A. Zamani, A. Yazdani, and T. S. Sidhu, "A control strategy for enhanced operation of inverter-based microgrids under transient disturbances and network faults," *IEEE Transactions on Power Delivery*, vol. 27, no. 4, pp. 1737–1747, 2012.

[204] L. Wen, X. Li, L. Gao, and Y. Zhang, "A new convolutional neural network-based data-driven fault diagnosis method," *IEEE Transactions on Industrial Electronics*, vol. 65, no. 7, pp. 5990–5998, 2017.

[205] M. Xia, T. Li, L. Xu, L. Liu, and C. W. De Silva, "Fault diagnosis for rotating machinery using multiple sensors and convolutional neural networks," *IEEE/ASME transactions on mechatronics*, vol. 23, no. 1, pp. 101–110, 2017.

[206] W. Sun, R. Zhao, R. Yan, S. Shao, and X. Chen, "Convolutional discriminative feature learning for induction motor fault diagnosis," *IEEE Transactions on Industrial Informatics*, vol. 13, no. 3, pp. 1350–1359, 2017.

[207] S. Hochreiter and J. Schmidhuber, "Long short-term memory," *Neural computation*, vol. 9, no. 8, pp. 1735–1780, 1997.

[208] K. Kravari and N. Bassiliades, "A survey of agent platforms," *Journal of Artificial Societies and Social Simulation*, vol. 18, no. 1, p. 11, 2015.